

# **Matrix-bound peptides modeling protein- protein interactions**

## **Dissertation**

zur Erlangung des akademischen Grades

Doctor rerum naturalium

Vorgelegt dem Fachbereich Biochemie / Biotechnologie  
der Mathematisch-Naturwissenschaftlich-Technischen Fakultät  
der Martin-Luther-Universität Halle-Wittenberg

von

**Chao Yu**

geb. am 25.06.1971 in Shanghai, P. R. China

Halle/S., Juni 2003

1. Gutachter: Prof. Dr. G. Fischer (MPG FS für Enzymologie der Proteinfaltung, Halle)
2. Gutachter: Prof. Dr. S. Reißmann (Friedrich-Schiller-Universität Jena)
3. Gutachter: Prof. Dr. K. Neubert (Martin-Luther-Universität Halle-Wittenberg)

Datum der Verteidigung: 20.10.2003

**urn:nbn:de:gbv:3-000005593**

[<http://nbn-resolving.de/urn/resolver.pl?urn=nbn%3Ade%3Agbv%3A3-000005593>]

# Table of contents

<b>1 Introduction</b>	1
<b>1.1 Sterically constrained oligopeptides with induced conformations</b>	1
1.1.1 Peptides bound to scaffolds	2
1.1.2 Peptides bound to solid phase	3
<b>1.2 Synthesis of peptide arrays on planar supports — SPOT technology</b>	6
1.2.1 SPOT-synthesis technique	7
1.2.2 The supports used in SPOT synthesis	9
1.2.3 Analysis of protein-protein/peptide contact sites based on SPOT synthesis	9
1.2.4 Mapping linear and discontinuous binding sites by standard SPOT strategy	11
<b>1.3 Prolyl <i>cis/trans</i> isomerization – a probe for structural dynamics of proline-containing polypeptides</b>	12
1.3.1 Prolyl <i>cis/trans</i> isomerization in peptides containing proline mimetics	14
1.3.2 Properties of <i>cis/trans</i> isomerization of peptide bond preceding fluorinated prolines	15
<b>1.4 Aims</b>	18
<b>2 Results and discussion</b>	20
<b>2.1 Prerequisites relating to Janus-peptide arrays by SPOT synthesis</b>	20
2.1.1 Scheme of screening matrix-bound peptide-peptide interaction in mapping protein-protein interaction sites — Janus-peptide array	20
2.1.2 Amino group loading on planar polymeric supports	22
2.1.3 Peptide quality on planar polymeric supports	22
2.1.4 Templates used in Janus-peptide arrays	25
<b>2.2 The examples of protein-peptide interaction</b>	26
2.2.1 Example I: Streptavidin/ <i>Strep</i> -tag II interaction	26
2.2.1.1 Self-recognition in streptavidin subunit association	27
2.2.1.2 Mapping binding epitopes on streptavidin to <i>Strep</i> -tag II by Janus-peptide arrays	29
2.2.1.3 Biotin blocks the binding of streptavidin to <i>Strep</i> -tag II in the Janus-peptide array	31
2.2.1.4 Comparison of two different templates used for Janus-peptide arrays	32
2.2.1.5 The quality of the synthetic Janus-peptide pairs	34
2.2.1.6 Peptide length variation for the minimized binding epitopes by Janus-peptide array	35
2.2.1.7 Failure in analyzing the binding epitopes on streptavidin by fluorescence labeled <i>Strep</i> -tag II using standard SPOT strategy	36
2.2.1.8 Janus-peptide arrays based on the reverse sequence of streptavidin and <i>Strep</i> -tag II	38
2.2.1.9 Using polypropylene membrane for Janus-peptide arrays	39
2.2.1.10 Conclusions	42

2.2.2	Example II: Protein 14-3-3/phosphopeptides interaction	43
2.2.2.1	Mapping binding epitopes on 14-3-3 to RQRSTpSTPNV (Raf peptide) by Janus-peptide arrays	45
2.2.2.2	Mapping binding epitopes on 14-3-3 to ARSHpSYPA (mT peptide) by Janus-peptide arrays	47
2.2.2.3	Trouble shooting for the synthesis of phosphopeptides on cellulose	48
2.2.2.4	Conclusions	49
<b>2.3</b>	<b>The examples of protein-protein interaction</b>	51
2.3.1	Example I: FKBP12/FAP48 interaction	53
2.3.1.1	Mapping binding epitopes on FAP48 to FKBP12 by standard SPOT strategy	53
2.3.1.2	Mapping binding epitopes on FKBP12 to FAP48 using Janus-peptide arrays	54
2.3.1.3	Conclusions	58
2.3.2	Example II: FKBP12/EGFR cytosolic domain (residues 645-1186) interaction	61
2.3.2.1	Mapping binding epitopes on EGFR (Arg <sup>645</sup> -Ala <sup>1186</sup> ) to FKBP12 by standard SPOT strategy	61
2.3.2.2	The inhibitory activities (IC <sub>50</sub> ) of several peptide epitopes derived from EGFR on the PPIase activity of FKBP12	64
2.3.2.3	Mapping binding epitopes on FKBP12 to EGFR (Arg <sup>645</sup> -Ala <sup>1186</sup> ) by using Janus-peptide arrays	65
2.3.2.4	Interactions between Janus-peptide pairs are sequence dependent	66
2.3.2.5	Conclusions	68
<b>2.4</b>	<b>General properties of Janus-peptide arrays</b>	68
2.4.1	The properties of Janus-peptide arrays	69
2.4.2	The potential drawbacks of Janus-peptide arrays	71
2.4.3	The evaluation of the results from Janus-peptide arrays	72
<b>2.5</b>	<b>Thermodynamic and kinetic parameters of the <i>cis/trans</i> isomerization of (4)-fluoroproline containing peptides and the influence of PPIases</b>	74
2.5.1	<i>Cis/trans</i> isomerization of (4)-fluoroproline containing peptides	74
2.5.2	Catalysis of the <i>cis/trans</i> isomerization of fluoroproline containing peptide substrates by PPIases	77
2.5.3	The influence of urea on the activity of different PPIases	80
2.5.4	Conclusions	83
<b>3</b>	<b>Materials and Methods</b>	85
<b>3.1</b>	<b>Materials</b>	85
<b>3.2</b>	<b>Methods</b>	91
3.2.1	Expression and purification of hCyp18	91
3.2.2	Expression and purification of hFKBP12	92
3.2.3	MALDI-TOF analysis of cellulose bound peptide spots	92
3.2.4	Modification of cellulose membrane with (β-Ala) <sub>2</sub> anchor functions	93

3.2.5	The synthesis of templates used in Janus-peptide arrays	94
3.2.6	The preparation of Janus-peptide membranes	95
3.2.7	Western blot analysis	96
3.2.8	Membrane regeneration	97
3.2.9	SDS-Polyacrylamide Gel Electrophoreses (SDS-PAGE)	97
3.2.10	Determination of urea concentration	97
3.2.11	Determination of protein concentration with UV/VIS-spectroscopy	98
3.2.12	Determination of protein concentration with Bradford method	98
3.2.13	The catalytic efficiency of peptidyl-prolyl <i>cis/trans</i> isomerases	99
3.2.14	Influence of PPIases on the <i>cis/trans</i> isomerization of (4)-fluoroproline containing peptides (protease-coupled assay)	100
3.2.15	Solvent-jump method (protease-free assay)	101
3.2.16	The inhibition of soluble peptides on the PPIase activity of <i>hFKBP12</i>	101
	<b>Summary</b>	102
	<b>References</b>	104
	<b>Acknowledgements</b>	
	<b>Appendix A</b>	
	<b>Appendix B</b>	

# Abbreviations

(4)-diF-Pro	4 <i>R</i> , 4 <i>S</i> - L-di-fluoroproline
(4 <i>R</i> )-FPro	(4 <i>R</i> )-L-fluoroproline
(4 <i>S</i> )-FPro	(4 <i>S</i> )- L-fluoroproline
4-Oxa	( <i>S</i> )-oxazolidine-4-carboxylic acid
4-Thz	( <i>R</i> )-thiazolidine-4-crboxylic acid
Abz	2-aminobenzoyl
Ac-	Acetyl-
APEG	amino PEG (Poly-ethylene-glycol) spacer
AU	Absorption Unit
b*pwt	Barstar pseudo-wildtype
Boc	<i>tert</i> -butyloxycarbonyl
BPB	bromophenol blue
BSA	Bovines Serumalbumin
Bzl	Benzyl
Cyp	Cyclophilin
DCC	N,N'-Dicyclohexylcarbodiimide
DCM	Dichloromethane
DIC	N,N'-Diisopropylcarbodiimide
Dde	1-(4,4-dimethyl-2,6-dioxocyclohex-1-ylidene)ethyl
DEAE	Diethylaminoethyl-
Dhbt	3-hydroxy-2,3-dihydroxy-4-oxo-benzotriazolyl
DIEA	Diisopropylethylamine
DIPCDI	N,N'-Diisopropylcarbodiimide
DMF	Dimethylformamide
DMSO	Dimethylsulfoxide
DTT	Dithiothreitol
ECL	Enhanced chemiluminescence
<i>E. coli</i> Par	<i>E. coli</i> Parvulin
<i>E. coli</i> TF	<i>E. coli</i> Trigger Factor
EDTA	Ethylenediamine-tetraaceticacid
EGFR	EGF receptor
ESI-MS	Electrospray ionization mass spectrometry
EtOH	Ethanol
FAP	FKBP-associated protein
FKBP	FK506-binding Protein
Flp	4( <i>R</i> )-fluoro-L-proline
flp	4( <i>S</i> )-fluoro-L-proline
FMDV	foot-and mouth disease virus
Fmoc	9-fluorenylmethoxycarbonyl
FT-IR	Fourier Transform Infrared Spectroscopy
HBTU	2-(1 <i>H</i> -Benzotriazole-1-yl)-1,1,3,3-tetramethyluronium hexafluorophosphate
HEPES	4-(2-Hydroxyethyl)-1-piperazine-1-ethanesulfonic acid
HF	hydrogen fluoride
HOBt	1-hydroxybenzotriazole
HRMAS	high-resolution magic angle spinning
HRP	Horse-Radish Peroxidase
Hyp	4( <i>R</i> )-hydroxy-L-proline

IPTG	Isopropyl $\beta$ -D-thiogalactopyranoside
ISP	Isomer-Specific Proteolysis
$k_{cat}$	catalytic constant
$K_d$	Dissociation constant
$K_m$	Michaelis-Menten constant
MALDI-TOF	Matrix assisted laser desorption ionisation time-of-flight
MBHA	Methylbenzylamine
MES	2-( <i>N</i> -Morpholin-o)ethanesulfonic acid
MLU	Martin-Luther-University
MS	Mass spectrometry
NMI	<i>N</i> -methylimidazole
NMP	<i>N</i> -methylpyrrolidin
NMR	Nuclear Magnetic Resonance
OD	optical density
PAGE	Polyacrylamide gelelectrophoresis
Par	Parvulin
Pbf	2,2,4,6,7-Pentamethyl-dihydrobenzofurane-5-sulfonyl
PEG	Polyethyleneglycol
PEGA	acrylamidopropyl-PEG- <i>N,N</i> -dimethylacrylamide
Pfp	Pentafluorophenyl
PMSF	Phenylmethylsulfonylfluoride
-pNA	- <i>para</i> -nitroaniline
POEPOP	polyoxyethylene-polyoxypropylene
PP	Polypropylene
PPIase	Peptidyl-Prolyl- <i>cis/trans</i> -Isomerase
PTFE	polytetrafluoroethylene
PyBOP	benzotriazole-1-yl-oxy-tris-pyrrolidino-phosphonium hexafluorophosphate
Rink	4-(2',4'-Dimethoxyphenyl-hydroxymethyl)-phenoxyacetic acid
RT	room temperature
SDS	Sodium dodecylsulfate
Sip	Silaproline
SPPS	Solid Phase Peptide Synthesis
Suc-	Succinyl-
TASP	template-assembled synthetic protein
TBS	Tris buffered saline
TBT	Tris buffered saline with Tween 20
TBTU	2-(1H-Benzotriazole-1-yl)-1,1,3,3-tetramethyluronium tetrafluoroborate
tBu	t-Butyl
TEMED	<i>N,N,N',N'</i> -Tetramethylethylenediamine
TF	Trigger factor
TFA	Trifluoroacetic acid
TOF-MS	Time-of-flight mass spectrometry
Tricine	<i>N</i> -Tris(hydroxymethyl)-methylglycine
Tris	2-Amino-2-(hydroxymethyl)-1,3-propane-1,3-diol
Trt	Trityl
UV/VIS	Ultraviolet/Visible
wt	Wild type
Xaa	amino acids

# 1 Introduction

## 1.1 Sterically constrained oligopeptides with induced conformations

Polypeptides with less than about 30 amino acid residues and devoid of disulfide bonds are unlikely to adopt a fixed conformation in aqueous solution (Dyson, H.J. and Wright, P.E. 1991). It can not be excluded that in some cases, peptides adopt some preferred structures, because polyproline (Stapley, B.J. and Creamer, T.P. 1999) or even a seven alanine residues (Shi, Z., et al. 2002) adopt the polyproline II helix under non-native conditions (e.g. at lower temperature). On the other hand, some *de novo* designed peptides can also form defined structures (Venkatraman, J., et al. 2001). However, short peptides have a tendency to exist in random structures in water. The lack of the long-range interactions to stabilize certain favorable energetic states in short peptides may be the main reason. Since the Gibbs free energy difference ( $\Delta G$ ) between the folded and unfolded state is caused by entropic and enthalpic contributions from both, the solvent and the polypeptide chain, the  $\Delta G$  of folding of small oligopeptides is much larger than for folding proteins (Dill, K.A. 1990, Makhatadze, G.I. and Privalov, P.L. 1995). Therefore, oligopeptides in solution adopt a manifold of conformations mostly separated by low energy barriers of interconversions.

However, previous studies have shown that it is possible to prepare relatively short peptides that are inclined towards adopting the desired conformation due to the incorporation of a single unnatural amino acid residue or template (Kemp, D.S., et al. 1991). NMR studies suggest that certain peptides immobilized on solid phase or displayed on bacteriophage coat protein are folded into a defined, stable conformation with less degree of motional freedom of the chains than for the same peptides in solution (Jelinek, R., et al. 1997, Warrass, R., et al. 2000). It is hypothesized that the chain entropy penalty associated with the folding of a short peptide chain can be decreased by lowering the conformational entropy of the unfolded state through covalently attaching to the conformationally restricted templates and solid phase, or forming peptide and protein chimeras. Accordingly, the sterically constrained short peptides can be induced to form stable structures.

### 1.1.1 Peptides bound to scaffolds

The concept of introducing a conformationally rigid scaffold into a peptide to stabilize a single bioactive conformation was first demonstrated by Hirschmann and co-workers (Freidinger, R.M., et al. 1980, Veber, D.F., et al. 1976).

Now a variety of templates have been incorporated into peptides and studied as folding nucleators, which are responsible for the attached peptides to form stable structures like  $\alpha$ -helices or  $\beta$ -sheets (Schneider, J.P. and Kelly, J.W. 1995a). These templates can typically transmit their conformational preferences to the peptide chain by hydrogen bonding or by a combination of hydrogen bonding and hydrophobic interactions to nucleate the desired structure.

Many efforts have been put in the *de novo* protein design based on this principle, like construction of template-assembled synthetic proteins (TASP) (Tuchscherer, G. and Mutter, M. 1995, Tuchscherer, G., et al. 1994). The TASP concept was often used to design proteins containing a 4-helix bundle or beta-barrel-like structure (Mutter, M., et al. 1989, Mutter, M. and Vuilleumier, S. 1989) (see also Table 1-1), through using cyclic peptide/peptidomimetic templates to generate common protein structural motifs in predominantly short peptides (Mutter, M. and Tuchscherer, G. 1997). The existence of possible driving forces for helix association on the template, such as packing effects (van der Waals interactions between closely packed helices) and interhelical polar interactions (hydrogen bonds and ion pairs), are also the reasons for 4-helix bundle TASP to adopt stable tertiary structure.

The importance of template size, shape and directionality has been investigated in TASPs (Wong, A.K., et al. 1998). The conformation of cyclic decapeptide template molecule has also been well studied by NMR (Peng, Z.H. 1999). Some successful examples of templates inducing regular structure in peptide and used in *de novo* design of proteins are summarized and listed in the following table (Table 1-1).

Not only templates, but also metal complexation can induce and stabilize the structure of peptides in aqueous solution (Arnold, F.H. and Zhang, J.H. 1994, Ghadiri, M.R. and Choi, C. 1990, Schneider, J.P. and Kelly, J.W. 1995b). This attempt has taken advantage of side chains of natural amino acids (His, Cys) or engineered unnatural amino acids like aminodiacetic acid (Ruan, F.Q., et al. 1990) in the polypeptide as metal-binding ligands. The results in the study of small helical motifs indicate that the helical stabilization observed is a result of metal mediated conformational restriction of the polypeptide (Zou, J. and Sugimoto, N. 2000).

Solution NMR studies of HIV-1 gp120 protein derived hexapeptide (GPGRAF) (Goudsmit, J., et al. 1988, Rusche, J.R., et al. 1988) embedded in 12 to 40 residue polypeptides can only detect transient turn-like structure elements ("nascent helix") (Chandrasekhar, K., et al. 1991, Zvi, A., et al. 1992), but not uniquely folded structure in any of these peptides in water. When GPGRAF sequence was inserted near the N terminus of major coat protein of filamentous bacteriophage, it adopts a well-defined double-turn structure similar to that in the native protein (Jelinek, R., et al. 1997). It is also known when a peptide containing a linear continuous epitope displayed on bacteriophage coat protein it can mimic very effectively the immunogenicity of the protein from which it is drawn (Veronese, F.D.M., et al. 1994). These results suggest that GPGRAF may be encouraged to adopt a persistent conformation in the context of phage coat protein, unlike the situation in free solution, and therefore it has an enhanced propensity to adopt a conformation similar to that found in the native protein from which it is derived.

### **1.1.2 Peptides bound to solid phase**

Synthetic peptides can exhibit biological activity (i.e. high binding affinity to acceptor molecules) while still attached to the solid supports (Geysen, H.M., et al. 1984, Lam, K.S., et al. 1991). Such phenomenon suggests that peptides covalently bonded to polymers can adopt biologically relevant conformations. Results of the two-dimensional NMR observation of a hexapeptide (GPGRAF) bound to polystyrene based Tentagel (TG) resin with PEG linker show that the peptide immobilized on beads is folded into a defined, stable conformation in comparison to the same peptide in solution (Jelinek, R., et al. 1997).

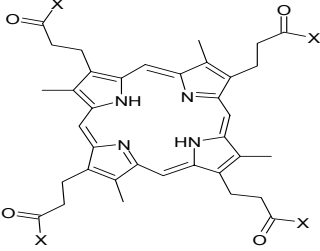
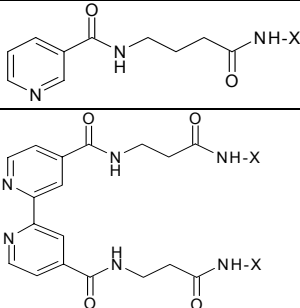
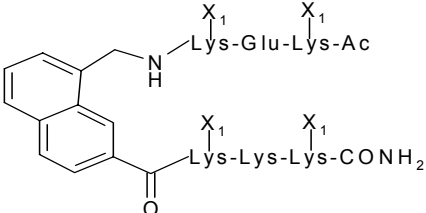
Recently, Furrer and co-workers have determined the influence of the chemico-physical nature of the three different resins, polystyrene-MBHA, PEGA (Meldal, M. 1992), and POEPOP (Renil, M. and Meldal, M. 1996) on the secondary structure of the covalently attached 19-mer foot-and-mouth disease virus (FMDV) peptide representing a highly immunogenic peptide of the virus by HRMAS NMR spectroscopy analysis (Furrer, J., et al. 2001). This study clearly shows that FMDV peptide linked to the three resins display ordered conformational behavior. The anchored FMDV peptide has a propensity to fold into an  $\alpha$ - or  $3_{10}$  helix in deuterated DMF, although the chemico-physical nature of different resins may have different influences on the conformation of the covalently attached peptide (Furrer, J., et al. 2001, Smythe, M.L., et al. 1995).

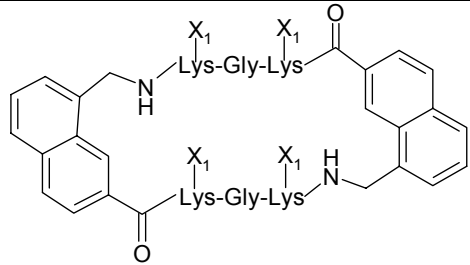
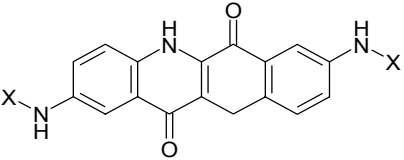
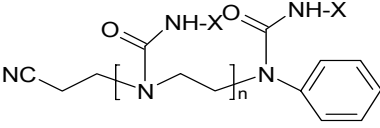
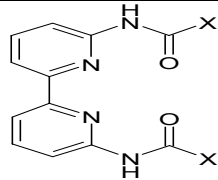
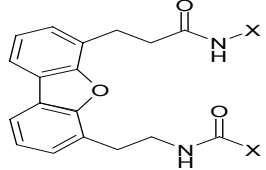
Another most concerned question regarding to the resin-linked peptide is the relationship between peptide length and density on beads and its preference to a certain conformation. As known, the interchain aggregation of the resin-bound peptides is a difficulty encountered in solid phase peptide chemistry. Polyalanine sequences of varying chain length have been used as model peptides to study folding and aggregation on solid support by different analytical techniques, such as infrared spectroscopy and NMR spectroscopy. It has been discovered that (Ala)<sub>5</sub>, (Ala)<sub>6</sub> and (Ala)<sub>7</sub> have propensity to form  $\beta$ -sheet conformation which leads to stable intermolecular sheets of neighboring peptide chains (Merrifield, R.B. 1995), therefore the yield of the coupling is decreased. Decreasing the peptide density by discharging the resin allows to study of longer polyalanine sequences without being restrained by aggregation. Lippens and co-workers have observed  $\alpha$ -helix formation in (Ala)<sub>12</sub> sequence by HRMAS NMR (Warrass, R., et al. 2000). These observations indicate that peptide length and density on solid phase have influences on the folding of the immobilized peptides.

Recently, Haehnel and co-workers have reported the design and combinatorial synthesis of *de novo* metalloproteins by TASP concept on cellulose membrane with the structure of an antiparallel four-helix bundle. Different sets of amphiphilic helices were assembled on cyclic peptide templates attached to the cellulose membrane. The variation of the amino acids of the hydrophobic binding pocket in the antiparallel four-helix bundle changed the binding ability of the *de novo* proteins to metals (Rau, H.K., et al. 2000, Schnepf, R., et al. 2001). The successful synthesizing and screening for a *de novo* protein on cellulose indicate that the stabilization and association of the immobilized peptides on template lead to a correct and functional conformation adopted by the *de novo* protein on solid support.

In addition, a WW protein domain consisting of 42 amino acids has been synthesized on cellulose (Toepert, F. 2001). The WW protein domain is a well-investigated model for studying  $\beta$ -sheet motifs (Koepf, E.K., et al. 1999, Kortemme, T., et al. 1998, Macias, M.J., et al. 1996). The binding properties of all single substitution of WW variants in the array towards the peptide ligand EYPPYPPPPYPSG have been investigated. The binding studies indicated that the synthetic WW domain on cellulose folded into a native-like conformation. The introduction of correctly folded protein domain on solid support opens a way to study structure-function relationships of proteins on solid support (Toepert, F. 2001).

**Table 1-1** Templates that induce a preferred conformation of attached peptides

Structural type	Template	Structure image	Reference
$\alpha$ -helical folding	Porphyrin based		Sasaki, T. and Kaiser, E.T. 1990 Akerfeldt, K.S., et al. 1992, Mihara, H., et al. 1992
	Pyridine and Bipyridine based		Ghadiri, M.R., et al. 1992 Ghadiri, M.R., et al. 1992, Lieberman, M. and Sasaki, T. 1991
Acyclic and cyclic peptide based		$\text{X}_1$ Ac-Lys-Pro-Lys-Lys-OH	Mutter, M. 1988, Mutter, M., et al. 1988
		$\text{X}_1$ $\text{X}_1$ $\text{X}_1$ $\text{X}_1$ Ac-Lys-Lys-Lys-Pro-Gly-Lys-Glu-Lys-OH	Mutter, M., et al. 1988 Tuchscherer, G., et al. 1993
		$\text{X}_1$ $\text{X}_1$ $\text{X}_1$ $\text{X}_1$ Ac-Lys*-Lys-Lys*-Pro-Gly-Lys*-Glu-Lys*-Gly-OH	Altmann, K.H. and Mutter, M. 1990, Mutter, M. and Altmann, K.H. 1986 *:Futaki, S., et al. 1999
		$\text{X}_1$ $\text{X}_1$ $\text{X}_1$ $\text{X}_2$ Ac-Cys-Lys-Ala-Lys-Pro-Gly-Lys-Ala-Lys-Cys-NH <sub>2</sub>	Mutter, M. 1985, Mutter, M., et al. 1988, Mutter, M. and Vuilleumier, S. 1989
		$\text{X}_1$ $\text{X}_2$ $\text{X}_3$ $\text{X}_4$ cydo-[Cys-Ala-Cys-Pro-Gly-Cys-Ala-Cys-Pro-Gly]	Rau, H.K., et al. 1998 Rau, H.K. and Haehnel, W. 1998 Schnepf, R., et al. 2001
			Tuchscherer, G., et al. 1993

			Mutter, M. 1985 Tuchscherer, G., et al. 1993 Mutter, M., et al. 1989, Tuchscherer, G., et al. 1992
β-sheet folding	Epindolidione based		Kemp, D.S. and Bowen, B.R. 1988, Kemp, D.S. and Bowen, B.R. 1988
	di- or triurea based	 n: 1 or 2	Holmes, D.L., et al. 1997
	Bipyridine based		Schneider, J.P. and Kelly, J.W. 1995b
	Dibenzofuran based		Diaz, H., et al. 1992 Tsang, K.Y., et al. 1994
	Acyclic peptide based	$\text{Ac-Lys}^{X_1}\text{-Lys}^{X_1}\text{-Lys}^{X_1}\text{-Lys}^{X_1}\text{-Pro-Gly-Lys}^{X_1}\text{-Lys}^{X_1}\text{-Lys}^{X_1}$	Mutter, M. and Vuilleumier, S. 1989 Mutter, M. 1988

Note: X represents the peptide chain C-terminally attached to the templates (via  $\epsilon\text{-NH}_2$  of Lys,  $\text{-SH}$  of Cys or other functional groups on the templates). The subscript of X indicates the use of different peptide chains.

## 1.2 Synthesis of peptide arrays on planar supports — SPOT technology

Planar supports represent a unique opportunity in designing novel approaches to solid phase synthesis of peptides and small organic molecules. Planar carriers allow the synthesis to be performed without any reaction vessels, construction of libraries with only one analytical representation of each structure (Lebl, M. 1998).

SPOT synthesis which was originally introduced by Frank (Frank, R. 1992, Frank, R., et al. 1991) is an easy and flexible technique for simultaneous and parallel chemical synthesis of peptides at distinct positions on a membrane support. Since its appearance, the SPOT

synthesis method has been developed extensively to permit rapid and highly parallel synthesis of not only peptides and peptide mixtures including unnatural building blocks, but also a growing range of organic compounds (Heine, N., et al. 2001, Scharn, D., et al. 2001). SPOT method has opened up unlimited opportunities to synthesize and subsequently screen large arrays of synthetic peptides and/or peptidomimetics. Such spatially addressable methodology for single compounds offers the advantage that the structure information of a molecule can be identified easily by its position. Peptide arrays prepared by SPOT synthesis can be used to study molecular recognition events, such as epitope mapping, the analysis of protein-protein and protein-nucleic acid interactions, and identification of biologically active peptides. Most impressively and advantageously is that peptide arrays can be applied to depict molecular recognition events on the single amino acid level precisely.

### **1.2.1 SPOT synthesis technique**

The principle of SPOT technology is based on that once a small droplet of activated amino acid solution being deposited directly onto a porous membrane (e.g. cellulose), the droplet is absorbed to form a circular spot. These spots can be considered as microreactors for a chemical reaction if a nonvolatile solvent system is used.

The scheme of SPOT synthesis method in the application of synthesizing peptides on cellulose is shown in Fig. 1-1. A commercially available filter paper (e.g. Whatman, Maidstone, UK) with hydroxyl functional group can be uniformly converted to amino functions through coupling with Fmoc- $\beta$ -Ala-OH activated by diisopropylcarbodiimide (Mathias, L.J. 1979) and the subsequent removal of the Fmoc-group (**I**). The spots are then predefined by dispensing small droplet of Fmoc- $\beta$ -Ala-pentafluorophenyl ester solution onto the distinct sites on the membrane (**II**). This process can be done either by a pipetting robot (Abimed GmbH, Langenfeld, Germany) or manually. After the removal of the Fmoc group, Fmoc- $\beta$ -Ala active ester or other activated building blocks can be coupled to the defined spots as spacer/linker (**III**). The following peptide chain elongation steps are conventional solid phase peptide synthesis (Merrifield, R.B. 1963, Merrifield, R.B. 1995). It is a repetitive procedure, each cycle starting with removal of N-terminal protecting group of the immobilized peptide chain on cellulose (**IV**), followed by coupling of the pre-activated amino acids with N-terminal and side chain suitably protected (**V**). The peptide chain is growing in the direction from carboxyl to amino-terminal (C->N). In between each step, the washing step is carried out by using respective reagents and solvents (**VI**). Finally, the peptide is generated

by the removal of all side chain protecting groups (**VII**), which is ready for subsequent chemical or biological screening directly on the cellulose membrane. The peptide can also be cleaved from the solid support by the use of ammonia vapor (Bray, A.M., et al. 1991) or via special linker molecules (Guillier, F., et al. 2000) between the membrane and the peptide. The different amino functions loading on different membrane supports (e.g. cellulose, polypropylene membrane) can be achieved in a range from 50 nmol/cm<sup>2</sup> up to 500 nmol/cm<sup>2</sup> depending on different derivatizing conditions (Scharn, D., et al. 2000, Wenschuh, H., et al. 2000).

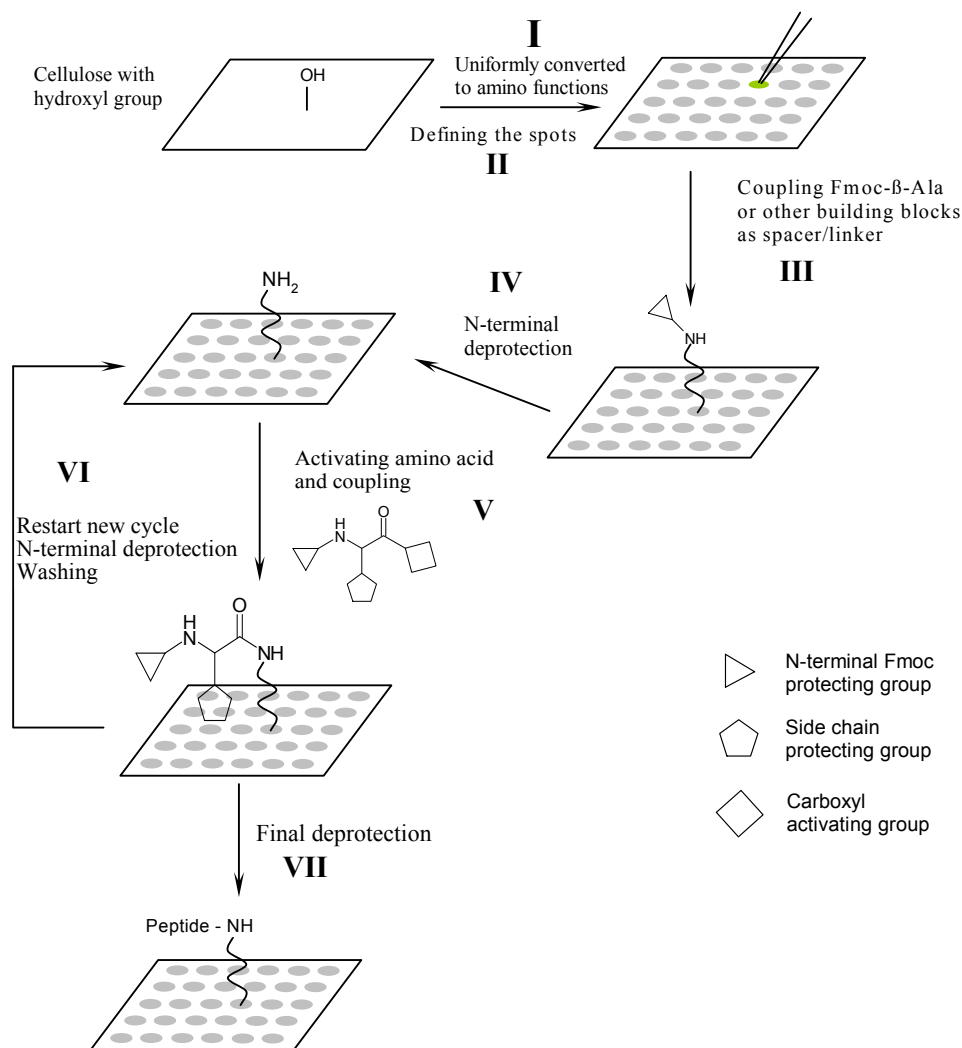


Fig. 1-1 Scheme of Spot synthesis on planar membrane

### **1.2.2 The supports used in SPOT synthesis**

The membrane support suitable for the successful spotwise assembly of peptides and subsequent screening must have several properties, such as:

- Chemical compatibility and stability with a variety of solvent systems and reaction conditions;
- Compatibility with physiological media and good hydrophilicity for the biological assay;
- Mechanical stability towards repetitive spotting, washing and cleavage steps;
- High porosity for good liquid permeability;
- Accessibility of surface functionalities for derivatization.

Two major types of the membrane supports are selected to be used in SPOT synthesis for assembly and biological screening of peptide arrays, namely cellulose membrane and polypropylene membranes.

Cellulose is known to have (1) hydroxyl functions which can be easily modified for peptide synthesis; (2) good surface hydrophilicity and wettability which allow the use of cellulose bound peptides for binding assays, and it is also known to be well compatible with mild Fmoc based peptide synthesis chemistry (Frank, R. and Doring, R. 1988). So nowadays, cellulose membranes are widely applied for the screening of immobilized peptides as well as the preparation of soluble peptides in the scale range from 1 to 100 nmol (Frank, R. and Overwin, H. 1996). These cellulose membranes include ester-derivatized amino functionalized cellulose (Frank, R. 1992) and CAPE (cellulose-amino-hydroxypropyl ether) membranes (Ast, T., et al. 1999, Licha, K., et al. 2000, Volkmer-Engert, R., et al. 1997).

For other chemistries not compatible with the polysaccharide (e.g. cellulose) support, the novel amino-functionalized polypropylene based membranes will be selected, such as, acrylate-grafted polypropylene membranes; acrylate-coated PTFE membranes; polystyrene-grafted PTFE membranes; polystyrene-grafted polyethylene films. All these membranes have been developed in the aim of being applicable for SPOT synthesis (Frank, R. 2002, Wenschuh, H., et al. 2000).

### **1.2.3 Analysis of protein-protein/peptide contact sites based on SPOT synthesis**

Protein-ligand and protein-protein interactions are essential to cellular mechanisms at all levels in biological processes. The determination of protein-protein interaction sites could be one of the powerful and efficient ways to characterize protein complexes. A number of

different methods have already been established and successfully applied in the analysis of protein-protein interactions. These methods include biochemical methods such as coimmunoprecipitation and cross-linking; molecular biological methods such as the two-hybrid system and phage display; and structural methods such as NMR spectroscopy and X-ray crystallography (Phizicky, E.M. and Fields, S. 1995). However many of these methods are either laborious (e.g. two-hybrid system) or difficult to handle (e.g. structural analysis), and depict protein interactions at whole molecular level.

Protein interactions can be studied at amino acid level since the use of protein-derived scans of overlapping peptides (Geysen, H.M., et al. 1984). SPOT technology allows the analysis and mapping of interaction sites of protein complexes in a rapid and straightforward way. However, it is not a method for direct detecting interactions of protein complexes. Therefore, further proof by complementary methods should be helpful to evaluate the preliminary interaction information obtained from SPOT method. Some advantages as well as potential drawbacks by using SPOT method to screen protein-protein contact sites are listed in [Table 1-2](#). SPOT method has been extensively applied to outline protein-protein/ligand interactions, especially in the field of immunological recognition, such as mapping of epitopes with polyclonal sera or monoclonal antibodies (Frank, R. and Schneider-Mergener, J. 2002).

**Table 1-2** Characteristics of SPOT method for the analysis of protein-protein/peptide interactions

Advantages	Disadvantages
1) Rapid and inexpensive, highly parallel synthesis of large amount of peptides or peptide mixtures 2) Not restricted to L-amino acids, unnatural building blocks can be used. 3) Cellulose or other membrane supports are compatible with many biological assays. 4) Synthesized arrays can be screened directly on solid phase simultaneously. 5) Depict molecular recognition events at the amino acid level. Sequence of target peptide can be identified easily by its position. 6) High peptide density on cellulose may increase the screen sensitivity.	1) The accessible peptide fragments from the protein core can cause unspecific hydrophobic interactions. 2) Non-linear, discontinuous, conformational dependent epitopes might not be measurable due to single binding regions contribute to low binding affinity. 3) Different solid supports might influence the folding of attached peptides, thus influence the recognition process. 4) The length of the attached peptide is limited (less than 20 amino acids) due to efficiency of stepwise peptide synthesis.

### 1.2.4 Mapping linear and discontinuous binding sites by standard SPOT strategy

Proteins interact via surface accessible interaction sites which involve amino acid residues and backbone contacts along a continuous segment of the protein chain (linear epitopes) or involve amino acid residues from at least two segments close in space by the folded conformation (conformational or discontinuous epitopes) but separated in the primary sequence (Fig. 1-2, B). The term “epitopes” mentioned here is defined as the contact sites of a protein that interacts with its binding partner (Frank, R. 2002).

In linear epitopes, the key amino acids mediating the contacts with the binding partner are located within one part of the primary structure and comprise no more than 15 amino acids in length, usually 8-12 amino acids. Peptides covering such epitopes are usually able to compete with the protein-protein interaction and have similar affinities as the intact protein from which they are derived (Reineke, U., et al. 1999).

The mapping of linear epitopes by standard SPOT method using overlapping peptides derived from the entire primary sequence of a protein is an easy and efficient approach (Frank, R. 1992). The whole protein sequence is fragmented and synthesized on cellulose with short overlapping peptides (normally 13-15 amino acids in length and shifted by 3 amino acids), so called peptide scan, which is subsequently probed for binding to the respective partner protein. The binding assay is either performed directly on peptide membrane through immunodetection of bound probe protein or autoradiograph of radiolabeled probe protein, or after transfer to a nitrocellulose membrane (Rudiger, S., et al. 1997). The sketch of mapping linear epitope is shown in Fig. 1-2(A). The sequences colored red are the linear contact site with detectable signals in binding assay.

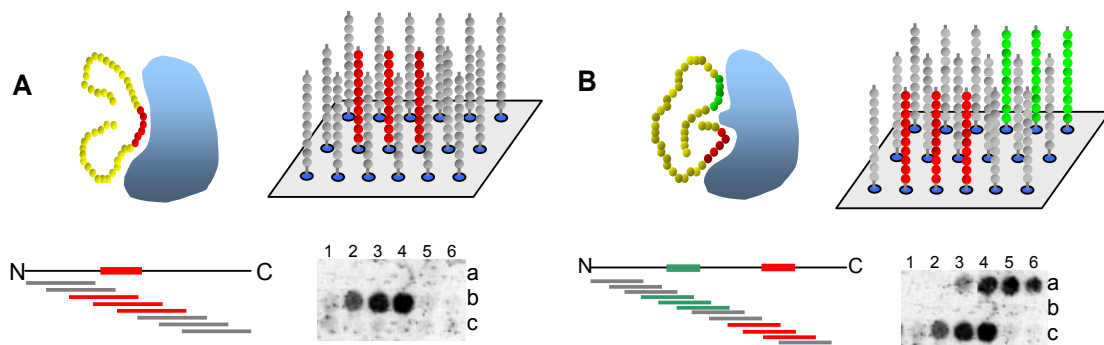


**Fig. 1-2** Scheme of mapping linear (A) and discontinuous (B) protein-protein interaction epitopes

Since protein-protein interactions are usually mediated by relatively large contact interface (Jones, S. and Thornton, J.M. 1996), in most cases proteins have more than one binding site to interact with their binding partners. In such discontinuous (conformational) binding sites the key residues contributing to the binding affinity are normally separated in the primary structure, but closer in the conformation on the surface of a folded protein to form a conjunct binding epitope (Fig. 1-2, B).

The mapping of discontinuous epitopes using fragments of protein either generated chemically or biologically suffers from the drawback that peptides comprising only single binding region of a discontinuous binding site generally have very low affinities for the binding partner in solution, even if the complete binding site mediates a high affinity interaction. Thus, the mapping of discontinuous epitopes with overlapping peptide scan on cellulose might be accordingly very difficult. However, SPOT approach has its unique advantage that the density of the immobilized peptides on membranes can be as high as 50 nmol/cm<sup>2</sup> or even higher, which achieves a high local peptide concentration (mM level or higher, estimated) and thus increases the screening sensitivity. In this way, the inherent defect that peptides comprising only the individual binding regions normally having low affinities for the binding partner can be overcome to a great extent by SPOT method. The scheme of mapping discontinuous epitopes is shown in Fig. 1-2(B), where the sequences colored red and green are separated in primary protein sequence with detectable signals individually in binding assay.

### **1.3 Prolyl *cis/trans* isomerization – a probe for structural dynamics of proline-containing polypeptides**

The peptide bond between the carbonyl carbon and the nitrogen shows partial double bond character, so peptide bonds are planar, and the flanking C $\alpha$  atoms can be in either the *trans* or the *cis* conformation. The *trans* state is mostly favored over *cis* in case the peptide bonds preceding residues other than proline (Ramachandran, G.N. and Sasisekharan, V. 1968). The non-prolyl *cis* peptide bonds are rarely found in folded proteins. However, for peptide bonds preceding proline (Xaa-Pro, prolyl bonds) the *trans* isomer is favored only slightly over the *cis* isomer (MacArthur, M.W. and Thornton, J.M. 1991, Stewart, D.E., et al. 1990), because the energy difference ( $\Delta G^\circ$ ) between the *cis* and *trans* state is small (< 2

kcal·mol<sup>-1</sup>) (Ramachandran, G.N. and Sasisekharan, V. 1968). Therefore, theoretically the two forms coexist in almost equal amounts (Fig. 1-3) in peptides. Indeed, the *cis* content is often between 10 % and 30 % in short unstructured peptides (Cheng, H.N. and Bovey, F.A. 1977, Grathwohl, C. and Wuthrich, K. 1981, Reimer, U., et al. 1998). The actual *cis/trans* ratio is largely depending on the chemical nature of the flanking amino acids, the charge distribution around the prolyl bond and the structural constraints, such as in folded proteins. Prolyl bonds often occur in the *cis* conformation in folded proteins, 7 % of all prolyl peptide bonds in folded proteins are in the *cis* conformation (MacArthur, M.W. and Thornton, J.M. 1991, Stewart, D.E., et al. 1990).

Prolyl *cis/trans* isomerizations are slow reactions with time constants between 10s and 100 s at 25 °C because they involve the rotation around a partial double bond. The prolyl isomerization often forms the rate-limiting step in folding and refolding of proteins (Fischer, G. and Schmid, F.X. 1990, Schmid, F.X., et al. 1993). In folded proteins, each prolyl peptide bond is usually in a defined conformation, being either *cis* or *trans* in every molecule (Brandts, J.F., et al. 1975). Incorrect prolyl isomers in a protein chain sharply decelerate its folding. Many proteins refold within few milliseconds when they contain correct prolyl isomers. If incorrect isomers are present, folding will usually require seconds to hours (Fischer, G. 2000, Schmid, F.X. 1993, Schmid, F.X. 2002, Stein, R.L. 1993). Peptidyl-prolyl *cis/trans* isomerases (PPIases) are ubiquitous and abundant enzymes (EC number 5.2.1.8) (Fischer, G. 1994, Galat, A. and Metcalfe, S.M. 1995, Pliyev, B.K. and Gurvits, B.Y. 1999) and can accelerate slow peptidyl-prolyl *cis/trans* interconversion in oligopeptides and proteins at different folding steps (Kiefhaber, T. and Schmid, F.X. 1992, Schiene, C. and Fischer, G. 2000, Schmid, F.X. 2002). In summary, dynamics of prolyl bond *cis/trans* isomerization gives rise to information on the conformational state of a particular backbone segments in proteins.

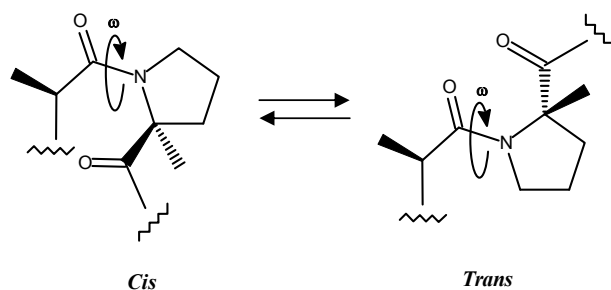


**Fig. 1-3** *Cis/trans* isomerization of peptidyl-prolyl bond. The peptide bond preceding proline residue has two stable conformations: *trans* ( $\omega$  about 180°) and *cis* ( $\omega$  about 0°).

### 1.3.1 Prolyl *cis/trans* isomerization in peptides containing proline mimetics

Proline (Pro) is unique among the gene-coded amino acids due to its side chain covalently bonded to the nitrogen atom of the peptide backbone. Prolyl residue plays an essential role in the three-dimensional structure of peptides and proteins. Since the prolyl peptide bond has energetically similar *cis* and *trans* isomers, proline may act as helix breaker or as the essential part of turns either in the state of *trans* or *cis* conformation (e.g., VIb type loop (Tugarinov, V., et al. 1999)).

In particular, Ac-Pro-NHMe (see Fig. 1-4) and Ac-Xaa-Pro-NHMe have been widely used as models for the studies on the conformational preferences and transition states for Xaa-Pro isomerization both experimentally (Beausoleil, E. and Lubell, W.D. 1996, Schoetz, G., et al. 2001) and theoretically (Fischer, S., et al. 1994, Kang, Y.K., et al. 1999).

In order to pursue a better understanding of the molecular events underlying such a slow interconversion, proline derivatives have been chosen and considered as tools to study the dynamics of Xaa-Pro bonds (where Pro can be substituted by other Pro derivatives), to determine the kinetics and thermodynamics of this *cis/trans* isomerisation.

A number of attempts have been made to constrain the Xaa-Pro bond to either *trans* or *cis* conformations by alkylation (An, S.S.A., et al. 1999, Beausoleil, E. and Lubell, W.D. 1996, Beausoleil, E. and Lubell, W.D. 2000, Kang, Y.K. 2002), cyclization (Chalmers, D.K. and Marshall, G.R. 1995), and heteroatomic substitution (Dumy, P., et al. 1997, Keller, M., et al. 1998, Mutter, M., et al. 1999). These experimental tools can be used to dissect conformational effects on prolyl isomerization. The fixation of specific conformational states is of much interest for structure-activity studies as well as the development of new drugs.

Pseudo-prolines ( $\Psi$ Pro) on the basis of oxazolidine and thiazolidine rings (Haack, T. and Mutter, M. 1992, Mutter, M., et al. 1995, Wöhr, T., et al. 1996) show different isomerization rates of the preceding tertiary amide bond as compared to that of a native prolyl-amide. NMR studies of a series of  $\Psi$ Pro (see Fig. 1-4) containing peptides have revealed that the introduction of  $\Psi$ Pro would change the *cis/trans* equilibrium of the Xaa- $\Psi$ Pro peptide bond in solution (Dumy, P., et al. 1997, Kern, D., et al. 1997). A considerable effect of 2-C substitution of  $\Psi$ Pro (identical to the 5-C position of Pro) on the *cis/trans* equilibrium has been observed (Keller, M., et al. 1998, Mutter, M., et al. 1999). Generally, the isomerization rates of Xaa- $\Psi$ Pro peptide bond in short model peptides can be accelerated as compared to that of Xaa-Pro peptide bond by lowering the transition state barrier energies, which largely depends on stereochemistry and the degree of substitution at the 2-C position of

$\Psi$ Pro (Keller, M., et al. 1998, Mutter, M., et al. 1999). In case of the analysis and comparison of conformational preference between Xaa-Sip, where Sip is 4-dimethylsila-proline, and Xaa-Pro peptide bonds, NMR results show that Sip has practically the same conformational preferences as found for Pro with similar *cis* content (Cavelier, F., et al. 2002). This investigation confirms the idea that a modified 4-C position of proline is usually expected to have weak influence on the proline conformational preferences (Haar, W., et al. 1976, McCafferty, D.G., et al. 1995).

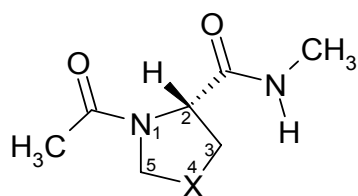


**Fig. 1-4** Definition of structural parameters for Ac- $\Psi$ Pro-NHMe: X = CH<sub>2</sub> for Pro; X = O for Oxa; X = S for Thz; X = Si for Sip

Note: the numbering is based on proline pyrrolidine ring structure

The investigation of the rotational barriers for *cis/trans* isomerization of different proline analogues by dynamic <sup>1</sup>H NMR spectroscopy has revealed that the rotational barrier of all observed cyclic proline analogues except for hydroxyproline are lower than that of proline by about 2.39 kcal·mol<sup>-1</sup> (Kern, D., et al. 1997).

Sterically restrained proline analogues, such as the alkylations at positions 2, 3, and 5 of proline have been shown to have sensitive influences on the backbone conformation of proline. Especially, for the alkylation at position 5 of proline pyrrolidine ring, the *cis/trans* equilibrium of the Xaa-Pro peptide bond is significantly affected ((Kang, Y.K. 2002) and references therein). As illustrated earlier that steric interactions can lower the barrier for tertiary amide bond isomerization of 5-alkylprolyl peptides (Beausoleil, E. and Lubell, W.D. 1996), whereas 3-alkylprolines can create steric interactions that raise the barrier for amide isomerization (Beausoleil, E., et al. 1998).

### 1.3.2 Properties of *cis/trans* isomerization of peptide bond preceding fluorinated prolines

Numerous investigations have been focused on the studies of hydroxyproline, normally denoting 4(*R*)-hydroxy-L-proline (Hyp) and 4(*S*)-hydroxy-L-proline (hyp). Hyp is the only stereoisomer found to be the major component of collagen, which is the most common protein in connective tissue. The basic structure of collagen is a triple helix structure with trimeric repeats of Xaa-Yaa-Gly where Pro and Hyp are in most cases found at positions

Xaa and Yaa, respectively. During the exploration of the role of hydroxyproline in maintaining the stability of collagen, fluorinated Pro derivatives including 4(*R*)-fluoro-L-proline (Flp) and 4(*S*)-fluoro-L-proline (flp) have been introduced in *de novo* synthetic collagen peptides to illustrate their contributions to the conformational stability of a protein.

In considering of the stereoelectronic effect on the equilibrium constant  $K_{trans/cis}$  and the rate constants  $k_{cis \rightarrow trans}$  or  $k_{trans \rightarrow cis}$ , the residue mimetics of the form Ac-Yaa-OMe have been synthesized (Fig. 1-5), where Yaa is Pro, Hyp, hyp, Flp, or flp. Related parameters can be found in Table 1-3 showing the effect of 4(*R*)- and 4(*S*)- substituents of Pro residues on the conformational stability of triple helical collagen (Bretscher, L.E., et al. 2001). The presence of electron-withdrawing atoms on the proline ring significantly affects the *cis/trans* equilibrium of the preceding peptide group, with *trans* isomer stabilized by 4(*R*) substituents and *cis* isomers by 4(*S*) substituents.

**Table 1-3** Effect of 4(*R*) and 4(*S*) substituents of Pro residues on the conformational stability of triple helical collagen and on related parameters.

Yaa	Ac-Yaa-OMe		triple-helical (Pro-Yaa-Gly) <sub>7</sub>
	$K_{trans/cis}$ <sup>a</sup>	$\nu_{ester}$ <sup>b</sup> (cm <sup>-1</sup> )	$T_m$ (°C) <sup>c</sup>
4( <i>R</i> )-fluoro-L-proline	6.7	1748	45
4( <i>R</i> )-hydroxy-L-proline	6.1	1746	36
Proline	4.6	1743	6-7 <sup>d</sup>
4( <i>S</i> )-hydroxy-L-proline	2.4	1725	< 5 <sup>e</sup>
4( <i>S</i> )-fluoro-L-proline	2.5	1754	< 2

According to ref. (Bretscher, L.E., et al. 2001). <sup>a</sup> Value of  $K_{trans/cis}$  ( $\pm 5\%$ ) were measured in D<sub>2</sub>O at 25 °C by integration of <sup>1</sup>H NMR spectra; <sup>b</sup> Value of  $\nu_{ester}$  ( $\pm 1\text{ cm}^{-1}$ ) were obtained in chloroform at 25 °C by FTIR spectroscopy with a Mattson Infinity instrument; <sup>c</sup> Values of  $T_m$  ( $\pm 1\text{ °C}$ ) were measured in 50 mM acetic acid by CD spectroscopy with an Aviv 62A DS instrument; <sup>d</sup> from ref. (Shaw, B.R. and Schurr, J.M. 1975); <sup>e</sup> Reported for (Pro-hyp-Gly)<sub>10</sub> in ref. (Inouye, K., et al. 1976).

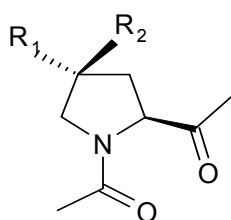


**Fig. 1-5** Definition of structural parameters for proline derivatives

$R_1 = \text{H}, R_2 = \text{H}$	<i>N</i> -acetyl-proline methyl ester
$R_1 = \text{OH}, R_2 = \text{H}$	<i>N</i> -acetyl-(4 <i>R</i> )-hydroxyl-proline methyl ester
$R_1 = \text{H}, R_2 = \text{OH}$	<i>N</i> -acetyl-(4 <i>S</i> )-hydroxyl-proline methyl ester
$R_1 = \text{F}, R_2 = \text{H}$	<i>N</i> -acetyl-(4 <i>R</i> )-fluoro-proline methyl ester
$R_1 = \text{H}, R_2 = \text{F}$	<i>N</i> -acetyl-(4 <i>S</i> )-fluoro-proline methyl ester
$R_1 = \text{F}, R_2 = \text{F}$	<i>N</i> -acetyl-(4)-diF-proline methyl ester

The FT-IR spectra of fluoroprolines containing substrates show that fluoro-derivatives caused a blue shift of the amide-I band (C=O stretching) as compared to that of Ac-Pro-OMe (Table 1-3). The similar results have also been observed by Renner et al. (Renner, C., et al. 2001), where Ac-(4)-diF-Pro-OMe caused a even larger blue shift as compared to Ac-(4*R*)-FPro-OMe and Ac-(4*S*)-FPro-OMe. The strengthening of the C=O bond accompanies weakening the double-bond character of the Ac-Pro amide bond. This inductive effect was caused by the electron withdrawing group fluorine, thus increased the stretching frequency of the carbonyl group (Eberhardt, E.S., et al. 1996).

The introduction of fluorine substituent(s) at position 4 of L-Pro, realized in the two diastereomeric compounds (4*S*)-F-Pro and (4*R*)-F-Pro, and in the (4)-diF-Pro, implicates only minor changes of steric requirements, but rather the introduction of the most electronegative atom causing a large inductive effect and influencing the ring pucker of the surrogate and the *cis/trans* isomerization.

There are data available from NMR measurements on the thermodynamics of the N-acetyl-proline-methylesters (Ac-Pro-OMe) of the respective (4)-fluoroproline derivatives showing varying ground state energy differences of the corresponding *cis* and *trans* conformers and of the activation parameters of the interconversion between them (Renner, C., et al. 2001). The reasons for  $K_{trans/cis}$  and rate constant differences between 4(*R*)- and 4(*S*)-substituents of Pro are mainly due to the *gauche* effect, that the (4*R*)-derivative shows an intrinsic preference for  $\gamma$ -*exo* puckering, the (4*S*)-derivative for  $\gamma$ -*endo* puckering (Bretscher, L.E., et al. 2001, DeRider, M.L., et al. 2002, Eberhardt, E.S., et al. 1996, Improta, R., et al. 2001, Vitagliano, L., et al. 2001).

Fluoroprolines are nowadays causing much attention, because  $^{19}\text{F}$  has excellent magnetic resonance properties (Gerig, J.T. 1994), and fluorinated amino acids are nearly isosteric to their natural counterparts and are equally (or more) chemically inert (Kukhar, V.P. 1994).  $^{19}\text{F}$  NMR spectroscopy has played a key role and become a useful tool for investigating structures and dynamics of fluorinated proteins or peptides. The correlations between the thermodynamics of the *cis/trans* isomerization of fluorinated prolines and the stability of the related *de novo* synthetic collagen (Bretscher, L.E., et al. 2001) or the protein mutants such as fluorinated prolines substitution of Pro<sup>48</sup> in barstar C40A/C82A/P27A denoted barstar pseudo-wildtype (b\*pwt) (Renner, C., et al. 2001) have also been well characterized. The results suggest that fluorination of proline substructures in peptides and proteins may provide new means of changing protein stability and thermodynamics, engineering protein assembly, and rationally strengthening receptor-ligand interactions.



spectroscopy has become a useful tool for investigating structures and dynamics of fluorinated peptides. The study of the properties of peptides containing (4)-fluoroproline substitutions would provide preliminary experimental data and accumulate experience for further introducing fluorinated amino acids into Janus-peptide pairs on solid support for  $^{19}\text{F}$  NMR investigation. We would expect the identification of peptide bond conformations of matrix-bound oligopeptides using dynamic  $^{19}\text{F}$  NMR spectroscopy in the presence of catalytic amounts of PPIases. Any approach developed, based on the idea of matrix-bound peptide-peptide interactions in modeling protein-protein interactions could become useful proteomic tools for analyzing the interaction sites of protein complexes. Because, in such case, the mapping of protein-protein interaction sites would not necessarily rely on the availability of native-state proteins, but only needs the primary sequences of the interacting proteins, which are easily obtainable in postgenomic era.

## 2 Results and discussion

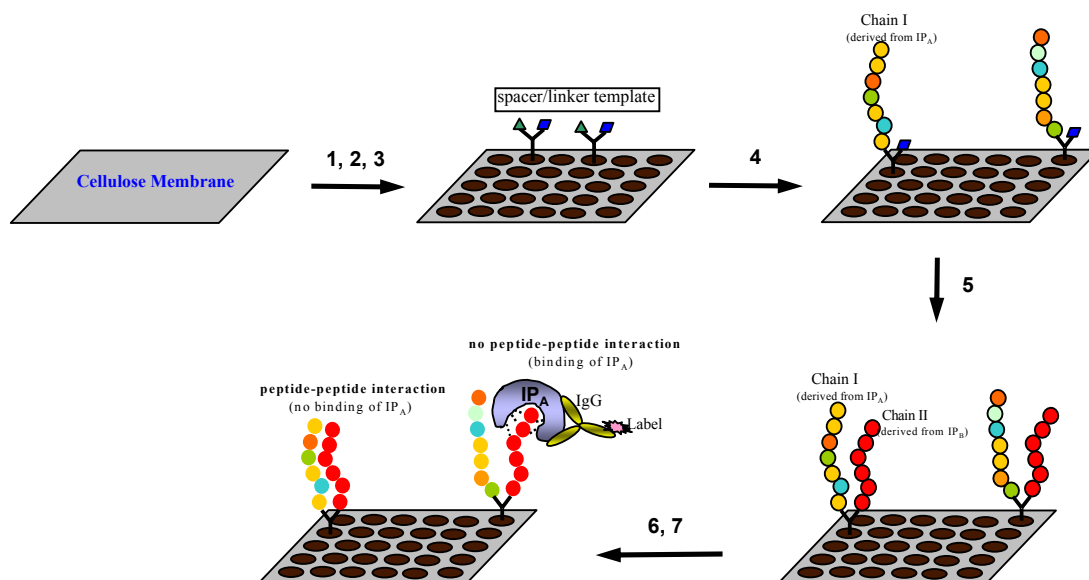
### 2.1 Prerequisites relating to Janus-peptide arrays by SPOT synthesis

#### 2.1.1 Scheme of screening matrix-bound peptide-peptide interaction in mapping protein-protein interaction sites — Janus-peptide array

The Janus-peptide array uses a bifunctional template anchored to a predefined spot on a planar surface with two amino function groups protected by two building blocks that can be selectively deprotected. Therefore, two different peptide chains can be synthesized sequentially. The schematics of the Janus-peptide array have been clearly depicted in [Scheme 2-1](#). To clarify potential application of the principle of Janus-peptide array, first we make an assumption that: 1) two interacting partners,  $IP_A$  (a protein) and  $IP_B$  (either a protein or a ligand to  $IP_A$ ) have interactions, and 2) only protein  $IP_A$  and its antibody are available in substance, but protein  $IP_B$  is not. The binding epitopes on protein  $IP_B$  to  $IP_A$  can be found by screening peptide scan of protein  $IP_B$  for binding of  $IP_A$ , using standard SPOT technology as illustrated in [Fig. 1-2](#). However, the detection of the contact sites on protein  $IP_A$  to protein  $IP_B$  has to use Janus-peptide array approach. The Janus-peptide array can be prepared by synthesis of a peptide scan derived from protein  $IP_A$  to chain I position, while chain II position can be synthesized with constant peptide epitopes derived from protein  $IP_B$ .

Afterwards, the prepared Janus-peptide membrane is incubated to equilibrium with protein  $IP_A$ . Binding of  $IP_A$  has to be probed either directly on Janus-peptide membrane or based on Western blot assay after transferring of the bound  $IP_A$  to a nitrocellulose membrane. The analysis of peptide-peptide interactions is based on the competition mechanism. The probe protein  $IP_A$  used for binding analysis has interaction with the constant peptide chain II (peptide epitope on protein  $IP_B$ ). When peptide chain I (scan of protein  $IP_A$ ) also has interaction with this invariable peptide chain II anchored on the same template, there exists competition between probe  $IP_A$  and peptide chain I derived from  $IP_A$  to the constant peptide chain II. It is reasonable to assume that once two peptides on one template have interaction the binding accessibility of protein  $IP_A$  to the constant peptide chain II might be perturbed, corresponding to weak signals observed by analysis of binding of protein  $IP_A$ . Through semi-

quantification of signals obtained from the binding assay, it is possible to determine which peptide pairs may have interactions and further depict the interaction sites of protein complexes. The related results of this part of work are described in sections 2.1 – 2.4.



**Scheme 2-1** Principle of Janus-peptide array in the screening of peptide-peptide interactions. 1) Membrane functionalization; 2) Spacer/linker attachment; 3) Template with two amino functions protected by Fmoc (▲) and Dde (■) protecting groups was introduced; 4) Deprotection of Fmoc group (20 % piperidine/DMF) and synthesis of the first peptide chain (variable sequence) onto template by SPOT synthesis; 5) Deprotection of Dde group (2 % hydrazine/DMF) and synthesis of the second peptide chain (constant sequence); 6) Deprotection of all side chain protecting groups (50 % TFA/DCM); 7) Solid phase screening assay by Western blot analysis.

Note: IP<sub>A</sub> and IP<sub>B</sub> are two interacting partners. IP<sub>A</sub> represents a protein, while IP<sub>B</sub> could be either a ligand or a binding protein to IP<sub>A</sub>.

### **2.1.2 Amino group loading on planar polymeric supports**

The polymeric support needs to be first chemically derivatized to introduce suitable anchor functions for peptide synthesis at the spot position. Cellulose filter membrane (Whatman, England) was modified by esterification of hydroxyl group with Fmoc- $\beta$ -Ala-OH activated by DIC (Frank, R. 1992), and then converted to amino functions by removal of N<sup>α</sup>-Fmoc protecting group. The amount of amino functions generated was determined by Fmoc deprotection with freshly prepared 20 % piperidine in DMF for 30 min and the measurement of the UV absorbance of the released dibenzofulvene/piperidine adduct ( $\epsilon_{301} = 7800 \text{ M}^{-1} \cdot \text{cm}^{-1}$ ) (Fields, G.B. and Noble, R.L. 1990, Fields, G.B., et al. 1992, Scharn, D., et al. 2000). Thus, the loading of the amino-functionalized cellulose membrane was determined, and each membrane has a loading range of 100 ~ 120 nmol/cm<sup>2</sup> of amino functions. The polypropylene membrane used, so called APEG-Amino-PP (AIMS Scientific Products GmbH, Germany), has modified amino-functional groups on the surface with the loading of about 60 ~ 80 nmol/cm<sup>2</sup>. The membranes used in the following experiments are mostly cellulose filter membrane unless being mentioned specifically.

### **2.1.3 Peptide quality on planar polymeric supports**

The quality of immobilized peptides on planar membrane is of great importance for getting reliable results from the subsequent chemical or biological screening based on these peptides. In contrast to synthesis of free peptides by SPPS, it is not possible to characterize purified peptides when they are attached to the solid supports. Higher yields of correct sequences can be obtained by prolonging the reaction time and acceleration of the reaction rate that can be obtained by the use of nonvolatile solvent and higher concentration of activated amino acids in SPOT strategy. Twenty natural amino acid Pfp or Dhbt esters are dissolved in DMF or NMP to a concentration of 0.3 M. DMF (b.p. 153 °C) or NMP (b.p. 203 °C) is often used as solvent because of the low volatility. The different coupling times (either 2 or 4 times) of each cycle for elongating peptides on cellulose were studied and the synthesis quality was evaluated by mass spectrometry analysis of model peptides synthesized (Fig. 2-1). Due to the introduction of the specific linkers, such as acid-labile Rink linker or photolabile nitrobenzyl-based linker (Guillier, F., et al. 2000) between peptides and membrane, peptides can be easily released from membranes for identification.

In some cases, it is apparent that each amino acid coupled only for two times might not be enough, especially for peptide sequences containing aromatic amino acids and prolines, or amino acids with a large side chain protecting group, such as Fmoc-His(Trt) or Fmoc-Arg(Pbf). The amino acids preceding proline are often difficult to be coupled to imide group since proline is prone to form a turn structure where the free imide function might not be freely accessible, unless the solid support could be swollen thoroughly (Fields, G.B., et al. 1992). As shown in Fig. 2-1 (panel A), the peptide Ac-PSRDPHYQDPHST-NH<sub>2</sub> in a 2-time coupling experiment gives dominantly the molecular mass of 1325.79 (missing one His and one Asp), and the mass of 1440.84 (missing one His), however the correct molecular mass 1577.88 of the peptide only shows a minor signal. In comparison with a 4-time coupling experiment, the same peptide shows a correct molecular mass of 1577.95 in dominant (Fig. 2-1, B).

In most cases, 4-time coupling of each amino acids can render the reaction to more than 95% completeness, and the residual amino functions on each spot are then blocked by acetylation (with 5% acetic anhydride in DMF for 30 min, using DIEA to adjust pH to 8 ~ 10). After the coupling of the last amino acids to the peptide chains and the subsequent removal of the N<sup>α</sup>-Fmoc protecting group, the free N<sup>α</sup>-amino groups are blocked by acetylation. The immobilized free peptides can be available by treatment with TFA to remove all the side-chain protecting groups (with 50 % TFA, 2 % triisobutylsilane and 2 % water in DCM (all v/v) for 3 h). The correct peptide sequences on individual spots are then in the majority (Fig. 2-1, panel C and D). It is necessary to be aware that all peptides synthesized on the polymeric supports performed in this dissertation are blocked with acetyl group.

MALDI-TOF-MS technique has been used for controlling the quality of peptides synthesized on planar surface. MALDI (Matrix assisted laser desorption ionization), a laser-based soft ionization method has been proven to be one of the most successful ionization methods for mass spectrometric analysis (Karas, M., et al. 1987). MALDI preferentially ionizes basic amino acids such as lysine or arginine containing peptides depending on the matrix used. The resulting ions are separated in the analyzer according to their mass/charge (m/z) ratios and collected by the detector. In the detector, the ions generate an electrical signal that is proportional to the number of ions and a data system records these signals and converts them into the mass spectrum. The amplitude of the mass spectrum is closely related to the degree of ionization of the observed peptides. So normally, lysine or arginine rich peptides show higher signals (amplitudes). In this regard, it is difficult to quantify the peptide amount simply depending on the amplitude of the mass got from MALDI-TOF-MS.

However, once peptides contain the same amount of basic amino acids, it is possible to judge the amounts of peptides by comparing the ratios of the amplitudes of the mass between different components. Based on this principle, it is apparent that the amounts of the correct peptides are higher by using 4-time coupling strategy than in the case of 2-time coupling.

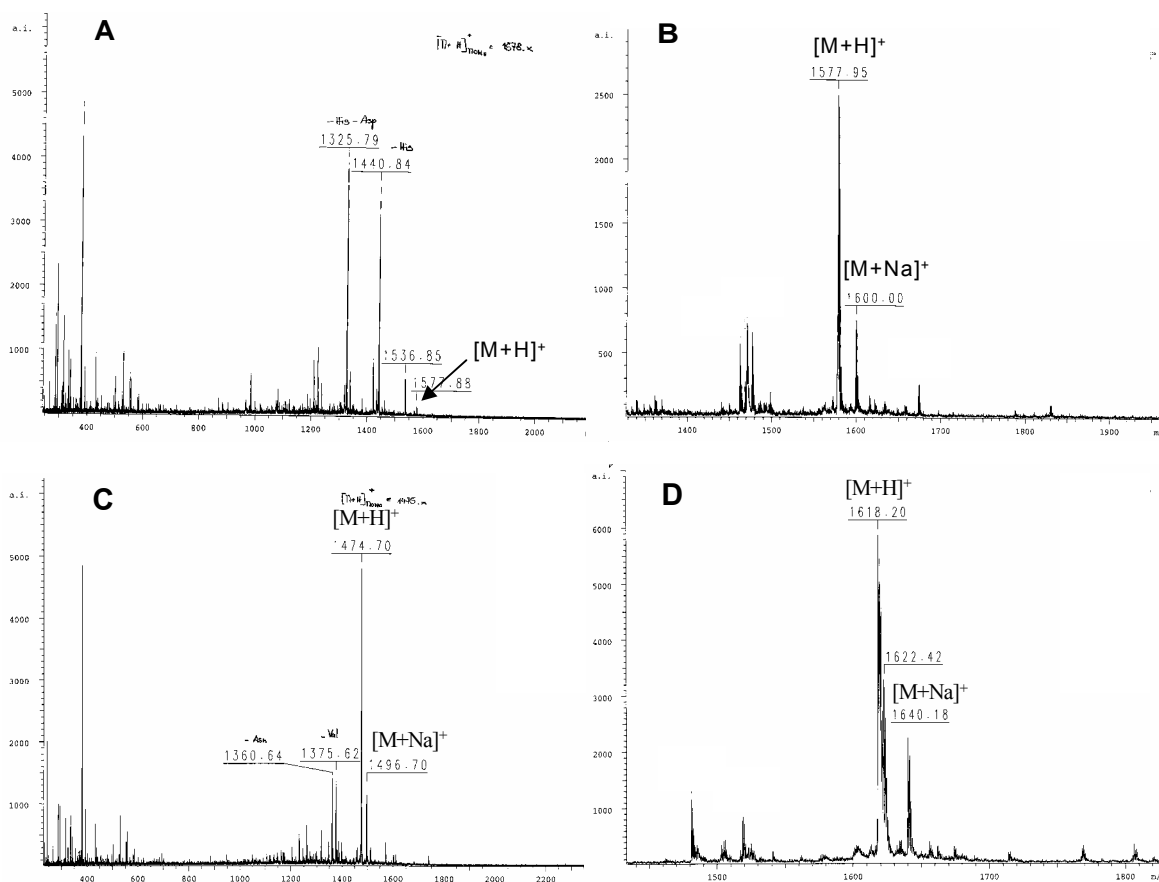


**Fig. 2-1** MALDI-TOF-MS analysis of several peptides after cleavage from cutout spots on cellulose. The analyzed peptides are immobilized on the planar surface via acid labile linker (Rink linker) and can be released from cellulose by TFA treatment to form a C-terminal amide. **(A)** MALDI-TOF-MS spectrum of peptide Ac-PSRDPHYQDPHST-NH<sub>2</sub> (theor. 1577.5) by coupling each amino acid two times. **(B)** MALDI-TOF-MS spectrum of peptide Ac-PSRDPHYQDPHST-NH<sub>2</sub> (theor. 1577.5) by coupling each amino acid four times **(C)** MALDI-TOF-MS spectrum of peptide Ac-PVYHNQPLNPAPS-NH<sub>2</sub> (theor. 1474.5) by coupling each amino acid four times. **(D)** MALDI-TOF-MS spectrum of peptide Ac-RIQTHQSDVWSYG-NH<sub>2</sub> (theor. 1619.6) by coupling each amino acid four times.

### 2.1.4 Templates used in Janus-peptide arrays

Based on the principle of Janus-peptide array as described in section 2.1.1, two different templates are synthesized and introduced to the defined spots on the membranes via a  $(\beta\text{-Ala})_2$  spacer. Both templates contain two amino functional groups protected by two building blocks, Fmoc and Dde that can be selectively deprotected. The Fmoc group can be deprotected by 20 % piperidine in DMF and the Dde group can be cleaved by 2 % hydrazine in DMF (Bycroft, B.W., et al. 1993). The structures of these templates are shown in Fig. 2-2.

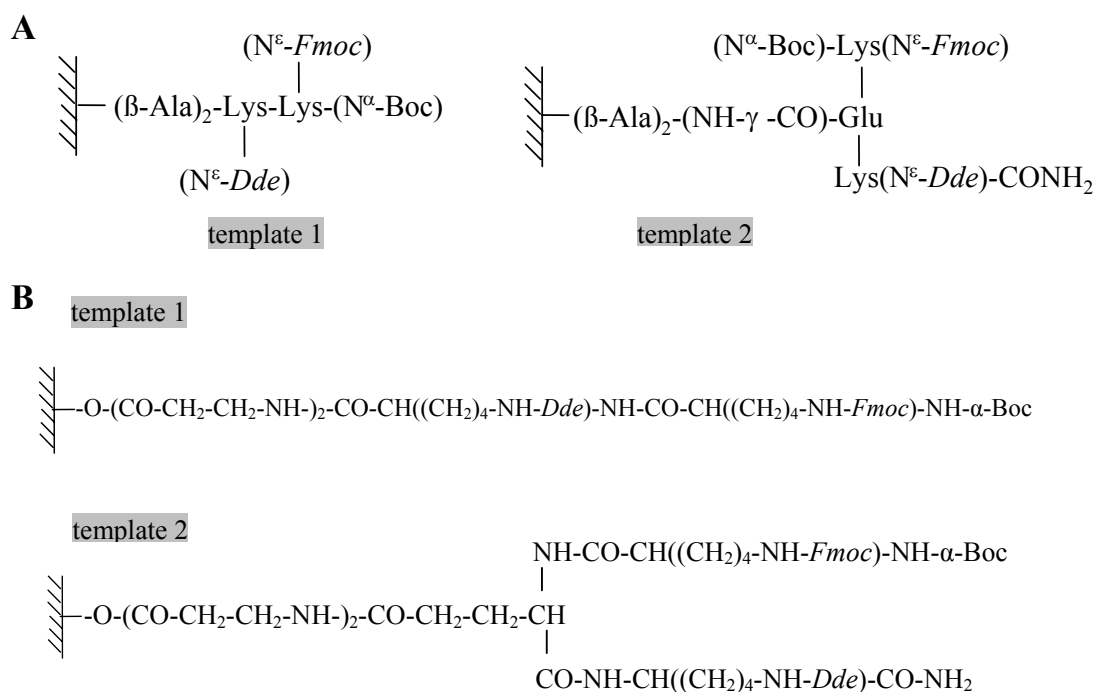


**Fig. 2-2** Templates used in the Janus-peptide arrays. **(A)** Structures of two different templates used in Janus-peptide arrays are attached to the membrane surface via two  $\beta\text{-Ala}$  amino acids as spacer. Both templates contain two different orthogonally protected Lys derivatives which are protected by Fmoc and Dde at  $\epsilon$ -amino group respectively. **(B)** Structure image of the peptide core of the templates.

Template 1 can be easily introduced through stepwise 2-time coupling of Fmoc-Lys(Dde)-OH and Boc-Lys(Fmoc)-OH to  $(\beta\text{-Ala})_2$  spacer on membrane, and the amino acid derivatives (0.3 M) are activated by PyBOP (0.3 M) in DMF containing DIEA (10%, v/v) as a base. Template 2 was prepared by solid phase synthesis of Fmoc-Glu(OtBu)-Lys(Dde)-Rink amide MBHA resin, followed by splitting Fmoc-Glu-Lys(Dde)-CONH<sub>2</sub> from resin by TFA with scavenger for 1 hr at room temperature. The purified Fmoc-Glu-Lys(Dde)-CONH<sub>2</sub> (0.3

M) was activated on  $\gamma$ -carboxyl group of Glu by PyBOP (0.3 M) in DMF with DIEA (10%, v/v) and then coupled to ( $\beta$ -Ala)<sub>2</sub> spacer on membrane. After cleavage of Fmoc group and coupling with Boc-Lys(Fmoc)-OH activated by PyBOP, template 2 was introduced onto the membrane and was ready for synthesis of array of Janus-peptide pairs. The amount of both peptides on different sites of the template can be measured and controlled by UV absorbance of the released Fmoc described in section 2.1.2. The quantification of Dde site can be simply determined using the same strategy after deprotection of Dde protecting group and coupling of first Fmoc protected amino acid. Since the efficiency of peptide synthesis is largely depending on the actual primary sequences of different peptides, it is not possible to perform the synthesis of various peptides in the same amounts. However, by increasing the coupling times of each amino acids and using higher concentrations up to 0.3 M of activated amino acid derivatives, the potential differences can be minimized.

## **2.2 The examples of protein-peptide interaction**

### **2.2.1 Example I: Streptavidin/*Strep*-tag II interaction**

To establish a new method for screening protein-protein/ligand interaction sites, known protein-ligand or protein-protein interacting combinations were selected to investigate the feasibility and reliability of the Janus-peptide array.

The interaction between streptavidin and *Strep*-tag II peptide has been well studied. The interacting interface and the key residues involved in binding have been clearly elucidated by X-ray crystallographic analysis (Schmidt, T.G., et al. 1996). Therefore, the mapping of interaction sites between streptavidin and *Strep*-tag II peptide was used as the first model for establishing and further evaluating the new method for analysis of peptide-peptide interactions on cellulose, known as Janus-peptide array.

The *Strep*-tag is a nine-amino acid peptide (NH<sub>2</sub>-AWRHPQFGG-COOH). It was selected from a random peptide library as an artificial ligand for the well-known protein reagent streptavidin (Schmidt, T.G. and Skerra, A. 1993) and has been used as an affinity tag for recombinant proteins. The variant *Strep*-tag II peptide (NH<sub>2</sub>-SNWSHPQFEK-COOH) was found by screening for a peptide with a higher affinity to streptavidin by employing a synthetic peptide spot assay (Schmidt, T.G., et al. 1996). The binding affinities of *Strep*-tag

and *Strep*-tag II to streptavidin measured by isothermal titration calorimetry revealed a  $K_d$  of 37  $\mu$ M and 72  $\mu$ M respectively. When immobilized on cellulose, *Strep*-tag II gave rise to significantly tighter binding of streptavidin than *Strep*-tag presented under identical conditions (Schmidt, T.G., et al. 1996), because C-terminal -COOH is important for the interaction, and the side chain of Glu near C-terminus of *Strep*-tag II has compensated for the missing of -COOH in *Strep*-tag due to attached to the solid support. Therefore, *Strep*-tag II is more suitable for studying in this work. The crystal structure of the complex between recombinant core streptavidin and the synthesized peptide showed that *Strep*-tag II sequence interacted with a part of streptavidin surface that was very close to the binding pocket of its natural ligand, biotin (Wilchek, M. and Bayer, E.A. 1989). The applications of *Strep*-tag affinity peptides in detection and purification of recombinant proteins are well known (Skerra, A. and Schmidt, T.G. 2000). Based on all the information available in literatures about *Strep*-tag II peptide, it seems to be very suitable for being introduced into Janus-peptide array system as a model system to portrait the molecular recognition properties between streptavidin and *Strep*-tag II peptide based on exploring peptide-peptide interactions by using Janus-peptide array.

### 2.2.1.1 Self-recognition in streptavidin subunit association

Before starting the screening, some control experiments had to be considered. It has to be known, whether the overlapping peptides from streptavidin can be recognized by streptavidin (sequence in [Fig. 2-3](#)) itself, and that which templates are appropriate to give a high signal to noise ratio in a reproducible manner.

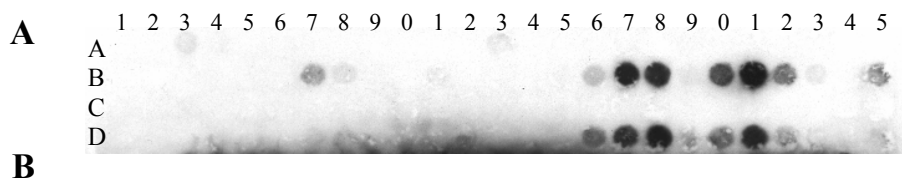
#### **Streptavidin sequence**

1	11	21	31	41	51
DPSKDSKAQV	SAAEAGITGT	WYNQLGSTFI	VTAGADGALT	GTYESAVGNA	ESRYVLTGRY
DSAPATDGSG	TALGWTVAWK	NNYRNAHSAT	TWSGQYVGGA	EARINTQWLL	TSGTTEANAW
KSTLVGHDTF	TKVKPSAASI	DAKKAGVNN	GNPLDAVQQ		

**Fig. 2-3** The sequence of streptavidin (Swiss-Prot: P22629) used in the immobilized peptide scan experiment. The signal sequence is not included here.

First, we synthesized only one peptide chain on each template with series of 12-mer peptides shifted by 3 amino acids spanning the complete streptavidin sequence (so called peptide scan of streptavidin). Since each template contains two amino functions protected by Fmoc group and Dde group, respectively (Fig. 2-2), the oligopeptides were synthesized at either the Fmoc or the Dde site of the template. The peptide membrane was probed by streptavidin and followed by electrotransfer of the bound streptavidin to nitrocellulose membrane. After incubation with anti-streptavidin antiserum and anti-rabbit IgG peroxidase conjugate, the visualization was performed by chemiluminescent reaction enhanced by ECL system (see materials and methods). The results are shown in Fig. 2-4 (panel A) for peptide scan synthesized either on the Fmoc site (row A-B) or on the Dde site (row C-D).

Only several spots give signals indicating that streptavidin binds to some peptide fragments derived from it (Fig. 2-4, A), and most other oligopeptides do not interact with streptavidin by Western blot analysis. The result is not unexpected, because natural streptavidin exists in a tetrameric form and His<sup>127</sup> which marked in bold from adjacent subunits is in close proximity (3.1 Å) to each other in natural streptavidin and locates in the subunit association interface (Reznik, G.O., et al. 1996, Sano, T., et al. 1997). Therefore, the peptide sequences found in this experiment might contribute to the subunit association.



Spot No. (positives)	The corresponding sequence of the spots	Location in streptavidin
B17 & D17	LVGHDTFTKVKP	Leu <sup>124</sup> – Pro <sup>135</sup>
B18 & D18	<b>H</b> DTFTKVKPSAA	His <sup>127</sup> – Ala <sup>138</sup>
B20 & D20	VKPSAASIDAAK	Val <sup>133</sup> – Lys <sup>144</sup>
B21 & D21	SAASIDAAKKAG	Ser <sup>136</sup> – Gly <sup>147</sup>

**Fig. 2-4** Streptavidin binds to several peptide fragments derived from it. **(A)** Peptide scans (12-mers with a 3-amino-acid shift) of streptavidin were synthesized on cellulose membrane to Fmoc site of template 1 (rows A-B), or to Dde site of template 1 (rows C-D) respectively. In both cases no secondary peptide chains were coupled to another free site, instead the free functional groups were acetylated. The peptide scans were probed by streptavidin (100 nM) and detected by Western blot analysis (see methods). The positive signals indicate streptavidin can interact with some fragments derived from it with the sequences given above. **(B)** The corresponding sequences of the visible spots and their locations in streptavidin are tabulated.

### *2.2.1.2 Mapping binding epitopes on streptavidin to Strep-tag II by Janus-peptide arrays*

In order to analyze the binding sites of streptavidin involved in the interaction to its ligand, *Strep-tag II* peptide, our Janus-peptide array (depicted in [Scheme 2-1](#)) has been used by exploring peptide-peptide interactions on cellulose to map the binding epitopes.

Series of 12-mer peptides spanning the complete streptavidin sequence with a 3-amino-acid shift were synthesized to one site of template 1 on the defined spots on cellulose, and afterwards *Strep-tag II* peptide is synthesized to the other site of the same template. The location order of two peptide chains on one template has two possibilities, being coupled either to the Fmoc site or to the Dde site. Such situation has been considered and the experiments have been practically performed ([Fig. 2-5](#)). Afterwards, the cellulose membrane was probed by streptavidin (100 nM) and the bound streptavidin was electrotransferred to nitrocellulose membrane. The detection was performed based on anti-rabbit IgG peroxidase conjugate recognizing anti-streptavidin antiserum bound to streptavidin on nitrocellulose. The visualization of the signals was performed by ECL Western blotting detection system.

The Janus hypothesis assumes that two peptides representing the linear interacting epitopes of proteins synthesized on one solid support are able to interact. If *Strep-tag II* interacts with a peptide derived from streptavidin, this peptide-peptide interaction of the matrix-bound Janus-peptide pairs would be detectable taking advantage of the higher densities of the anchored peptides on each spot. Thus, the potential binding of *Strep-tag II* to soluble streptavidin probe should be decreased due to the existence of competitive interactions between the neighboring immobilized peptide epitope derived from streptavidin and the soluble streptavidin probe to *Strep-tag II*. So a possible interaction between two peptide chains would be indicated by a less pronounced binding of streptavidin. According to the conditions of the experiments, a weaker signal during Western blot analysis can be expected.

There are two regions marked with pink underline and light blue underline respectively, give prominent and continuous weak signals in [Fig. 2-5](#). The same result patterns have been found both in panel A and B by using template 1, denoting that the location order of the peptide pair on certain template would not influence the result output significantly. Based on our hypothesis, the results indicated that there exist interactions between two peptide chains on the spots that gave weak signals. Therefore it can reveal the potential interacting epitopes of streptavidin in binding to *Strep-tag II* peptide. The corresponding sequences of these two regions have been shown in [Fig. 2-5](#) (panel C).

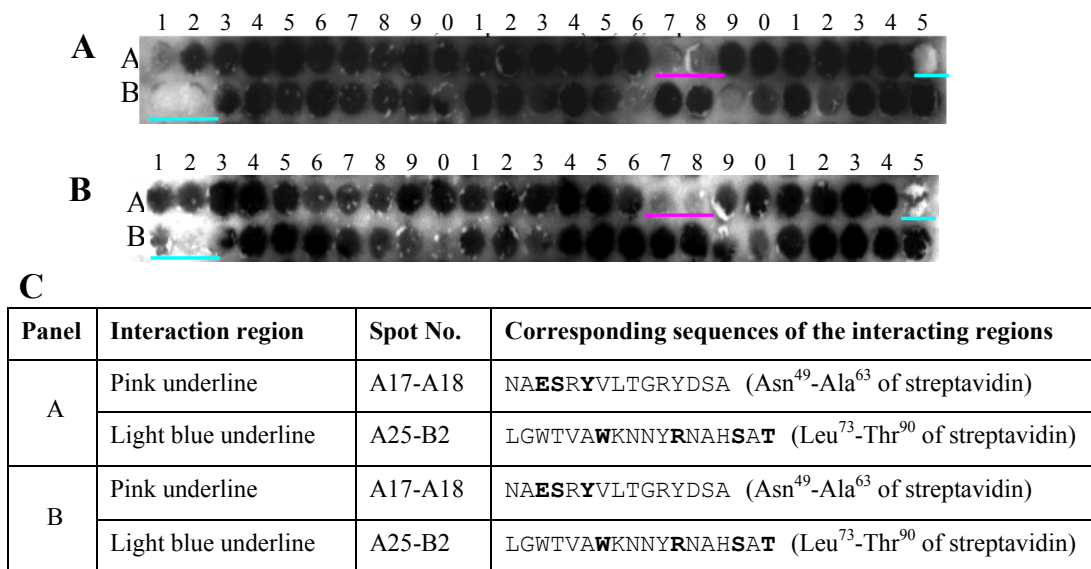


**Fig. 2-5** The interactions between 50 Janus-peptide pairs consist of overlapping dodecapeptides derived from streptavidin and *Strep*-tag II. The peptide membrane was probed by streptavidin (100 nM) and followed by Western blot analysis (see methods). **(A)** Peptide scans (12-mers with a 3-amino-acid shift) of streptavidin were synthesized on Fmoc site of template 1 while *Strep*-tag II peptide was coupled to Dde site. **(B)** Peptide scans (12-mers with a 3-amino-acid shift) of streptavidin were synthesized on Dde site of template 1 while *Strep*-tag II peptide was coupled to Fmoc site. **(C)** The corresponding sequences of the interacting regions are tabulated.

Interestingly, they represent segments of streptavidin shown to be in close proximity to *Strep*-tag II in the X-ray structure (Schmidt, T.G., et al. 1996). They include the key amino acids which are involved in the intermolecular contacts through hydrogen bonds between streptavidin and the bound *Strep*-tag II, such as Glu<sup>51</sup>, Ser<sup>52</sup>, Tyr<sup>54</sup> of the flexible loop in streptavidin, and Arg<sup>84</sup>, Ser<sup>88</sup>, Thr<sup>90</sup> (Schmidt, T.G., et al. 1996). These important amino acids are shown in bold (Fig. 2-5). *Strep*-tag II binds specifically to streptavidin and occupies the same pocket with which biotin is normally complexed. So the key amino acids such as Trp<sup>79</sup>, Trp<sup>108</sup>, and Trp<sup>120</sup> involved in biotin binding (Chilkoti, A., et al. 1995) might also play an important role in *Strep*-tag II binding. Here Trp<sup>79</sup> (in bold) has been found by Janus-peptide array. Since the low signal variation in this Janus-peptide array assay has been observed (Fig. 2-5), it is difficult to judge the differences of the spots with similar strong signal intensities. This problem can be solved either by densitometry analysis of each spots or by optimizing the experimental conditions to obtain a larger signal variation, such as using different template or optimizing the concentrations of antibody and the probe protein.

ECL Western blotting analysis system has been used for the detection and visualization of the signals in the experiments. It is known that Hyperfilm ECL exhibits a linear response to the light produced from enhanced chemiluminescence. This relationship can be used for the quantification of proteins analyzed by ECL Western blots according to the manual book in the ECL Western blotting detection kit (Amersham Pharmacia Biotech). So the signal intensity of each spots observed is direct proportion to the amount of the bound protein. However, saturation of the signal intensity should be considered which could be prevented by optimizing the Western blot conditions, like decreasing the amount of the antibodies used. In this regard, the discrimination of the interacting peptide pairs from non-interacting peptide pairs in Janus-peptide array assay is based on the signal intensity obtained. So the weaker signal observed corresponds to the potential interaction between two peptide chains on the template on solid support.

### *2.2.1.3 Biotin blocks the binding of streptavidin to Strep-tag II in Janus-peptide array*

To evaluate the specificity of Janus-peptide array in streptavidin/*Strep*-tag II interaction, the natural ligand of streptavidin, biotin, has been used as an inhibitor. At first, streptavidin was incubated with biotin in a molar ratio of around 1:8 for 1 hr at room temperature. Subsequently, the mixture was used to probe the Janus-peptide membranes (same membranes as used in [Fig. 2-4](#) and [Fig. 2-5](#) after regeneration), followed by Western blot assay.

From the results shown in [Fig. 2-6](#) (panel B), we obtained a binding pattern comparable to the binding pattern in the complete absence of *Strep*-tag II ([Fig. 2-4](#), A). It is clear that biotin has blocked the interaction between streptavidin and *Strep*-tag II. The visible signals got in [Fig. 2-6](#) indicate, that biotin is not able to block the binding of streptavidin to epitopes derived from its own sequence. It is already well known, that the subunit association of streptavidin is not influenced by biotin (Hendrickson, W.A., et al. 1989, Sano, T., et al. 1997, Weber, P.C., et al. 1989). Thus, this experiment shows that streptavidin has the same or at least the similar binding pocket to biotin as well as *Strep*-tag II, which is in good agreement with the known conclusions in the literature (Schmidt, T.G., et al. 1996).

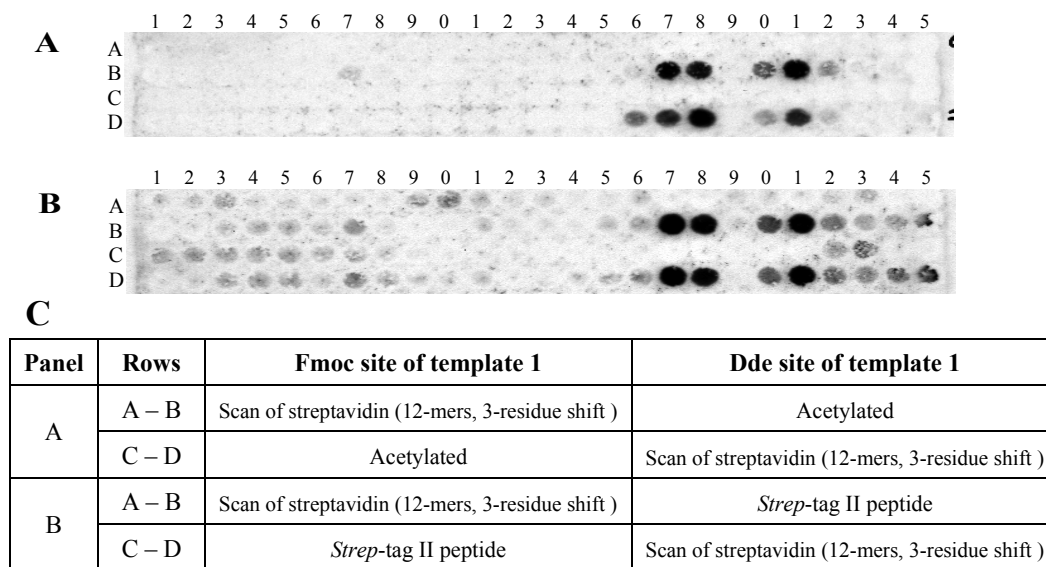


**Fig. 2-6** Biotin blocks the binding of streptavidin to *Strep*-tag II peptide. Janus-peptide arrays (fragments of streptavidin and *Strep*-tag II pairs) were probed by streptavidin and biotin complex. Streptavidin (60  $\mu$ g) was pre-incubated with Biotin (6  $\mu$ g) in MP buffer (see materials) for 60 min. Then the complex was used as probe to perform standard Western blot analysis as described in methods section. **(A)** On the template each spot, only one site is synthesized with oligopeptides of streptavidin scan. **(B)** On the template each spot, both sites are synthesized with oligopeptides derived from streptavidin and *Strep*-tag II respectively. **(C)** The different Janus-peptide array patterns are given in the table.

#### 2.2.1.4 Comparison of two different templates used for Janus-peptide arrays

Two different templates (Fig. 2-2), template 1 and template 2, have been introduced in Janus-peptide arrays. They are evaluated by using the streptavidin/*Strep*-tag II model system. As shown in Fig. 2-7, array of Janus-peptide pairs, peptide scans of streptavidin (12-mer peptides with a 2-amino-acid shift) and *Strep*-tag II pairs, have been synthesized on cellulose by using template 1 (panel A) and template 2 (panel B). The peptide membranes were probed with streptavidin (100 nM). Under the parallel Western blot analysis conditions, the visible result patterns are similar using both templates (Fig. 2-7, panel A and B). Continuous spots with weak signals are concerned. Some differences have been observed between panel A and B that two regions of spots (spots A10-A12 and C1-C2) in panel B show prominently weak signals while not in panel A. Other three regions of spots with weak signals are all detected in both cases, two of them had already been observed as shown in Fig. 2-5. The corresponding sequences are shown in the table of Fig. 2-7 (panel C). The key amino acids (Chilkoti, A., et

al. 1995, Schmidt, T.G., et al. 1996) either existing in the ligand binding pocket like Trp<sup>79</sup> and Trp<sup>120</sup>, or involved in hydrogen bonds formed between streptavidin and the bound *Strep*-tag II, such as Asn<sup>23</sup>, Ser<sup>27</sup>, Ser<sup>45</sup>, Ala<sup>46</sup>, Val<sup>47</sup>, Glu<sup>51</sup>, Ser<sup>52</sup>, Tyr<sup>54</sup>, Arg<sup>84</sup>, Ser<sup>88</sup> and Thr<sup>90</sup> are marked in bold. It seems successful that most of the important amino acids involved in the binding interfaces of streptavidin to *Strep*-tag II have been found by Janus-peptide array.

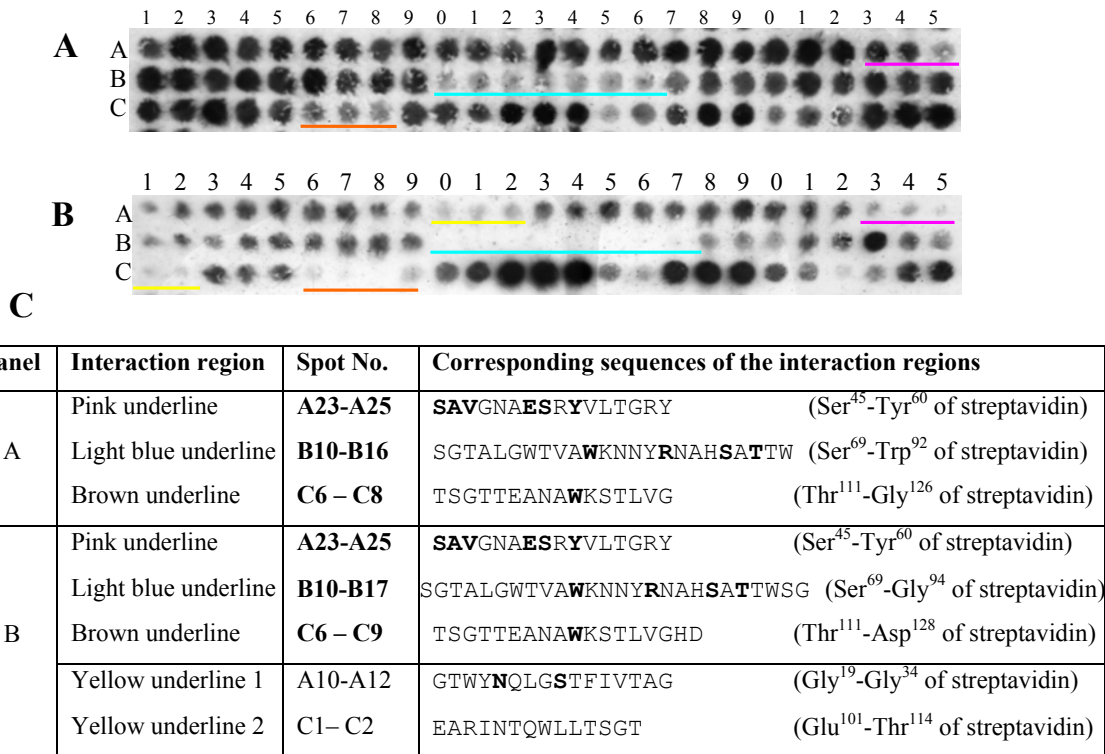


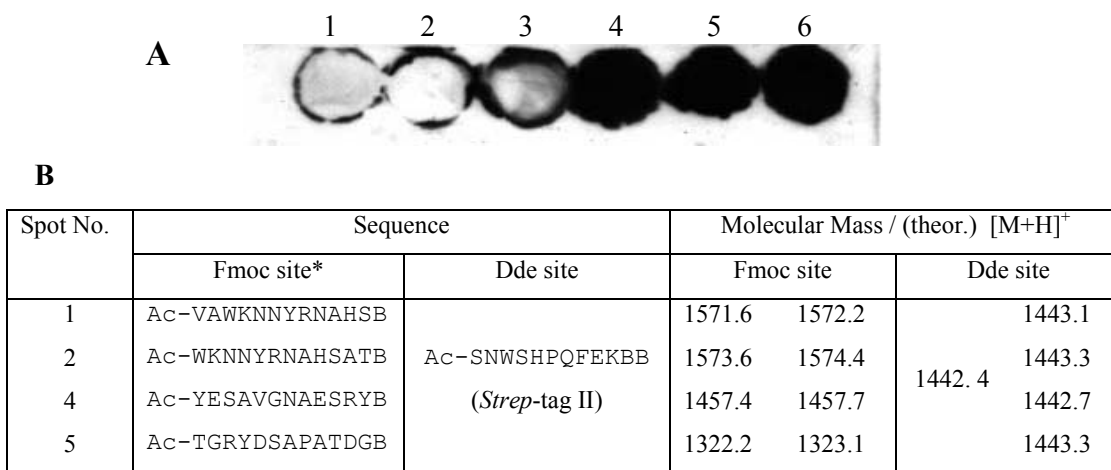
**Fig. 2-7** Comparison of two different templates used in Janus-peptide array. Analysis of the interactions between 75 Janus-peptide pairs (overlapping dodecapeptides derived from streptavidin and *Strep*-tag II peptide) using different templates. The Janus-peptide membranes were probed by streptavidin (100 nM) and followed by Western blot analysis. **(A)** Peptide scans (12-mers with a 2-amino-acid shift) of streptavidin were synthesized on Fmoc site and *Strep*-tag II peptide was coupled on Dde site using template 1. **(B)** Peptide scans (12-mers with a 2-amino-acid shift) of streptavidin were synthesized on Fmoc site and *Strep*-tag II peptide was synthesized on Dde site using template 2. **(C)** The corresponding sequences of the interacting regions are tabulated.

Another region of interest is the spots C15-C22 in both panel A and B where several spots showing weak signals. However, the correct judgement of whether peptide pairs in this region have interactions or not was disturbed by the overlay signals caused by the recognition of streptavidin to its own subunit association epitopes found in [Fig. 2-4](#).

The differences of the outputs by using these two templates are small. However, template 2 shows a high signal to noise ratio, and the ability to discover more potential interacting peptide pairs. It might be due to that template 2 has a more symmetric structure than template 1. In this respect, template 2 is preferred and has been applied in the following Janus-peptide array experiments.

### 2.2.1.5 The quality of the synthetic Janus-peptide pairs

Several peptide pairs either having interactions or not had been manually synthesized in parallel in two groups by using template 2. Both groups of peptide pairs had been attached to the template anchored on pre-defined spots through photolabile nitrobenzyl-based linker (Guillier, F., et al. 2000). All peptide pairs should be synthesized in dark conditions. One group of peptide pairs had been used to perform Western blot experiment probed by streptavidin (Fig. 2-8, panel A). While another group of peptide pairs attached to dry spots were exposed to UV light and split from solid surface with C-terminal amide peptides for MALDI-TOF mass spectrometry analysis. The relevant mass spectrometry data of the corresponding peptide pairs are shown in Fig. 2-8 (panel B).



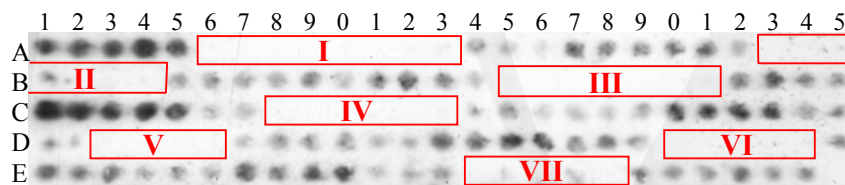
Note: \*: peptides synthesized on Fmoc site derived from streptavidin; B:  $\beta$ -Alanine.

**Fig. 2-8** Analytical data of several Janus-peptide pairs attached to the template in defined spots. **(A)** Western blot results of several peptide pairs probed by streptavidin. **(B)** Tabulated relevant MALDI-TOF-MS data of the corresponding peptide pairs.

The MALDI-TOF-MS analysis showed that the selected Janus-peptide pairs from certain spots contain two correct peptide chains immobilized on template each spot. The results from Western blot analysis probed by streptavidin (Fig. 2-8, panel A) were also reproducible compared to the results from Fig. 2-7, where spots no. 1, 2, 3, 4, 5 and 6 here corresponding to spots B14, B15, C9, A22, B4 and B5 of Fig. 2-7 (panel A or B) respectively. It was observed that spots no. 1 to 3 showed visible signals on the rim of each spots. This observation looks similar to the so-called “ring-spot” effects because of the high peptide loading already described (Kramer, A., et al. 1999). However, it was not the case here since spots 4 to 6 do not have such effects. The visible signals on the rim were due to manual synthesis of two different peptide chains and it was difficult to maintain exact control of spot size during synthesis. The spot size during synthesis of *Strep*-tag II might be larger than that during the synthesis of the other chain, or the synthesis on the rim was not complete, so that it led to such kind of “ring-spot” effect. Such kind of phenomena also cannot be completely avoided by automatic synthesis using the robot because of the slight changes in the shape of the polymeric membranes during washing and deprotection procedures.

### *2.2.1.6 Peptide length variation for the minimized binding epitopes by Janus-peptide array*

To analyze if the Janus-peptide array approach can be used to detect specific epitope requirements like the minimum epitope length, one binding epitope region was then analyzed in more detail by synthesis of series of peptides of different length derived from sequence Arg<sup>59</sup>-Ala<sup>100</sup> of streptavidin (Fig. 2-9) using template 2. The 12-mer peptides corresponding to spots from A1 to A16 are identical to those corresponding to spots from B5 to B20 of Fig. 2-7 (A or B) and give the same results after Western blot analysis probed by streptavidin (50 nM), where spots with continuous weak signals corresponding to the interacting epitopes. All shorter peptide series clearly demonstrate the minimum binding site in this region, corresponding to Trp<sup>75</sup>-Ser<sup>88</sup> sequence of streptavidin. From the results we can clearly see that using the strategy performed here it is possible to map the minimum binding epitope between two interacting partners.



Length	Spot No.	interaction regions	Corresponding sequences of the interaction regions	Locations in streptavidin
12-mers	A1-A16	block I	SGTALG <b>WTVAWKNNYRNAHS</b> ATTWSG	Ser <sup>69</sup> – Gly <sup>94</sup>
11-mers	A17-B8	block II	TALG <b>WTVAWKNNYRNAHS</b> ATTWS	Thr <sup>71</sup> – Ser <sup>93</sup>
10-mers	B9-B25	block III	TALG <b>WTVAWKNNYRNAHS</b> ATTW	Thr <sup>71</sup> – Trp <sup>92</sup>
9-mers	C1-C18	block IV	LG <b>WTVAWKNNYRNAHS</b> ATT	Leu <sup>73</sup> – Thr <sup>91</sup>
8-mers	C19-D11	block V	<b>VAWKNNYRNAHS</b> AT	Val <sup>77</sup> – Thr <sup>90</sup>
7-mers	D12-E5	block VI	<b>WTVAWKNNYRNAHS</b> A	Trp <sup>75</sup> – Ala <sup>89</sup>
6-mers	E6-E24	block VII	<b>WTVAWKNNYRNAHS</b>	Trp <sup>75</sup> – Ser <sup>88</sup>

**Fig. 2-9** Length variation (size-scan) of one binding epitope of streptavidin (Arg<sup>59</sup>-Ala<sup>100</sup>) to *Strep*-tag II. The peptide scans (varied from 12-mers to 6-mers with 2-amino-acid shift) of streptavidin sequence from Arg<sup>59</sup> to Ala<sup>100</sup> were synthesized to the Fmoc site of the template 2, while *Strep*-tag II as constant peptide being synthesized to the Dde site of the template 2. The peptide membrane was probed by streptavidin (50 nM) and followed by Western blot analysis. The minimized binding epitope is marked in bold between dashed lines in the table.

#### 2.2.1.7 Failure in analyzing the binding epitopes on streptavidin by fluorescence labeled *Strep*-tag II using standard SPOT strategy

In order to analyze the ligand binding epitopes of streptavidin, we also screened cellulose-bound peptide scan (Reineke, U., et al. 1996) representing the complete sequence of streptavidin for the binding to labeled *Strep*-tag II using standard SPOT synthesis (Frank, R. 1992) as a comparison. Peptide scan of streptavidin composed of 12-mer peptides with a 2-amino-acid shift was synthesized onto cellulose membrane via a (β-Ala)<sub>2</sub> spacer. A soluble form of fluorescence labeled *Strep*-tag II (Abz-SNWSHPQFEK-NH<sub>2</sub>) was used to probe the peptide membrane for the binding activity. The membrane was illuminated with a UV lamp upon excitation at 330 nm and the emitted fluorescence from the bound labeled peptide was recorded by a CCD camera (raytest Isotopenmessgeraete, Germany) (Fig. 2-10). Several concentrations of labeled *Strep*-tag II were tested up to 400 μM, and they were incubated with the peptide membrane overnight at 4 °C. However, no spots with prominent strong fluorescence signals had been found, but only the unspecific background signals which caused by non-sequence specific affinities between labeled peptide and cellulose anchored peptides.

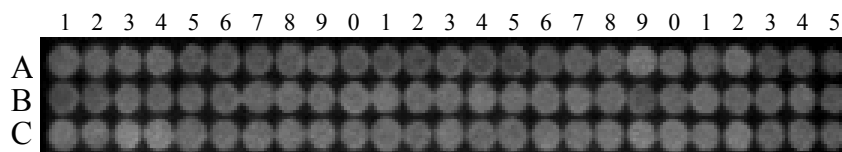


**Fig. 2-10** Peptide scan of streptavidin-derived dodecapeptides with Abz labeled *Strep*-tag II. Membrane-bound dodecapeptides overlapping by ten amino acids were probed with Abz labeled *Strep*-tag II (200  $\mu$ M), followed by extensive washing. Bound fluorescence was illuminated by excitation at 330 nm and recorded by a CCD camera.

Probably, it is not possible to obtain interaction signals, because the binding affinity of soluble peptide is not high enough to interact with cellulose bound peptides. Major differences between the soluble and the cellulose bound peptides are the relatively low local concentration and high degree of conformational freedom of soluble peptide in comparison to the cellulose bound peptides.

In standard SPOT experiment the final concentration of soluble peptide ( $\mu$ M level) is often much lower than that when it is immobilized on solid support. Because the concentration of soluble peptide is largely depended on its solubility in aqueous, while immobilized peptide has no such limitation. The high density of immobilized peptide on membrane can achieve higher local peptide concentration. We estimated that a density of 50 nmol/cm<sup>2</sup> of peptides on solid support could represent a high local concentration (estimated from 2D density to 3D concentration). As such, in Janus experiment the weak interaction between two peptide chains is favored and therefore detectable, whereas in standard SPOT experiment performed here not.

It is known that a soluble peptide normally has a high degree of conformational freedom and adopts flexible conformation. When a peptide is immobilized on a solid support, its conformational freedom and molecular motion are greatly limited by lowering the conformational entropy. We assume that once two peptides, potentially able to interact, are immobilized on a solid support, the entropy penalty associated with interaction between two peptides on template can be decreased because of the reduction of conformational entropy. So thermodynamically, the weak interactions between two configurationally constrained peptide chains would be more preferred as compared to the case in standard SPOT experiment when one of the interacting peptide is soluble. The possible driving forces for two peptide chains association on the template, such as hydrogen bonds and ion pairs are also the reasons for allowing the weak interaction between two immobilized peptides detectable.

## 2.2.1.8 Janus-peptide arrays based on the reverse sequence of streptavidin and Strep-tag II

Series of overlapping peptides (12-mer peptides with a 2-amino-acid shift) derived from the reverse sequence of streptavidin were synthesized to prepare Janus-peptide pairs with *Strep-tag II* (original sequence) using template 2. “Reverse” means that the C-terminal amino acid in normal protein sequence becomes the N-terminal amino acid in the reverse sequence. The Janus-peptide membrane was probed with streptavidin (50 nM), followed by electrotransfer of the bound streptavidin to nitrocellulose membrane. After incubation with anti-streptavidin antiserum and anti-rabbit IgG peroxidase conjugate, the visualization was performed by ECL system (Fig. 2-11, A).

Sometimes the judging of weak signals was difficult. The simplest way to roughly distinguish which spots giving weak signals is mainly according to the comparison of the signal intensity of one spot to the neighboring spots. Once several consecutive spots showing sharply decreased signal intensities in comparison to the neighboring spots, these continuous spots can be regarded as giving weak signals. However, in a region enclosed by brown circular (Fig. 2-11, A), all spots show very weak signal, it seems that these weak signals are caused by unevenly electrotransferring of the bound streptavidin to nitrocellulose. Such kind of inhomogeneity caused by the experimental system is sometimes observed in the other experiments. In this respect, the spots in this region will not be discussed in detail here.

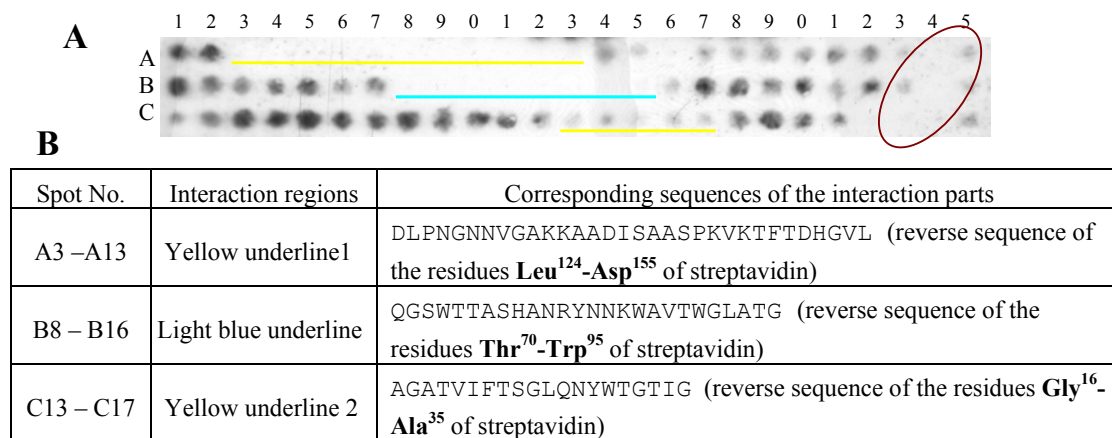


**Fig. 2-11** Analysis of interactions between 75 overlapping dodecapeptides derived from the reverse sequence of streptavidin and *Strep-tag II* peptide on cellulose. **(A)** Peptide scans (12-mers with a 2-amino-acid shift) of the reverse sequence of streptavidin were synthesized on cellulose to Fmoc site of template 2 while *Strep-tag II* peptide was synthesized to the Dde site. The Janus-peptide arrays were probed by streptavidin and detected by Western blot analysis (see methods). **(B)** The corresponding sequences of the interacting regions are tabulated.

Several regions of spots with continuous and significantly weak or no signals have been marked with colored underlines below the spots (Fig. 2-11, A). The corresponding sequences of these interacting regions are shown in the table (Fig. 2-11, B). Interestingly, two of the binding epitopes (spots B8-B16 and C13-C17) which corresponding to the residues Thr<sup>70</sup>-Trp<sup>95</sup> and Gly<sup>16</sup>-Ala<sup>35</sup> of streptavidin respectively have also been found as the binding epitopes in the previous Janus-peptide array assay containing peptide scan of streptavidin and *Strep*-tag II peptide pairs (Fig. 2-7, B, spots B10-B17 and A10-A12). Both forward and reverse sequences of residues Thr<sup>70</sup>-Trp<sup>95</sup> and Gly<sup>16</sup>-Ala<sup>35</sup> of streptavidin discovered to be the potential binding epitopes to *Strep*-tag II in Janus-peptide array denoted that the interactions of these epitopes (either forward or reverse sequences) to *Strep*-tag II might be independent on the backbone structures of the sequences but rather be dominated by the peptide side chains. The same conclusion can be deduced from the crystal structure of streptavidin/*Strep*-tag II complex that the interactions between the bound *Strep*-tag II and streptavidin are dominated by the peptide side chains (Schmidt, T.G., et al. 1996).

Another region of interest (spots A3-A13) corresponds to residues Leu<sup>124</sup>-Asp<sup>155</sup> of streptavidin and the relevant spots from the experiment of Fig. 2-7 (panel B), C10-C22. However, spots C10-C22 in Fig. 2-7 (panel B) do not show continuous weak signals instead that most of the spots in this region give strong signals due to the recognition of streptavidin to the fragments derived from its own sequence (subunit binding epitopes) as already observed in Fig. 2-4. In such case, we might be able to assume that the subunit association of streptavidin is depending on the backbone chain structure (primary sequence) of streptavidin, because in the reverse sequence such interactions are abolished. The results indicate that also residues Leu<sup>124</sup>-Asp<sup>155</sup> of streptavidin form part of the binding site to *Strep*-tag II. Unfortunately, the proof of the concept for this region is missing, because there is no structural information about this part of the protein in the crystal structure (Schmidt, T.G., et al. 1996, PDB entry 1RSU).

### *2.2.1.9 Using polypropylene membrane for Janus-peptide arrays*

Cellulose membrane seems to be suitable for Janus-peptide array in exploring peptide-peptide interactions in streptavidin/*Strep*-tag II model system. Now the question occurred, whether the supporting material itself has an influence on the Janus method. This question

arises because it has been already observed that the chemico-physical nature of different supports can influence the conformation adopted by the covalently attached peptide (Furrer, J., et al. 2001). Therefore, another membrane support was tested in Janus-peptide array to compare it with the cellulose membrane. The APEG-amino-polypropylene membrane (AMIS Scientific Products GmbH, Germany) was selected and used in Janus-peptide array by using streptavidin/*Strep*-tag II interaction system. Polypropylene is known to have an increased mechanical stability compared to the filter membrane. However it has no functional groups easy for chemical reactions and it is not compatible for being used in biological assays, so novel amino-functionalized polypropylene based membranes have been developed (Frank, R. 2002, Wenschuh, H., et al. 2000). To improve the compatibility for biological assay, polyethyleneglycol (PEG) has been copolymerized onto the surface of polypropylene membrane to make the surface more hydrophilic and compatible to proteins or antibodies for different assays.

Arrays of Janus-peptide pairs, peptide scans of streptavidin (12-mer peptides with a 2-amino-acid shift) and *Strep*-tag II pairs, have been synthesized on APEG-amino-polypropylene (APEG-PP) membrane (Fig. 2-12). After Western blot analysis of the bound streptavidin and the visualization step, two regions of spots with continuous weak signal have been observed with colored underlines below the spots (Fig. 2-12, A). From the results, we found that light blue underline region (spots B10-B16) which had already been found as the major binding epitope in the experiment by using cellulose membrane, had also been found here by using APEG-Amino-PP membrane. The regions A23-A25 (residues Ser<sup>45</sup>-Tyr<sup>60</sup> of streptavidin) and C6-C8 (residues Thr<sup>111</sup>-Gly<sup>126</sup> of streptavidin) which had been found to give weak signals (Fig. 2-7, B) by using cellulose membrane, could not be detected by using APEG-PP membrane here (Fig. 2-12, A).

On the other hand, spots C11-C22 have shown consecutive weak signals by using polypropylene membrane but not by using cellulose, instead of some strong signals. It is known that the strong signals given in this region (spots C11-C22) in Fig. 2-7 (panel B) by using cellulose membrane are probably due to the recognition of streptavidin to its own subunit association epitopes already observed in Fig. 2-4. However, it was not the same by using APEG-PP membrane. The reason why there seems to be no self-interaction of streptavidin to its own fragments in the same region (spots C11-C22) by using APEG-PP membrane (Fig. 2-12) was not clear, most probably due to the influences from APEG-PP support. The control experiment of synthesizing only the peptide scan of streptavidin on APEG-PP membrane was not performed, because of the limited amount of APEG-PP

membrane available. The accurate estimation of whether peptide pairs each spots in this region having interactions appears to be difficult. No crystal structure data can prove whether the corresponding residues His<sup>127</sup>-Leu<sup>154</sup> of streptavidin in this region (spots C11-C22) really have interactions with *Strep*-tag II or not, because only the core sequence of streptavidin (Met<sup>13</sup>-Pro<sup>135</sup>) has been crystallized.

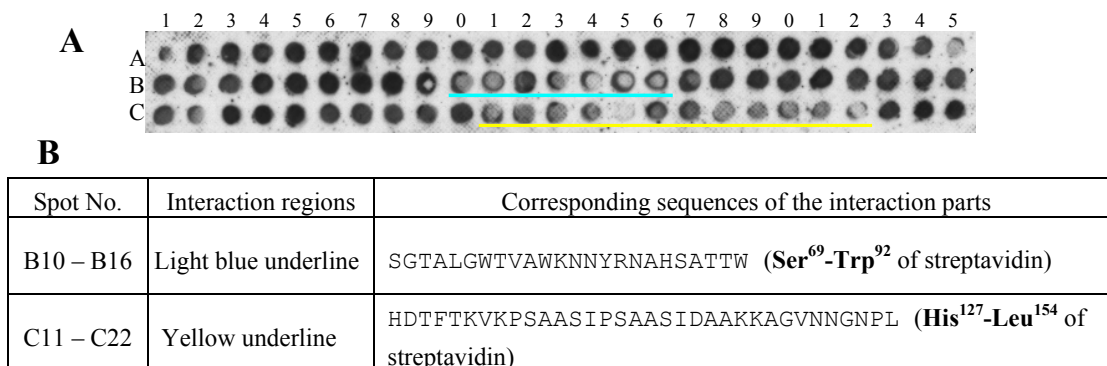


**Fig. 2-12** Analysis of interactions between 75 overlapping dodecapeptides derived from streptavidin and *Strep*-tag II peptide on APEG-Amino-Polypropylene membrane (80 nmol/cm<sup>2</sup>). **(A)** Peptide scans (12-mers with a 2-amino-acid shift) of streptavidin were synthesized on APEG-Amino-PP membrane to Fmoc site of template 2 while *Strep*-tag II peptide was synthesized to the Dde site. The Janus-peptide arrays were probed by streptavidin (50 nM) and detected by Western blot analysis (see methods section). **(B)** The corresponding sequences of the interacting regions are tabulated.

The study of the compatibility of some amino-modified polypropylene (PP) membranes for peptide-antibody binding assays elucidated that the modified PP membranes work as well as cellulose in terms of signal intensity and background (Wenschuh, H., et al. 2000). It is true also within our study that APEG-PP membrane showed good mechanical property and good compatibility for protein binding assay. We have clearly found one binding epitope corresponding to Ser<sup>69</sup>-Trp<sup>92</sup> of streptavidin in streptavidin/*Strep*-tag II model system by using APEG-PP membrane (Fig. 2-12). This epitope has also been found by using cellulose membrane indicating that in principle, similar interactions of peptide pairs are occurring on both solid supports and therefore their interactions were detectable. It is known that once a peptide is immobilized on a solid support, its conformational freedom is limited resulting in a propensity to form a stable structure. In this respect, the detection of peptide-peptide interaction using different solid supports is similar. Nevertheless, there are some differences in the outputs because of using different solid supports. It could be due to the following reasons: 1) the peptide pairs on different polymeric surfaces might adopt different

structures inducing different interacting patterns, as already elucidated that different chemicophysical properties of solid supports having different influences on secondary structure of the covalently attached peptide (Furrer, J., et al. 2001); 2) the loading of the peptide pairs (density) on different polymeric surfaces might lead to the different outputs, as shown in the relating study that the binding varied largely depending on different densities of immobilized peptides in peptide-antibody binding assays (Wenschuh, H., et al. 2000).

Since more potential interaction sites could be screened out by using cellulose, cellulose membrane was chosen and applied in the following experiments as solid surface to perform Janus-peptide array experiments at a first glance to verify the idea of Janus-peptide array. It does not mean that modified PP membranes cannot be a good planar support for Janus experiments. It is just a matter of putting more efforts for further screening analysis and optimizing processes.

### *2.2.1.10 Conclusions*

Most of the potential binding epitopes found by Janus-peptide array, which are derived from the interacting Janus-peptide pairs, are located in the binding pocket of streptavidin through interpreting all the data at hand and taking a close view of the structure of the binding sites between streptavidin and *Strep*-tag II. The colored flat ribbon regions shown in [Fig. 2-13](#) represent the binding epitopes found by Janus-peptide array. They are including sequence Ser<sup>45</sup>-Tyr<sup>60</sup> of streptavidin (pink flat ribbon), sequence Trp<sup>75</sup>-Ser<sup>88</sup> of streptavidin (light blue flat ribbon) and sequence Thr<sup>111</sup>-Asp<sup>128</sup> of streptavidin (brown flat ribbon). The interaction was already described according to the crystal structure of streptavidin/*Strep*-tag II complex. It is known that Asn<sup>23</sup>, Ser<sup>27</sup>, Tyr<sup>43</sup>, Ser<sup>45</sup>, Ala<sup>46</sup>, Val<sup>47</sup>, Glu<sup>51</sup>, Ser<sup>52</sup>, Tyr<sup>54</sup>, Arg<sup>84</sup>, Ser<sup>88</sup>, Thr<sup>90</sup> and Asp<sup>128</sup> are involved in intermolecular contact through hydrogen bonds or via hydrogen-bonded water molecules between streptavidin and the bound *Strep*-tag II, while Trp<sup>79</sup> and Trp<sup>120</sup> exist in the ligand binding pocket (Chilkoti, A., et al. 1995, Schmidt, T.G., et al. 1996). The three observed binding epitopes contain most of the key amino acids involved in binding of streptavidin to *Strep*-tagII, which were displayed with their complete side chains ([Fig. 2-13](#)). They are including Ser<sup>45</sup>, Glu<sup>51</sup>, Tyr<sup>54</sup>, Trp<sup>79</sup>, Arg<sup>84</sup>, Ser<sup>88</sup> and Trp<sup>120</sup> which are known to play important roles in binding of streptavidin to *Strep*-tag II, such as involved in forming intermolecular (like Ser<sup>45</sup>, Glu<sup>51</sup>, Tyr<sup>54</sup>, etc.) hydrogen bonds with the ligand (Chilkoti, A., et al. 1995, Schmidt, T.G., et al. 1996). The successful investigation and mapping of the interaction sites of the known complex streptavidin/*Strep*-tag II by using Janus-peptide array

has verified that two peptides, potentially having interactions, could interact when they were side-by-side immobilized on the solid support, and elucidated that Janus-peptide array was feasible in exploring peptide-peptide interactions. Janus-peptide array has to be proved now by other examples.

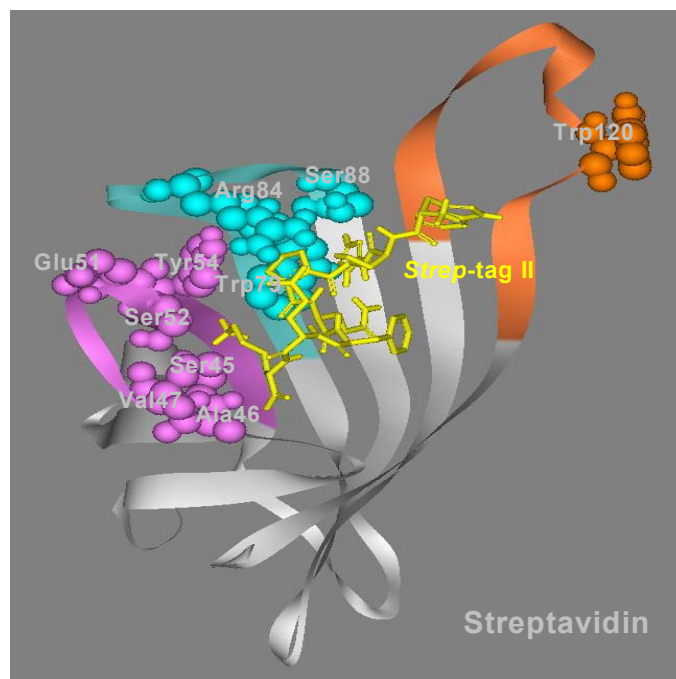


**Fig. 2-13** View of the structure of streptavidin and *Strep-tag II* complex. A grey flat ribbon representation of streptavidin core sequence (Met<sup>13</sup>-Pro<sup>135</sup>) bound to *Strep-tag II* (missing N-terminal Ser and Asn) is shown (Schmidt, T.G., et al. 1996, PDB entry 1RSU). The colored flat ribbon regions are the binding epitopes found in [Fig. 2-7](#) (panel A or B). They are including sequence Ser<sup>45</sup>-Tyr<sup>60</sup> of streptavidin (pink), sequence Trp<sup>75</sup>-Ser<sup>88</sup> of streptavidin (light blue) and sequence Thr<sup>111</sup>-Asp<sup>128</sup> of streptavidin (brown). The important amino acids involved in the interaction to *Strep-tag II* in the binding pocket of streptavidin are shown in CPK, such as Ser<sup>45</sup>, Ala<sup>46</sup>, Val<sup>47</sup>, Glu<sup>51</sup>, Ser<sup>52</sup>, Tyr<sup>54</sup>, Trp<sup>79</sup>, Arg<sup>84</sup>, Ser<sup>88</sup> and Trp<sup>120</sup>.

### 2.2.2 Example II: Protein 14-3-3/phosphopeptides interaction

14-3-3 proteins are abundant in all eukaryotic cells (Aitken, A. 1996). They are involved in important cellular processes such as signal transduction, cell-cycle control and apoptosis. More than 100 different cellular binding partners for the 14-3-3 have been reported (van Hemert, M.J., et al. 2001). The 14-3-3 proteins form a highly conserved family of acidic

dimeric proteins with a subunit mass of approximately 30 kDa. Multiple isoforms have been identified plus their phosphorylated versions. The 14-3-3 family of proteins mediates biological functions by binding to phosphoserine-containing proteins. A number of different motifs have been identified in proteins that bind to 14-3-3 proteins. Many of these motifs contain a phosphoserine (pS) residue flanked by an arginine and proline, e.g., RSXpSXP (Muslin, A.J., et al. 1996, Yaffe, M.B., et al. 1997),  $RX_{1-2}SX_{2-3}pS$  (Liu, Y.C., et al. 1997),  $RX(Y/F)-XpSXP$  or  $RXSX(S/T)XP$  (Yaffe, M.B., et al. 1997). 14-3-3 proteins also bind to serine-rich regions containing a  $X_3SXSX_3SX_2SX$  motif (Vincenz, C. and Dixit, V.M. 1996).

A phosphopeptide comprised of residues 251-265 of Raf-1, named pS-Raf-259 (LSQRQRSTpSTPNVHMV), bound several isoforms of 14-3-3, inhibited the association of 14-3-3 with Raf-1 *in vitro*, with a  $K_i$  of 510 nM (Muslin, A.J., et al. 1996). The crystal structure of the  $\zeta$  isoform of 14-3-3 in complex with pS-Raf-259 had been reported (Petosa, C., et al. 1998).

Another phosphopeptide containing the sequence RSHpSYP corresponding to the 14-3-3 binding site in polyoma middle-T (mT) which appears to mimic an activated growth-factor receptor, recruiting a variety of signaling molecules, had a  $K_i$  of 435 nM to 14-3-3. The crystal structure of 14-3-3 $\zeta$  complexed to a phosphopeptide (ARSHpSYPA) based on the sequence around Ser<sup>276</sup> in mT (sequence MARSHpSYPAKK) was solved and the interaction profiles had been described extensively (Yaffe, M.B., et al. 1997).

Based on the knowledge about the binding profiles of phosphopeptides to 14-3-3s in the literature, and with respect to the importance of biological functions of 14-3-3s, the 14-3-3 and phosphopeptides interactions can be another good model to be introduced in Janus-peptide arrays system. The mapping of the interaction sites between 14-3-3s and phosphopeptides by exploring peptide-peptide interactions on solid phase could be helpful to evaluate this new Janus-peptide array methodology described.

The 14-3-3 sequence used for peptide scan in Janus-peptide array is the  $\zeta$  isoform with the sequence shown in [Fig. 2-14](#). Since 14-3-3s always form homo- or hetero-dimers, the 14-3-3 used here as a probe protein is a recombinant protein expressed in *E.coli* which is in a heterodimer form as a  $\zeta/\delta$  form (kindly provided by Dr. Holger Bang). Two different phosphopeptides have been chosen for Janus-peptide arrays, they are RQRSTpSTPNV derived from pS-Raf-259 (Muslin, A.J., et al. 1996) and ARSHpSYPA originally from polyoma mT antigen (Rittinger, K., et al. 1999, Yaffe, M.B., et al. 1997), respectively.

**14-3-3 $\zeta$  sequence**

1	11	21	31	41	51
MDKNELVQKA	KLAEQAERYD	DMAACMKSVT	EQGAELSNEE	RNLLSVAYKN	VVGARRSSWR
VVSSIEQKTE	GAEKKQOMAR	EYREKIETEL	RDICNDVLSL	LEKFLIPNAS	QAESKVFYLK
MKGDYYRYLA	EVAAGDDKKG	IVDQSQQAYQ	EAFEISKKEM	QPTHPIRLGL	ALNFSVFYEE
ILNSPEKACS	LAKTAFDEAI	AELDTLSEES	YKDSTLIMQL	LRDNLTWLTS	DTQGDEAEAG
EGGEN					

**Fig. 2-14** The sequence of  $\zeta$  isoform of 14-3-3 (NCBI protein\_id: AAA36446.1) used for peptide scan in Janus-peptide array.

### 2.2.2.1 Mapping binding epitopes on 14-3-3 to RQRSTpSTPNV (Raf peptide) by Janus-peptide arrays

An array of Janus-peptide pairs, containing peptide scans of 14-3-3 (12-mers with a 3-amino-acid shift) and peptide RQRSTpSTPNV pairs, has been synthesized on cellulose using template 2 (Fig. 2-15). After probing the array by 14-3-3 protein (150 nM), the bound protein was electrotransferred to nitrocellulose, and recognized by anti-14-3-3 monoclonal antibody (Santa Cruz) and anti-mouse IgG peroxidase conjugate, followed by final visualization using ECL system. Three regions of spots with continuous weak signals have been observed. They are depicted as regions with colored underlines (Fig. 2-15, A) corresponding to the spots with continuous higher positive arbitrary units (Fig. 2-15, B). Densitometry analysis has been used to quantify the signal intensity of each spots when the variance of the visible signals cannot be easily judged by eyes. The definition of the ‘arbitrary unit’ used for the densitometry analysis can be found in the legend of Fig. 2-15.

The corresponding sequences of each region and the localizations of them in 14-3-3 are listed (Fig. 2-15, C). Especially, the found region of spots A16 – A18 (Fig. 2-15, A) covering the sequence Ala<sup>47</sup> – Ser<sup>64</sup> (in helix  $\alpha$ 3) of 14-3-3 contains a cluster of basic residues (Lys<sup>49</sup>, Arg<sup>56</sup>, Arg<sup>60</sup>) which were very important for the interactions with the phosphoserine of pS-Raf-259 (Petosa, C., et al. 1998). This major epitope region has been recognized as the binding epitope by Janus-peptide array with continuous weak signals, relevant to the higher positive arbitrary units of spots (Fig. 2-15, B). It had been discovered that Raf peptide made unique contacts to Leu<sup>227</sup> and Trp<sup>228</sup> from helix  $\alpha$ 9 of 14-3-3 (Petosa, C., et al. 1998). This interaction site has also been detected here (Fig. 2-15) corresponding to spots D16-D18 covering the residues Thr<sup>226</sup> – Gly<sup>243</sup> (in helix  $\alpha$ 9) of 14-3-3. The results obtained here by

using Janus-peptide array have again shown that Janus method is a useful method in finding out the major binding sites of protein complexes.

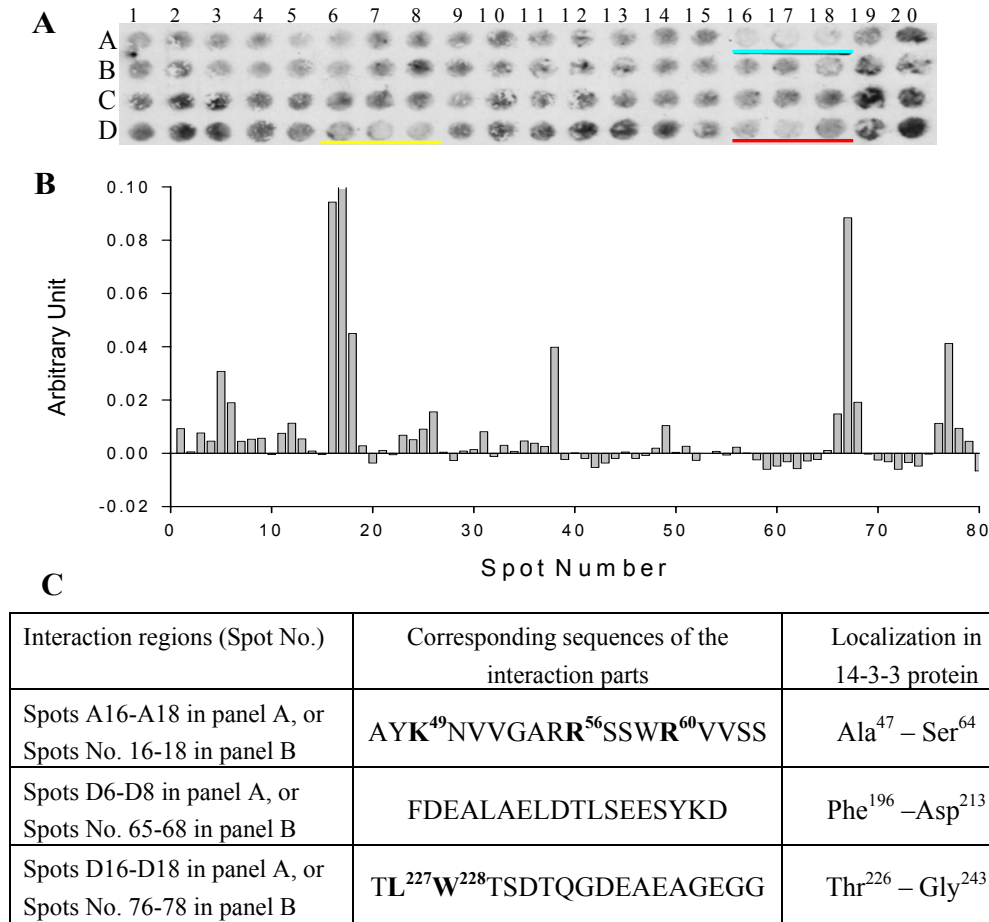


**Fig. 2-15** Interactions between overlapping dodecapeptides derived from 14-3-3 protein and phosphopeptide RQRSTpSTPNV. Peptide scans (12-mers with a 3-amino-acid shift) of 14-3-3 were synthesized on cellulose membrane to Fmoc site of template 2 while peptide RQRSTpSTPNV was coupled to Dde site with a  $\beta$ -Ala as spacer. The Janus-peptide membrane was probed by 14-3-3  $\zeta/\delta$  (150 nM) and the binding was detected after electrotransfer of cellulose-bound 14-3-3 to a nitrocellulose membrane by Western blot analysis (see methods section). **(A)** The visualized signals of Western blot assay, with colored underlines for spots giving weak signals. **(B)** Densitometry analysis of each spot in panel A by Gel-Pro Analyzer (Media Cybernetics). **(C)** The corresponding sequences of each underlined regions and their locations in 14-3-3 have been tabulated, with key amino acids involved in the interaction marked in bold.

The **Arbitrary Units**: The reciprocal of the intensities of each spots analyzed by Gel-Pro Analyzer 3.1 minus the reciprocal of the average intensity of all spots tested. The larger the positive arbitrary unit values correspond to the weaker the signals got from blot experiments that indicate the potential interaction peptide pairs. The definition is always the same in the following densitometry analysis of the spots.

### 2.2.2.2 Mapping binding epitopes on 14-3-3 to ARSHpSYPA (mT peptide) by Janus-peptide arrays

The same strategy has been used in depicting the binding interfaces between 14-3-3 and the mT peptide. An array of Janus-peptide pairs, peptide scans of 14-3-3 (10-mers with a 2-amino-acid shift) and peptide ARSHpSYPA pairs, has been synthesized on cellulose using template 2 (Fig. 2-16). After probing the array by 14-3-3 (200 nM), the bound protein was electrotransferred to nitrocellulose, and recognized by anti-14-3-3 monoclonal antibody (Santa Cruz) and anti-mouse IgG peroxidase conjugate, followed by the final visualization using ECL system.

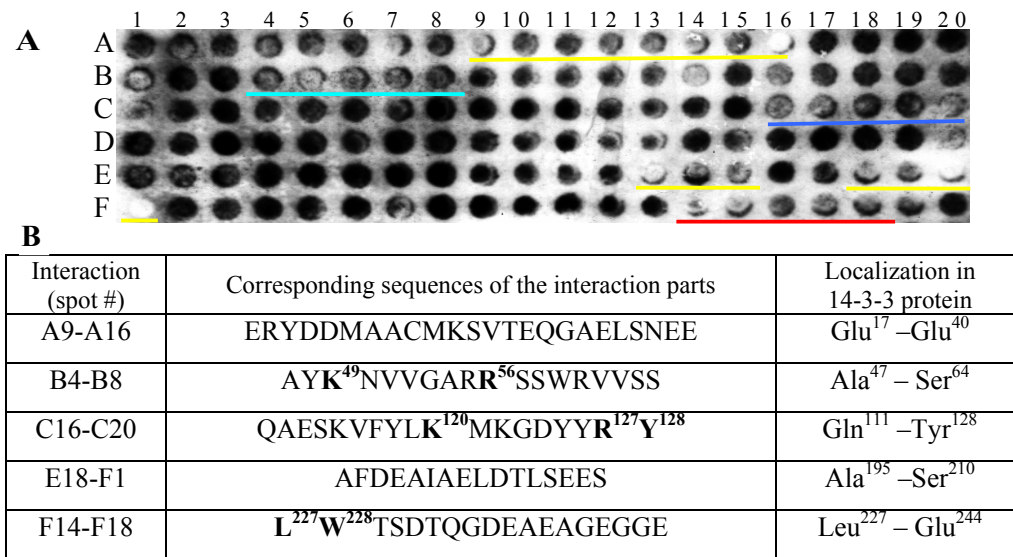


**Fig. 2-16** Interactions between overlapping dodecapeptides derived from 14-3-3 protein and phosphopeptide ARSHpSYPA. Peptide scans (10-mers with a 2-amino-acid shift) of 14-3-3 were synthesized on cellulose membrane to Fmoc site of template 2, while peptide ARSHpSYPA was coupled to the Dde site with ( $\beta$ -Ala)<sub>2</sub> as spacer. The Janus-peptide membrane was probed by 14-3-3  $\zeta/\delta$  (200 nM) and the binding was detected after electrotransfer of cellulose-bound 14-3-3 to a nitrocellulose membrane by Western blot assay (as described in material and methods). **(A)** The visualized signals of Western blot assay, with colored underlines for spots giving weak signals. **(B)** The corresponding sequences of each underlined regions and their locations in 14-3-3 have been tabulated, with key amino acids involved in the interaction marked in bold.

Several regions of spots have been concerned with colored underlines showing continuous weak signals (Fig. 2-16, A). Since the background is not equal therefore some spots seems to be brighter than they are. The sizes of each spots are also dissimilar therefore it is not suitable to quantify the signal intensity using densitometry analysis which records

grey density of each spots in the same area size. The judging of weak signal can base on visually comparing the intensities of the neighboring spots. The corresponding sequences of each selected regions and the localizations of them in 14-3-3 are listed in [Fig. 2-16](#) (panel B). Three regions are the same as found in 14-3-3 and Raf peptide model system (for comparison see [Fig. 2-15](#)). They are the residues Ala<sup>47</sup> – Ser<sup>64</sup> (in helix  $\alpha$ 3), Ala<sup>195</sup> – Ser<sup>210</sup> and Leu<sup>227</sup> – Glu<sup>244</sup> (in helix  $\alpha$ 9) of 14-3-3. Crystal structure had clearly demonstrated that the conservative Arg<sup>56</sup> and Lys<sup>49</sup> from helix  $\alpha$ 3 played key roles in coordinating the phosphoserine residue in mT (Rittinger, K., et al. 1999, Yaffe, M.B., et al. 1997). Additional one region of spots C16-C20 covering residues Gln<sup>111</sup> – Tyr<sup>128</sup> (in helix  $\alpha$ 5) of 14-3-3 have been observed in this model system ([Fig. 2-16](#)), including very conserved Lys<sup>120</sup>, Arg<sup>127</sup> and Tyr<sup>128</sup> in all 14-3-3 isotypes which exposed to the binding groove and involved in binding the peptide ([Fig. 2-18](#)).

### *2.2.2.3 Trouble shooting for the synthesis of phosphopeptides on cellulose*

Special attentions should be paid on the synthesis of phosphopeptides on the filter surface, such as the coupling of phosphoserine building block into the peptide chains here. It is known that the use of bis-protected phosphoserine will cause side reactions when treated with piperidine during the standard deprotection cycle leading to  $\beta$ -elimination with loss of the phosphate group (Lacombe, J.M., et al. 1990). However, Wakamiya, et al. (Wakamiya, T., et al. 1994) have demonstrated that this kind of side reaction could be prevented by the use of a mono-protected derivative, such as Fmoc-Ser(PO(OBzl)OH)-OH, for incorporation of the phosphoserine residue.

Fmoc-Ser(PO(OBzl)OH)-OH had been used for the synthesis of phosphopeptides in preparing Janus-peptide arrays. The coupling method for Fmoc-Ser(PO(OBzl)OH)-OH was based on HBTU (or TBTU)/HOBt/DIEA (1:1:2) activation (Perich, J.W., et al. 1999). An addition of an extra equivalent of base is beneficial. The benzyl side-chain protecting group was removed in 1-2 hours by 95% TFA. Considering the mechanical stability of cellulose, when using 95% TFA for the final cleavage of side chain protecting groups, it is necessary to treat membrane only with very gentle shaking. Otherwise, the cellulose membrane will become very fragile, and unsuitable for performing further assays on it.

The quality of the phosphopeptides on certain spots can be monitored by MALDI-TOF-MS. Still the incomplete coupling of phosphoserine in peptide chains had been observed by MS ([Fig. 2-17](#)). A simple way to overcome the incompleteness is to increase the

amount of the coupling reagents. As already discussed before, MALDI-TOF-MS analysis cannot provide quantitative information (section 2.1.3), so the amount of peptides relates not directly proportional to the peak height of each component.

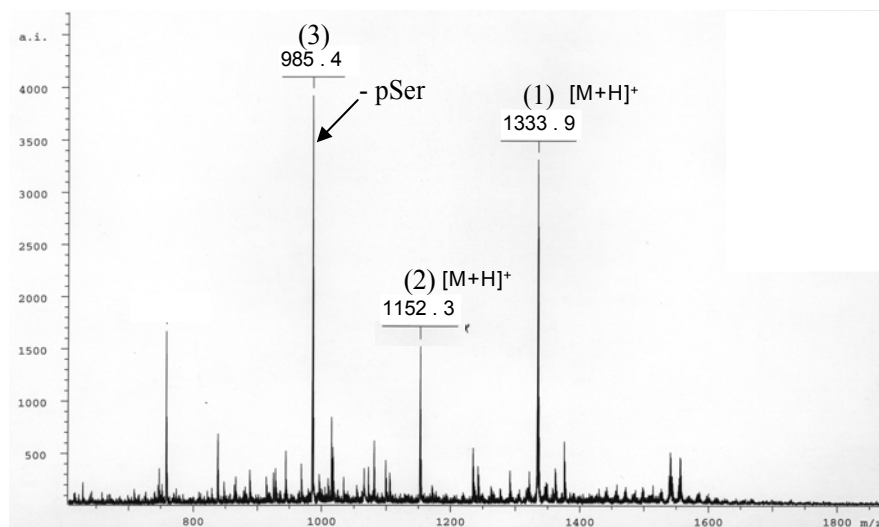


**Fig. 2-17** MALDI-TOF Mass spectrometry of the peptide pair on selected spot (corresponding to spot B4 of Fig. 2-16). Peak (1) shows the mass of 1333.9 [M + H]<sup>+</sup> representing the mass of peptide Ac-AYKNVVGARRSB-NH<sub>2</sub> (theor. 1332.5) on Fmoc site. Peak (2) shows the mass of 1152.3 [M + H]<sup>+</sup> representing the mass of peptide Ac-ARSHpSYPABB-NH<sub>2</sub> (theor. 1151.2) on Dde site. Peak (3) shows the mass of 985.4 [M + H]<sup>+</sup> representing the mass of peptide missing one phosphoserine in Ac-ARSHpSYPABB-NH<sub>2</sub> (theor. 1151.2) on Dde site. Note, B is β-alanine; Ac is Acetyl; pS is phosphoserine.

#### 2.2.2.4 Conclusions

The binding sites of 14-3-3ζ towards peptide like ARSHpSYPA (Fig. 2-18), represent an amphipathic binding groove, formed by helices α3, α5, α7, and α9. Three binding epitopes found by Janus-peptide array locate directly in the amphipathic binding groove. The corresponding sequences and the locations of the observed epitopes have been illustrated (Fig. 2-18), such as residues Ala<sup>47</sup>-Ser<sup>64</sup> (in helix α3) shown in light blue ribbon, residues Gln<sup>111</sup>-Tyr<sup>128</sup> (in helix α5) shown in blue ribbon and residues Leu<sup>227</sup>-Glu<sup>244</sup> (in helix α9) shown in red ribbon. Only residues Leu<sup>227</sup>-Thr<sup>232</sup> are visible in the crystal structure, so it is not possible to compare the data for residues Gln<sup>233</sup>-Glu<sup>244</sup>. The interaction was already described according to the crystal structure of 14-3-3ζ/ARSHpSYPA complex (Rittinger, K., et al. 1999, PDB entry 1QJB). It is known that side chains of Asn<sup>224</sup>, Asn<sup>173</sup>, and Lys<sup>120</sup> maintain an extended peptide backbone, which appears to be important for positioning the serine

phosphate of ARSHpSYPA for interactions within the basic pocket. Meanwhile, a hydrophobic pocket comprised of Val<sup>176</sup> and Tyr<sup>179</sup> (from helix  $\alpha$ 7), and Leu<sup>227</sup> and Trp<sup>228</sup> (from helix  $\alpha$ 9) is important for the interaction with ARSHpSYPA as well. In ARSHpSYPA structure, the proline is in the *cis* conformation, stabilized by a hydrogen bond between the  $\epsilon$ -amino group of Lys<sup>49</sup> of 14-3-3 and the Pro carbonyl oxygen in the next amide linkage (Rittinger, K., et al. 1999). The conserved and the key amino acids in all 14-3-3 isotypes engaged in the peptide binding found by Janus experiment in this model are displayed with their complete side chains (Fig. 2-18). The results obtained here using 14-3-3/phosphopeptide models analyzed by Janus-peptide array have again shown that Janus-peptide array is a useful method in finding out the major binding sites of protein complexes based on the interactions of matrix-bound Janus-peptide pairs.

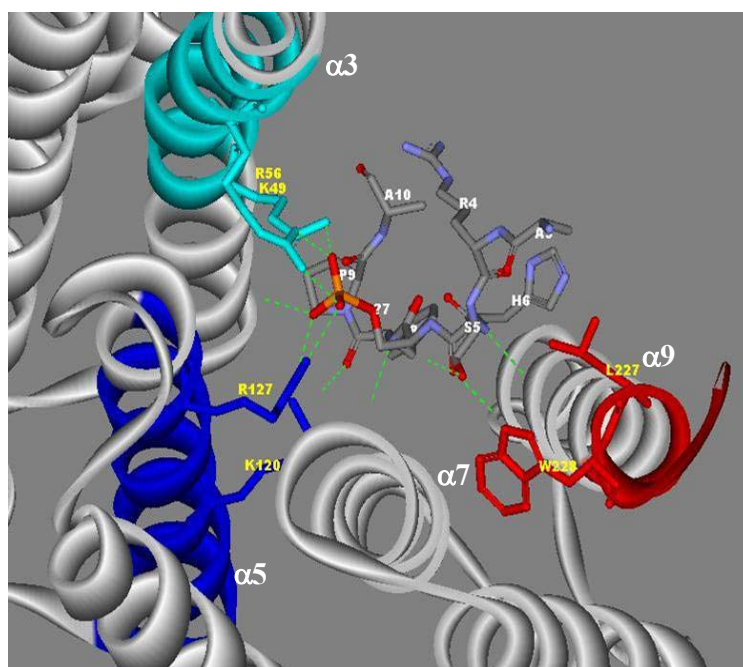


**Fig. 2-18** View at the binding sites of the complex of 14-3-3 $\zeta$  and ARSHpSYPA. 14-3-3 $\zeta$  (Met<sup>1</sup>-Thr<sup>232</sup>) is shown in grey solid ribbon and ARSHpSYPA shown in stick (Rittinger, K., et al. 1999, PDB entry 1QJB). The colored ribbon regions are the binding epitopes found by Janus-peptide array (Fig. 2-16). They are including the sequence Ala<sup>47</sup> – Ser<sup>64</sup> (in helix  $\alpha$ 3) of 14-3-3 $\zeta$  (light blue ribbon), sequence Gln<sup>111</sup> – Tyr<sup>128</sup> (in helix  $\alpha$ 5) of 14-3-3 $\zeta$  (blue ribbon) and sequence Leu<sup>227</sup> – Thr<sup>232</sup> (in helix  $\alpha$ 9) of 14-3-3 $\zeta$  (red ribbon). The important basic amino acids involved in binding to ARSHpSYPA in the binding interface of 14-3-3 $\zeta$  are shown in sticks, such as Lys<sup>49</sup>, Arg<sup>56</sup>, Lys<sup>120</sup> and Arg<sup>127</sup>. The small green dash lines represent the hydrogen bond forming.

### **2.3 The examples of protein-protein interaction**

Human FKBP12 is the prototypic member of the growing family of FK506-binding proteins (FKBPs), one of the three families of peptidyl prolyl *cis/trans* isomerases (PPIases, EC number 5.2.1.8) (Fischer, G. 1994, Galat, A. and Metcalfe, S.M. 1995, Gothel, S.F. and Marahiel, M.A. 1999). PPIases are enzymes evolved to catalyze the isomerization of peptide bonds preceding proline. FKBP12, the receptor for the immunosuppressant drugs FK506 and rapamycin (two related macrolides) (Bierer, B.E. 1994, Schreiber, S.L. 1991, Standaert, R.F., et al. 1990), has various biological functions *in vivo* (Schiene-Fischer, C. and Yu, C. 2001). The association of FKBP12 and FK506 leads to the inhibition of the catalytic activity of the binding partner of FKBP12-FK506 complex, the calcium-activated serine phosphatase calcineurin (Cardenas, M.E., et al. 1994) and therefore mediates immunosuppression. The association of FKBP12 with rapamycin leads to the interaction with a target protein termed rapamycin and FKBP12 target (RAFT) (Sabatini, D.M., et al. 1994) or FKBP-rapamycin-associated protein (FRAP) (Brown, E.J., et al. 1994) and appears to block the T cell response at a later stage. Among the various *in vivo* functions of FKBP12, a remarkable feature is the association with different types of receptors. FKBP12 is tightly associated with calcium release channel proteins, the ryanodine receptor, and the inositol-1,4,5-triphosphate receptor, which mediate calcium flux (Cameron, A.M., et al. 1995a, Cameron, A.M., et al. 1995bb) and play important roles *in vivo*. Additionally, the isomerase activity of FKBP12 can also be involved in the catalysis of proteins restructuring (Schiene, C. and Fischer, G. 2000).

A novel 48-kDa FKBP-associated protein (FAP48) has been found to interact with FKBP12 by yeast two-hybrid system, and the formation of complex between FKBP12 and FAP48 can be prevented by FK506 and rapamycin in a dose dependent manner (Chambraud, B., et al. 1996). Very recently, the relevant biological functions upon the interactions between these two proteins have been revealed that FAP48-FKBP complexes increase IL2 production (Krummrei, U., et al. 2003). Site-directed mutagenesis of all proline sites on FAP48 to Ala, indicating the importance of Pro<sup>219</sup> and Pro<sup>309</sup> in FAP48 for the binding to FKBP12 (Neye, H. 2001). There is no information about additional amino acid residues of FAP48 to be important for this interaction. On the other hand, which amino acid residues of FKBP12 are involved in the binding interface to FAP48 can be only deduced by the assumption that binding occurs at the active site of FKBP12 due to that binding of FAP48 to FKBP12 can be inhibited by FK506 (Neye, H. 2001). Since the key amino acids involved in the active site of FKBP12 are

only deduced by the structure of FKBP12-FK506 complex (PDB entry: 1FKJ) (Wilson, K.P., et al. 1995), yet it does not actually represent the real binding interface of FKBP12 to a protein or peptide ligand. In such situation, it is necessary to analyze the interaction sites of FAP48-FKBP12 complex in more detail.

The effects of FKBP12 on autophosphorylation of the epidermal growth factor (EGF) receptor had been reported. It was shown that FKBP12 inhibited tyrosine kinase activity of EGF receptor in a concentration dependent manner, and the inhibition of autophosphorylation of EGFR by FKBP12 was PPIase activities dependent (Lopez-Illasaca, M., et al. 1998). The lack of FKBP12 effects on the dephosphorylation kinetics of EGFR in pulse chase experiments and the detection of the physical interaction of FKBP12 and EGFR indicate a direct influence of FKBP12 on EGFR (Schiene, C., dissertation, 1999). A similar mechanism elucidated in the case that FKBP12 inhibited tyrosine kinase activities of type I TGFbeta receptor (TβR-I) by direct binding to the GS region of TβR-I (Chen, Y.G., et al. 1997, Huse, M., et al. 1999). The study of the direct binding sites that might exist between FKBP12 and the cytosolic domain of EGFR may shed light on the mechanism how FKBP12 inhibits EGFR autophosphorylation. Because FKBP12 is already known as a cytosolic protein (Schreiber, S.L. 1991), the assumption is that the direct interactions between FKBP12 and EGFR should be at the cytosolic domain.

The detection of the interaction sites of two proteins often meets limitations, because one of the binding partners is not available or the chemical properties of the protein do not allow handling in interaction assays. Such as the cases encountered here, FAP48 was not available as a probe protein in substance, while EGFR is not easy to handle and difficult to obtain at a considerable concentration. Therefore, we cannot simply use standard SPOT method by synthesizing peptide scan of one protein for the binding of another interaction protein that is lack as depicted in [Fig. 1-2](#). However, we still want to get the information about the interactions between FKBP12 and FAP48 or between FKBP12 and EGFR at amino acid level, since it will be helpful to elucidate the biological essentials of these protein-protein interactions. What we can do is to use Janus-peptide arrays to analyze peptide-peptide interactions in deciphering the code of protein-protein interaction sites. These experiments will also provide us indications to answer the question whether peptide-peptide interactions can be used to model protein-protein interactions.

### 2.3.1 Example I: FKBP12/FAP48 interaction

Human recombinant FKBP12 was expressed in *E.coli* and purified sequentially by ion exchange column, blue affinity column and gel filtration column according to published procedures (Standaert, R.F., et al. 1990). The activity of purified FKBP12 was measured by protease coupled assay established by Fischer (Fischer, G., et al. 1984), using Suc-Ala-Leu-Pro-Phe-pNA as a substrate. The  $k_{cat}/K_m$  of FKBP12 to this substrate was  $2.57 \times 10^6 \text{ M}^{-1} \text{ S}^{-1}$ , which is in the same range as reported about  $1.24 \times 10^6 \text{ M}^{-1} \text{ S}^{-1}$  to the same substrate (Tradler, T., et al. 1997).

#### 2.3.1.1 Mapping binding epitopes on FAP48 to FKBP12 by standard SPOT strategy

In the first step, it was necessary to map the binding sites on FAP48, which are involved in the contact to FKBP12. We screened cellulose-bound peptide scan of FAP48 for the binding to FKBP12 by standard SPOT technology as described in [Fig. 1-2](#). Series of 13-mer peptides with a 2-amino-acid shift spanning the complete FAP48 sequence ([Fig. 2-19](#)) were synthesized on a cellulose membrane. The peptide membrane was then probed by FKBP12 (200 nM) and followed by stepwise electrotransfer of the bound FKBP12 to nitrocellulose membrane. The stepwise electrotransfer of bound ligates onto nitrocellulose as described (Vandenbroeck, K., et al. 2002) has the benefits to find out the strongest binding epitopes. After incubation with anti-FKBP12 antiserum and anti-rabbit IgG peroxidase conjugate, the visualization was performed by ECL system ([Fig. 2-20](#)).

#### Human FAP48 sequence

1	11	21	31	41	51
MAVEELQSII	KRCQILEEQD	FKEEDFGLFQ	LAGQRCIEEG	HTDQLLEIIQ	NEKNKVIIKN
MGWNLVGPVV	RCLLCKDKED	SKRKVYFLIF	DLLVKLCNPK	ELLLGLLELI	EEPSGKQISQ
SILLLLQPLQ	TVIQKLHNKA	YSIGLALSTL	WNQLSLLPVP	YSKEQIQMDD	YGLCQCCKAL
IEFTKPFVEE	VIDNKENSLE	NEKLDKDELLK	FCFKSLKCPL	LTAQFFEQSE	EGGNDPFRYF
ASEIIGFLSA	IGHFPFKMIF	NHGRKKRTWN	YLEFEEEEENK	QLADSMASLA	YLVFVQGIHI
DQLPMVLSPL	YLLQFNMGHI	EVFLQRTEES	VISKGLELLE	NSLLRIEDNS	LLYQYLEIKS
FLTVPQGLVK	VMTLCPIETL	RKSLAMLQL	YINKLDSQ GK	YTLFREHVTT	NGLQDHS

**Fig. 2-19** The sequence of human FAP48 (Swiss-Prot: Q92990) used for the immobilized peptide scan experiments.

Three distinct regions of FAP48 peptides have been found to have strong interactions with FKBP12 (Fig. 2-20, A) with the corresponding peptide sequences shown in the table (Fig. 2-20, B). The deduced binding sites in these three regions all contain one proline in the sequence, which is very important for being the binding targets for FKBP12, because FKBP12 as a PPIase binds to substrates containing proline. Three out of total fifteen prolines in FAP48 have been observed to be involved in the binding epitopes to FKBP12. Especially, the found epitopes corresponding to spots C27-C30 and D30-D35 contain Pro<sup>219</sup> and Pro<sup>309</sup>, respectively. These two Pro residues had already been elucidated to be very important for the binding of FAP48 to FKBP12. The substitution of Pro<sup>219</sup> or Pro<sup>309</sup> by Ala individually leads to a loss or decrease of the interaction between FAP48 to FKBP12 (Neye, H. 2001).

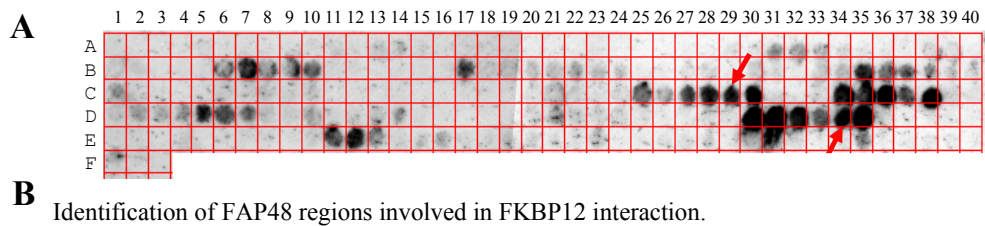


**Fig. 2-20** Binding of FKBP12 to peptide scans derived from the FKBP associated protein 48 (FAP48). The overlapping 13-mer peptides frame-shifted by two residues spanning the sequence of FAP48 were synthesized on cellulose by SPOT method. The peptide scans were probed with FKBP12 (200 nM) and the binding was detected after second electrotransfer of cellulose-bound FKBP12 to nitrocellulose membranes by Western blot assay (see methods section). **(A)** The visualized signals of the second-round transferring of the bound FKBP 12 to nitrocellulose (0.8 mA/cm<sup>2</sup>, 60 min) detected by Western blot assay. **(B)** The main binding regions with the corresponding sequences on FAP48 were shown in the table.

The peptide sequences of the spots pointed with red arrow correspond to spot (C29) with sequence of Ac-KCPLLTAQFFEQS and spot (D34) with sequence of Ac-LSPLYLLQFNMGH showing signals (positive). Spot (E21) with sequence of Ac-FLTVPQGLVKVMT gives no signal (negative).

### 2.3.1.2 Mapping binding epitopes on FKBP12 to FAP48 using Janus-peptide arrays

The easy way to map the binding epitopes on FKBP12 involved in the interactions would use the same strategy by synthesizing peptide scan of FKBP12 and probing with

FAP48. However, such strategy is not feasible because FAP48 and its antibody are not available in substance. This problem could be solved by using Janus-peptide array described ([Scheme 2-1](#)) and through this way; the interaction sites on FKBP12 to FAP48 can be characterized.

Series of 13-mer peptides spanning the complete FKBP12 sequence ([Fig. 2-21](#)) and with a 2-amino-acid shift were synthesized to Fmoc site of template 2 on predefined spots. Another Dde site of the template was synthesized with one of the three peptides derived from FAP48. Two of them are involved in the already known binding epitopes to FKBP12 containing the key Pro<sup>219</sup> in sequence KCPLLTAQFFEQS (Lys<sup>217</sup>-Ser<sup>229</sup> of FAP48) and Pro<sup>309</sup> in sequence LSPLYLLQFNMGH (Leu<sup>307</sup>-His<sup>319</sup> of FAP48), which corresponded to spots C29 and D34 in [Fig. 2-20](#), respectively. The last peptide, not a binding epitope on FAP48 to FKBP12, was derived from spot E21 which gave no signal in [Fig. 2-20](#) with the sequence FLTVPQGLVKVMT (Phe<sup>361</sup>-Thr<sup>373</sup> of FAP48). After synthesis of the Janus-peptide arrays on cellulose, the peptide membranes were incubated to equilibrium with FKBP12 (200 nM) and the detection is performed based on anti-FKBP12 antiserum and anti-rabbit IgG peroxidase conjugate recognitions after electrotransfer of the bound FKBP12 onto nitrocellulose.

### Human FKBP12 sequence

1	11	21	31	41	51
GVQVETISPG	DGRTFPKRGQ	TCVVHYTGML	EDGKKFDSSR	DRNKPFKFML	GKQEVIRGWE
EGVAQMSVGQ	RAKLTISPDY	AYGATGHPGI	IPPHATLVFD	VELLKLE	

**Fig. 2-21** The sequence of human FKBP12 (Swiss-Prot: P20071) used for peptide scan in Janus-peptide arrays experiments.

Peptides KCPLLTAQFFEQS and LSPLYLLQFNMGH, corresponding to spot C29 and spot D34 respectively ([Fig. 2-20](#)), are the binding epitopes on FAP48 to FKBP12. The binding epitopes on FKBP12 to FAP48 can be judged by Janus peptide array through exploring the peptide-peptide interactions between peptide scan of FKBP12 and peptide Ac-KCPLLTAQFFEQS pairs ([Fig. 2-22](#)), or between peptide scan of FKBP12 and peptide Ac-LSPLYLLQFNMGH pairs ([Fig. 2-23](#)). The similar regions, either spots no. A15 to A25 in [Fig. 2-22](#) or spots no. A13 to A25 in [Fig. 2-23](#), have been found showing continuous weak signals (panel A) relevant to the higher positive arbitrary units (panel B). These results indicate that the residues of FKBP12 corresponding to these spots are involved in the

interactions to the peptide epitopes derived from FAP48. The corresponding sequences are residues Met<sup>29</sup>-Glu<sup>61</sup> of FKBP12 in [Fig. 2-22](#) and residues His<sup>25</sup>-Glu<sup>61</sup> of FKBP12 in [Fig. 2-23](#), respectively, which are considered to be the binding sites on FKBP12 to FAP48.

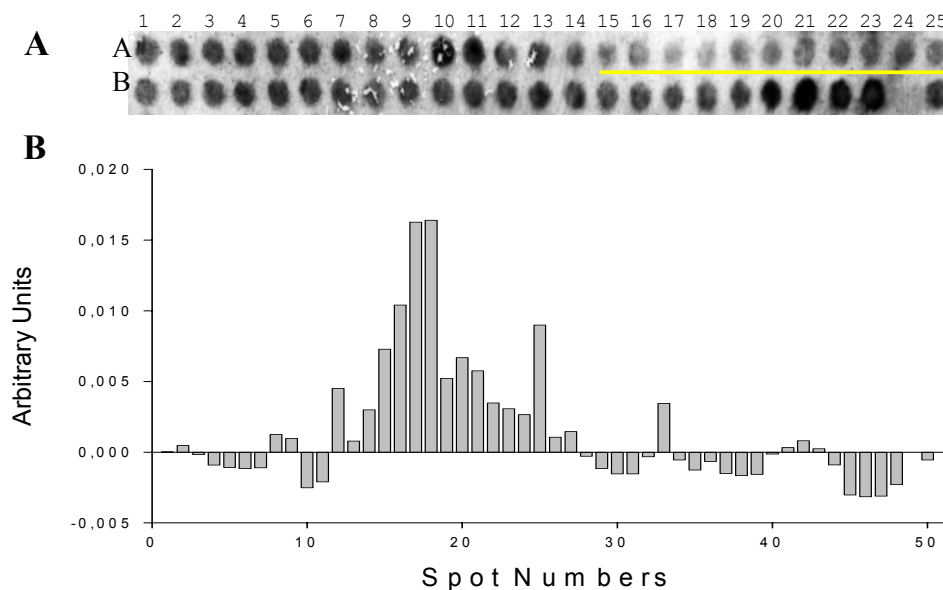


**Fig. 2-22** Interactions between 48 overlapping peptides derived from FKBP12 and peptide Ac-KCPLLTAQFFEQS from FAP48 (Lys<sup>217</sup>-Ser<sup>229</sup>). Peptide scan (13-mers with a 2-amino-acid shift) of FKBP12 were synthesized on cellulose membrane to Fmoc site of template 2 while peptide Ac-KCPLLTAQFFEQS was synthesized to Dde site. The Janus-peptide membrane was probed by FKBP12 (200 nM) and the binding was detected after electrotransfer of cellulose-bound FKBP12 onto a nitrocellulose membrane by Western blot assay (see methods section). **(A)** The visualized signals of Western blot assay, with yellow underline for spots giving weak signals. **(B)** Densitometry analysis of each spots in panel A by Gel-Pro Analyzer (Media Cybernetics). Note: spots A1-A25 (panel A) correspond to spots 1-25 (panel B), and spots B1-B25 correspond to spots 26-50 (panel B). The definition of ‘Arbitrary Units’ see legend in [Fig. 2-15](#).

Spots (No. A15-A25) in panel A with yellow underline as well as spots (15-25) in panel B showing continuous positive units represent the interaction sequences in FKBP12 from residues Met<sup>29</sup> to Glu<sup>61</sup>.

Spot (No. B25) as a control represents that only peptide Ac-KCPLLTAQFFEQS was immobilized on template to the Dde site, no another peptide chain on the Fmoc site.

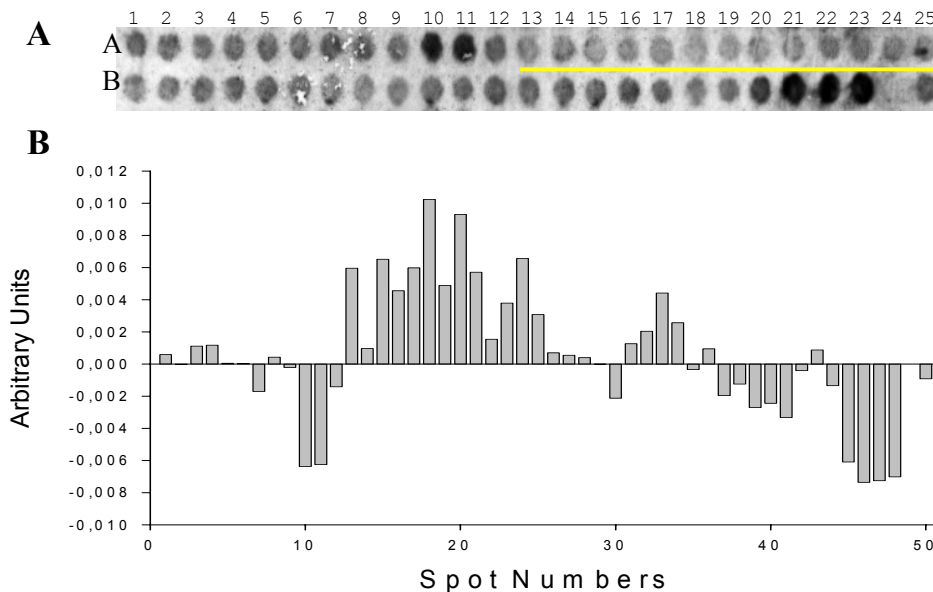


**Fig. 2-23** Interactions between 48 overlapping peptides derived from FKBP12 and peptide Ac-LSPLYLLQFNMGH from FAP48 (Leu<sup>307</sup>-His<sup>319</sup>). Peptide scan (13-mers with a 2-amino-acid shift) of FKBP12 were synthesized on cellulose membrane to Fmoc site of template 2 while peptide Ac-LSPLYLLQFNMGH was synthesized to Dde site. The Janus-peptide membrane was probed by FKBP12 (200 nM) and the binding was detected after electrotransfer of cellulose-bound FKBP12 onto a nitrocellulose membrane by Western blot assay (as described in material and methods). **(A)** The visualized signals of Western blot assay, with colored underlines for spots giving weak signals. **(B)** Densitometry analysis of each spot in panel A by Gel-Pro Analyzer (Media Cybernetics). Note: spots A1-A25 (panel A) correspond to spots 1-25 (panel B), and spots B1-B25 correspond to spots 26-50 (panel B). The definition of ‘**Arbitrary Units**’ see legend in [Fig. 2-15](#). Spots (No. A13-A25) in panel A with yellow underline as well as spots (13-25) in panel B showing continuous positive units represent the interaction sequences in FKBP12 from residues His<sup>25</sup> to Glu<sup>61</sup>. Spot (No. B25) as a control represents that only peptide Ac-LSPLYLLQFNMGH was synthesized on template to the Dde site, no another peptide chain on the Fmoc site.

As a comparison (control experiment), peptide Phe<sup>361</sup>-Thr<sup>373</sup> of FAP48, which represents non binding epitope for FKBP12 was chosen to create Janus-peptide arrays for the investigation of the interactions between overlapping peptides derived from FKBP12 and this peptide (Phe<sup>361</sup>-Thr<sup>373</sup> of FAP48) ([Fig. 2-24](#)). Since sequence Phe<sup>361</sup>-Thr<sup>373</sup> (corresponding to spot E21 in [Fig. 2-20](#)) was not a binding epitope on FAP48 to FKBP12, it is expected (as it is) to observe no signals in most of the spots shown in [Fig. 2-24](#). Except that several spots (B21-B23) showed signals due to the binding of FKBP12 to the FKBP12 derived peptides (data not shown here, but with the same signal pattern as shown in [Fig. 2-24](#) after probing of FKBP12 to peptide scan of FKBP12 membrane and being detected by Western blot analysis).



**Fig.2-24** Interactions between 48 overlapping peptides derived from FKBP12 and peptide Ac-FLTVPQGLVKVMT of FAP48 (Phe<sup>361</sup>-Thr<sup>373</sup>). Peptide scans (13-mers with a 2-amino-acid shift) of FKBP12 were synthesized on cellulose membrane to Fmoc site of template 2 while peptide Ac-FLTVPQGLVKVMT was synthesized to Dde site. The Janus-peptide membrane was probed by FKBP12 (200 nM) and the binding was detected after electrotransfer of cellulose-bound FKBP12 onto a nitrocellulose membrane by Western blot assay (see methods section).

Once, pre-incubation of FK506, the natural ligand of FKBP12 ( $K_d$  in a nM level) with FKBP12 in a molar ratio of 5:1 at room temperature for one hour, and then using this mixture to probe the same Janus-peptide membranes used in [Fig. 2-22](#) or [Fig. 2-23](#), which were regenerated for reusing, the visible signals were not detectable ([Fig. 2-25](#)). It was clear that FK506 had blocked the interactions between FKBP12 and the peptide epitopes derived from FAP48 in the assay. Such results indicate that the binding pocket of FKBP12 to the peptide epitopes on FAP48 might be similar as that to FK506. The spots giving signals (B21-B23) are due to the binding of FKBP12 to the FKBP12 derived peptides, however the reasons for the self binding are not clear. This result indicates that this self-binding epitope is not involved in the FK506 binding site of FKBP12.



**Fig. 2-25** FK506 can block the binding of FKBP12 to peptide Ac-KCPLLTAQFFEQS, the binding epitope derived from FAP48 (Lys<sup>217</sup>-Ser<sup>229</sup>). Peptide scans (13-mers with a 2-amino-acid shift) of FKBP12 were synthesized on cellulose membrane to Fmoc site of template 2 while peptide Ac-KCPLLTAQFFEQS was synthesized to Dde site. FKBP12 (0.2  $\mu$ M) was pre-incubated with FK506 (1  $\mu$ M) in MP buffer for 60 min. Then the complex was used as probe to incubate with the Janus-peptide membrane. The binding was detected after electrotransfer of cellulose-bound FKBP12 onto a nitrocellulose membrane by Western blot assay (as described in material and methods).

### 2.3.1.3 Conclusions

Based on all the data we got from the Janus-peptide array experiments and considering that FK506 can block the interactions between FKBP12 and the peptide epitopes derived from

FAP48 (Fig. 2-25), it would not be difficult to depict the binding sites on FKBP12 involved in the binding to FAP48 even the crystal structure of the complex is not available.

The binding epitopes (residues Met<sup>29</sup>-Glu<sup>61</sup>) of FKBP12 to FAP48 found by Janus-peptide array experiments (Fig. 2-22 or Fig. 2-23) were displayed in yellow solid ribbon (Fig. 2-26) locating in the binding pocket of FKBP12 to FK506 already known from crystal structure analysis (Van Duyne, G.D., et al. 1991, Van Duyne, G.D., et al. 1993). The key amino acids known to be important to the interaction with FK506 (Fischer, G. 1994, Wilson, K.P., et al. 1995), such as Phe<sup>36</sup>, Asp<sup>37</sup>, Arg<sup>42</sup>, Phe<sup>46</sup>, Val<sup>55</sup>, Ile<sup>56</sup> and Trp<sup>59</sup>, which were included in the found epitope Met<sup>29</sup>-Glu<sup>61</sup> of FKBP12, were displayed with their side chains in red CPK (Fig. 2-26) or red stick (Fig. 2-27).

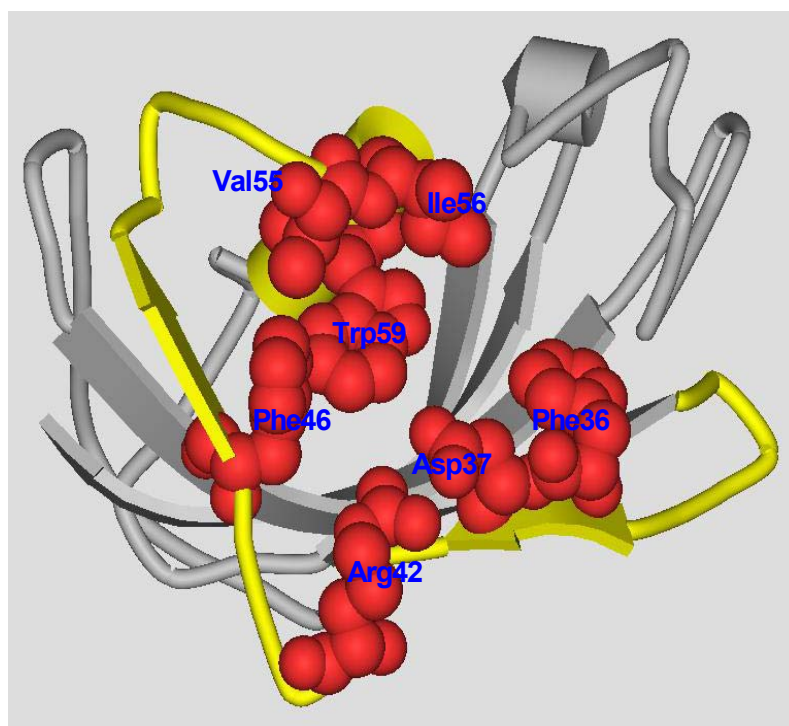


**Fig. 2-26** The structure of FKBP12 is shown in grey solid ribbon (Wilson, K.P., et al. 1995, PDB entry 1FKK). The yellow solid ribbon region is the binding site of FKBP12 to peptide epitopes on FAP48 found by Janus-peptide array experiments (Fig. 2-22 and Fig. 2-23). The corresponding sequence of this region is Met<sup>29</sup>-Glu<sup>61</sup> of FKBP12 including the key amino acids in the binding pocket of FKBP12 to FK506, such as Phe<sup>36</sup>, Asp<sup>37</sup>, Arg<sup>42</sup>, Phe<sup>46</sup>, Val<sup>55</sup>, Ile<sup>56</sup>, Trp<sup>59</sup> (displayed in red CPK).

Some of the other key amino acids that were not observed by Janus-peptide array experiments but also involved in the binding to FK506, such as Tyr<sup>26</sup>, Tyr<sup>88</sup>, His<sup>87</sup>, Ile<sup>91</sup> and Phe<sup>99</sup>, were shown in blue stick (Fig. 2-27).

If FAP48 were a substrate protein to FKBP12, we would expect binding to the active site. Interpretation of Janus experiment results, we can clearly see that the found binding epitopes on FKBP12 are exactly located in the known binding pocket of FKBP12 to FK506. Additionally, FK506 can block the binding between peptide epitope derived from FAP48 and FKBP12 (Fig. 2-25) also indicating that both FK506 and peptide epitope bound to the similar binding pocket of FKBP12. Therefore, by using Janus-peptide array strategy, we found the expected binding site between FAP48 and FKBP12. However, the FKBP12 structure is only known in complex with FK506, but not with peptide substrate. The binding region for natural substrate was deduced from above mentioned structure (Van Duyne, G.D., et al. 1991) illustrating the interacting sequence stretches. In the case of binding to proteins or peptide substrates, a different extended binding region would be possible. Therefore, although it was known that FKBP12 only has one hydrophobic binding pocket, it is possible that the binding regions to the peptide epitopes on FAP48 are not exactly the same as those to FK506.

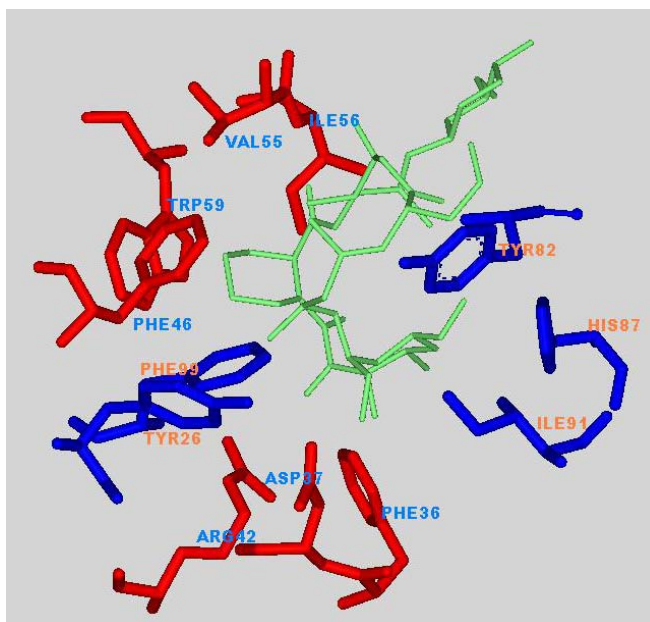


**Fig. 2-27** View of the key residues in the binding pocket of FKBP12 complexed with FK506 (Wilson, K.P., et al. 1995, PDB entry 1FKJ). FK506 is displayed as light green sticks. Key amino acids in FKBP12 binding pocket found by Janus-peptide array are displayed with their side chains in red sticks while the unfound key amino acids in blue sticks.

### 2.3.2 Example II: FKBP12/EGFR cytosolic domain (residues 645-1186) interaction

#### 2.3.2.1 Mapping binding epitopes on EGFR (Arg<sup>645</sup>-Ala<sup>1186</sup>) to FKBP12 by standard SPOT strategy

First, we wanted to find out the potential binding epitopes on EGFR cytosolic domain (Fig. 2-28) which might be involved in the binding to FKBP12. The potential binding epitopes on EGFR cytosolic domain can be easily mapped by applying the standard SPOT technology through synthesis of the peptide scan of EGFR (residues 645-1186) on cellulose membrane with overlapping oligopeptides of 13-mers shifted by one amino acids and probed by FKBP12, followed by Western blot analysis (Fig. 2-29). The stepwise electrotransfer of bound FKBP12 to nitrocellulose had been performed to screen out the strongest binding epitopes.

#### EGF receptor cytosolic domain's sequence (645-1186)

650	660	670	680	690	700
RRRHIV	RKRTLRLRLQ	ERELVEPLTP	SGEAPNQALL	RILKETEFKK	IKVLGSGAFG
TVYKGLWIPE	GEKVKIPVAI	KELREATSPK	ANKEILDEAY	VMASVDNPHV	CRLLGICLTS
TVQLITQLMP	FGCLLDYVRE	HKDNIGSQYL	LNWCVQIAKG	MNYLEDRLV	HRDLAARNVL
VKTPQHVKIT	DFGLAKLLGA	EEKEYHAEGG	KVPIKWMAL	SILHRIYTHQ	SDVWSYGVTV
WELMTFGSKP	YDGIPASEIS	SILEKGERLP	QPPICTIDVY	MIMVKCWMID	ADSRPKFREL
IIEFSKMARD	PQRYLVIQGD	ERMHLPSPTD	SNFYRALMDE	EDMDDVVDAD	EYLIPQQGFF
SSPSTSRTP	LSSLSATSNN	STVACIDRNG	LQSCPIKEDS	FLQRYSSDPT	GALTEDSIDD
TFLPVPEYIN	QSVPKRPAGS	VQNPVYHNQP	LNPAPSRDPH	YQDPHSTAVG	NPEYLNTVQP
TCVNSTFDSP	AHWAQKGS HQ	ISLDNPDYQQ	DFFPKEAKPN	GIFKGSTAEN	AEYLRVAPQS
SEFIGA					

**Fig. 2-28** The sequence of human EGFR (SWISS : P00533) cytosolic domain (residues 645-1186) used for the immobilized peptide scan experiments. The residues of signal sequence are not counted here.

Several regions show continuous strong signals. With yellow underlines (Fig. 2-29, A) depicted, they are considered to be the binding epitopes on EGFR cytoplasmic domain (Arg<sup>645</sup>-Ala<sup>1186</sup>) to FKBP12. In this experiment, only the regions that contain six or more than six continuous spots giving strong signals are of interest, because the overlapping peptides

only shifted by one amino acid. Therefore, the peptide sequences corresponding to six continuous spots here are just relevant to two continuous spots in standard peptide scan strategy where the overlapping peptides are shifted by three amino acids. The corresponding peptide sequences are shown in [Fig. 2-29](#) (B). The corresponding sequences of these regions all contain one proline that is necessary for being the substrate for FKBP12. Among all these potential binding epitopes, spots H22-H27, which correspond to the sequence Lys<sup>946</sup>-Met<sup>963</sup> of EGFR contain the distinctive three amino acid sequence Leu<sup>955</sup>-Val<sup>956</sup>-Ile<sup>957</sup> found previously to regulate the transphosphorylation of substrate tyrosines in oligomerized EGFR family complexes. The substitution of Leu<sup>955</sup> impaired the phosphor-transfer activity greatly. A model suggesting direct contact between this segment and another protein has been proposed for the ErbB2/ErbB3 system (Schaefer, G., et al. 1999). However, from the crystal structure of EGF receptor kinase domain, it has been found that Leu<sup>955</sup> was completely buried, which strongly suggested that Leu<sup>955</sup> side chain does not contact another protein (Stamos, J., et al. 2002). Nevertheless, crystal structure only represents one state of conformation proteins adopt under certain condition. It is possible that EGFR cytosolic part underlies complicated conformational changes when it carries out biological functions *in vivo*.

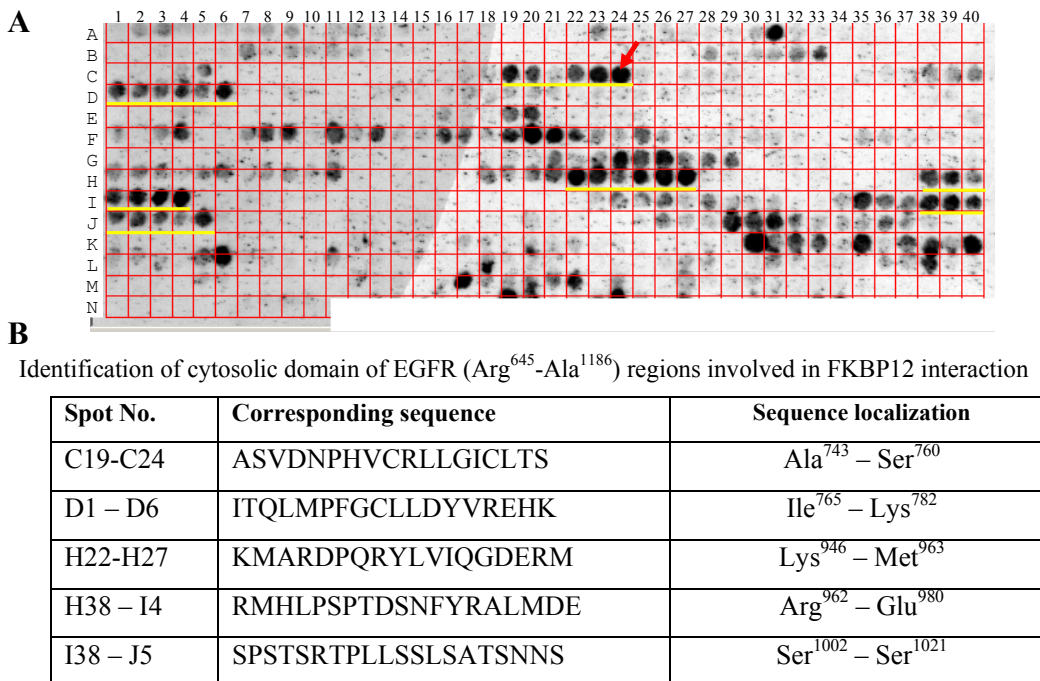


**Fig. 2-29** Binding of FKBP12 to peptide scans derived from the cytosolic domain of EGF receptor (Arg<sup>645</sup>-Ala<sup>1186</sup>). The overlapping 13-mer peptides frameshifted by one residue spanning the sequence from 645 to 1186 of EGF receptor cytosolic domain were synthesized on cellulose by SPOT method. The peptide scans were probed with FKBP12 (200 nM) and the binding was detected after stepwise electrotransfer of cellulose-bound

FKBP12 to a nitrocellulose membrane by Western blot (see methods section). The binding regions were focused on the regions with six or more than six continuous positive spots and were given in the table herein. **(A)** The visualized signals of the second round transferring of the bound FKBP 12 to nitrocellulose ( $0.8 \text{ mA/cm}^2$ , 60 min) detected by Western blot assay. **(B)** The main binding regions with the corresponding sequences on EGFR (Arg<sup>645</sup>-Ala<sup>1186</sup>) were shown in the table. Arrow points to spot (C24) corresponding to N-acetylated peptide PHVCRLLGICLTS.

FK506 has been used as an inhibitor to evaluate the active site-directed specificity of the experiment performed in [Fig. 2-29](#) by SPOT methodology. Firstly, FK506 was pre-incubated with FKBP12 in a molar ratio of 4:1 for 1 hr at room temperature. Subsequently, the mixture was used to probe the peptide membrane, the same membrane used in the experiment of [Fig. 2-29](#) after regeneration (materials and methods). After first round electrotransfer of the possible bound protein onto nitrocellulose and Western blot analysis, all regions with strong signals in [Fig. 2-29](#) did not show any visible signals ([Fig. 2-30](#)). It is clear that FK506 has blocked the binding of FKBP12 to the potential binding epitopes found in [Fig. 2-29](#), which are considered to interact with the same binding pocket as that to FK506. The binding study of FKBP12 to the peptide scan derived from the reverse sequence of EGFR cytosolic domain showed no interactions (data not shown). These results indicated that the epitopes found by SPOT method in [Fig. 2-29](#) were specific.

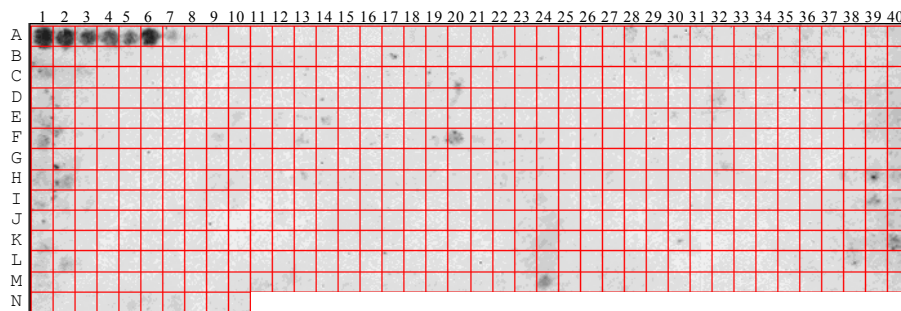


**Fig. 2-30** FK506 blocks the binding of FKBP12 to peptide scans of the cytosolic domain of EGF receptor (Arg<sup>645</sup>-Ala<sup>1186</sup>). The overlapping 13-mer peptides frameshifted by one residue spanning the sequence from 645 to 1186 of EGF receptor cytosolic domain were synthesized on cellulose by SPOT method. FKBP12 (50  $\mu\text{g}$ ) was pre-incubated with FK506 (10  $\mu\text{g}$ ) in MP buffer at room temperature for 60 min. The immobilized peptide membrane was then probed with the FKBP12/FK506 complex with the final concentrations of 200 nM FKBP12 and 800 nM FK506. The binding was detected after electrotransfer of cellulose-bound FKBP12 to a nitrocellulose membrane by Western blot assay (as described in material and methods). The figure shows the result of the first round transferring of the bound FKBP 12 to nitrocellulose ( $0.8 \text{ mA/cm}^2$ , 90 min) followed by Western blot assay. The only region found to interact, spots A1-A6, corresponds to sequence RRRHIVRKRTLRLQLQER (residues Arg<sup>645</sup>-Arg<sup>662</sup> of EGFR).

Only spots A1-A6 show continuous visible signals (Fig. 2-30) with the corresponding sequences of RRRHIVRKRTLRLQLER (residues Arg<sup>645</sup>-Arg<sup>662</sup> of EGFR). The interaction of FKBP12 to this region indicates that another binding site might exist which is distinct from the known binding pocket of FKBP12 to FK506. However, the interaction between FKBP12 to this region is weak, because such kind of interaction cannot be detected after the second round electrotransfer of the bound FKBP12 onto nitrocellulose (Fig. 2-29, spots A1-A6). The reason for the interaction of FKBP12 to this epitope is not clear yet.

### *2.3.2.2 The inhibitory activities (IC<sub>50</sub>) of several peptide epitopes derived from EGFR on the PPIase activity of FKBP12*

Several peptide epitopes that had been found to be the binding epitopes on EGFR to *h*FKBP12 by standard SPOT method (Fig. 2-29) have been synthesized to evaluate their inhibitory activities on the PPIase activity of FKBP12. They are Ac-DNPHVCRLLGICLTS-NH<sub>2</sub> (residues Asp<sup>746</sup>-Ser<sup>760</sup> of EGFR), Ac-QLMPFGCLLDYVREH-NH<sub>2</sub> (residues Gln<sup>767</sup>-His<sup>781</sup> of EGFR) and Ac-MARDPQRYLVIQGDE-NH<sub>2</sub> (residues Met<sup>947</sup>-Glu<sup>961</sup> of EGFR) which correspond to spots C22-C24, D3-D5 and H23-H25 in Fig. 2-29, respectively. Another peptide which was not involved in the binding epitopes of EGFR to *h*FKBP12 active site was also synthesized to be used as a negative control. This peptide is Ac-ETEFKKIKVLGSGA-NH<sub>2</sub> (residues Glu<sup>685</sup>-Ala<sup>698</sup>) corresponding to spots B1-B2 in Fig. 2-29.

The inhibitory activities of the peptides on the PPIase activity of FKBP12 were analyzed by first incubating of *h*FKBP12 with various concentrations of soluble peptides for 30 min at 10 °C and then measuring the residual PPIase activity of *h*FKBP12 by using the protease-free assay (Janowski, B., et al. 1997) towards substrate Suc-Ala-Phe-Pro-Phe-pNA. The inhibitory constant (IC<sub>50</sub>) of each peptide was then calculated and tabulated (Table 2-1). The results had clearly shown that three peptide epitopes on EGFR found by standard SPOT method (Fig. 2-29) showed inhibitory activities on PPIase activity of *h*FKBP12 as soluble peptides with the IC<sub>50</sub> at the μM level (Table 2-1, entry 1 to 3). The control peptide which was not found to be a binding epitope to *h*FKBP12 showed no or very weak inhibitory activity as a soluble peptide and its IC<sub>50</sub> was higher than 5 mM (Table 2-1, entry 4). The results for the inhibition of FKBP12 by the corresponding soluble peptides showed good agreement with the results found by standard SPOT method. The found binding epitopes showed inhibitory activities on PPIase activity of *h*FKBP12, however, the IC<sub>50</sub> of them was

not directly proportional to the binding intensity in the solid phase binding assay. It is known that most peptide substrates of FKBP12 have high  $K_m$  values (hundreds of  $\mu\text{M}$ ) for binding to FKBP12, e.g. Suc-Ala-Leu-Pro-Phe-pNA revealing a  $K_m$  of around 520  $\mu\text{M}$  (Kofron, J.L., et al. 1991). The  $\text{IC}_{50}$  values of EGFR derived peptides, in terms of active site affinity, are also in the same range (Table 2-1, entry 1 to 3), therefore these peptides are considered to be the substrates for binding to the active site of FKBP12. The results indicate that the direct interaction could be occurred between FKBP12 and EGFR cytosolic domain.

**Table 2-1**  $\text{IC}_{50}$  of EGFR derived peptides on the PPIase activity of hFKBP12

	Peptides	$\text{IC}_{50}$ of hFKBP12 inhibition <sup>a</sup>
1.	Ac-DNPHVCRLLGICLTS-NH <sub>2</sub>	390 $\mu\text{M}$ <sup>b</sup>
2.	Ac-QLMPFGCLLDYVREH-NH <sub>2</sub>	350 $\mu\text{M}$ <sup>b</sup>
3.	Ac-MARDPQRYLVIQGDE-NH <sub>2</sub>	230 $\mu\text{M}$ <sup>b</sup>
4.	Ac-ETEFKKIKVLGSG-NH <sub>2</sub>	> 5 mM

<sup>a</sup> Protease-free assay. <sup>b</sup> Deviation is less than 20 %.

### 2.3.2.3 Mapping binding epitopes on FKBP12 to EGFR (Arg<sup>645</sup>-Ala<sup>1186</sup>) by using Janus-peptide arrays

We used the same Janus-peptide array strategy as performed in previous protein-ligand or protein-protein interaction models to map the binding sites on FKBP12 involved in the interactions to EGFR cytoplasmic domain. For this reason Janus-peptide array was synthesized with a peptide scan of FKBP12 (13-mer peptides with a 2-amino-acid shift) on Fmoc site of template 2 and one of the peptide epitopes (Ac-PHVCRLLGICLTS) which was found to be the binding epitope on EGFR corresponding to the spot C24 (Fig. 2-29) on Dde site. After probing the Janus-peptide membrane by FKBP12 and visualization by the detection system, the visible signals have been quantified by densitometry analysis (Fig. 2-31, B). The similar results have been obtained as compared to the previous experiments (Fig. 2-22 or Fig. 2-23). Spots with continuous weak signals (higher positive arbitrary units in panel B of Fig. 2-31) were focused in the regions from spot no. A15 to B3 corresponding to the residues Met<sup>29</sup> to Ser<sup>67</sup> of FKBP12 (Fig. 2-31).

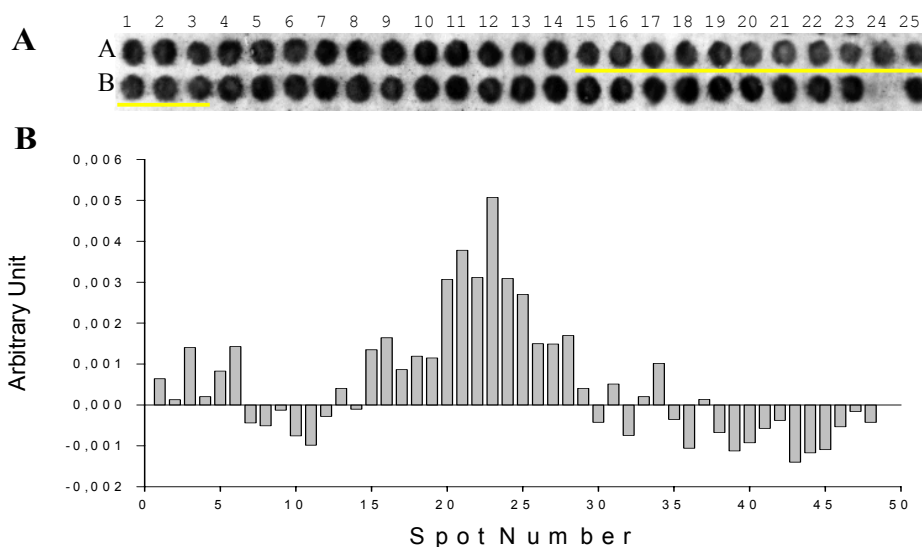
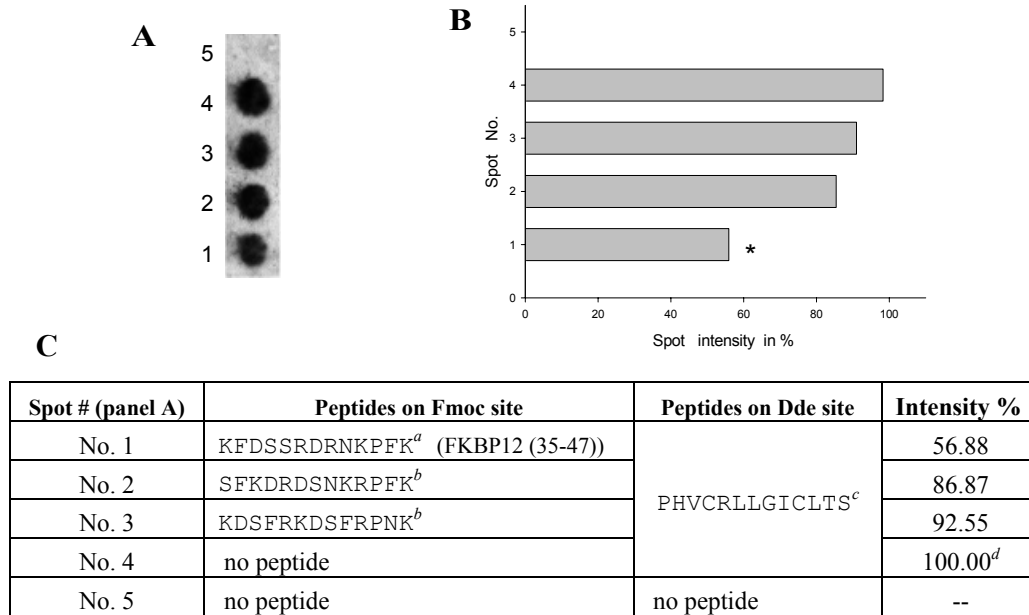


**Fig. 2-31** Interactions between 48 overlapping peptides derived from FKBP12 and peptide Ac-PHVCRLLGICLTS from EGFR (Pro<sup>748</sup>-Ser<sup>760</sup>). **(A)** Peptide scans (13-mers with a 2-amino-acid shift) of FKBP12 were synthesized on cellulose membrane to Fmoc site of template 2 while peptide Ac-PHVCRLLGICLTS was synthesized to Dde site. The Janus-peptide arrays were probed by FKBP12 and the binding was detected after electrotransfer of cellulose-bound FKBP12 onto a nitrocellulose membrane by Western blot analysis (see methods section). **(B)** Densitometry analysis of each spot in panel A by Gel-Pro Analyzer (Media Cybernetics). Note: spots A1-A25 (panel A) correspond to spots 1-25 (panel B), and spots B1-B25 correspond to spots 26-50 (panel B). The definition of ‘Arbitrary Units’ see legend in Fig. 2-15. Spots (No. A15-B3) in panel A with yellow underline as well as spots (15-28) in panel B showing continuous positive units represent the interaction sequences in FKBP12 from amino acid Met<sup>29</sup> to Ser<sup>67</sup>. Spot (No. B25) as a control represents that only peptide Ac-PHVCRLLGICLTS was synthesized on template to the Dde site, no another peptide chain on the Fmoc site.

#### 2.3.2.4 Interactions between Janus-peptide pairs are sequence dependent

One control experiment to evaluate the specificity of the interactions between Janus-peptide chains has been performed as shown in Fig. 2-32. Several Janus-peptide pairs had been synthesized based on one interacting peptide pair derived from spot no. 18 in Fig. 2-31.

As shown in Fig. 2-32, spot no. 1 corresponds to this original interacting peptide pair, with residues Lys<sup>35</sup>-Lys<sup>47</sup> of FKBP12 on Fmoc site and Pro<sup>748</sup>-Ser<sup>760</sup> of EGFR (peptide epitope for binding to FKBP12) on Dde site. The peptide chains on Fmoc site of spot no. 2 and 3 are the randomized sequence orders derived from residues Lys<sup>35</sup>-Lys<sup>47</sup> of FKBP12 (Fig. 2-32, C). After performing the blot experiment probed by FKBP12 and detected by antibodies, the visible signals were shown in Fig. 2-32 (A), and the corresponding quantified densities of each spots were shown in Fig. 2-32 (B).



<sup>a</sup> This peptide has interaction with the peptide coupled on Dde site (spot 18 in Fig. 2-31). <sup>b</sup> These peptides are the random sequence order of residues Lys<sup>35</sup>-Lys<sup>47</sup> of FKBP12 synthesized on spot no. 1. <sup>c</sup> This peptide is derived from EGFR (Pro<sup>748</sup>-Ser<sup>760</sup>) and was the epitope recognized by FKBP12 (spot C24 in Fig. 2-29), <sup>d</sup> This spot with the highest intensity was set to 100%. \* The intensity of spot no.1 has prominent difference to that of spot no. 4.

**Fig. 2-32** Investigation of the interactions between some controlled Janus-peptide pairs to evaluate the specificities. **(A)** Some immobilized Janus-peptide pairs are probed by FKBP12, and visualized by Western blot experiment (see materials and methods). **(B)** The Janus-peptide pairs vary in their interactions which showing different binding abilities to FKBP12 probe. The degree of binding to FKBP12 was determined by densitometry analysis of each spot by Gel-Pro Analyzer (Media Cybernetics). **(C)** The detailed information of Janus-peptide pairs synthesized on membrane for probing by FKBP12 is shown in panel A. The N-terminal of all Janus-peptide pairs is blocked by an acetyl group.

From the results we can clearly see that only the peptide pair (synthesized on spot no.1) containing the original primary sequence from FKBP12 (residues Lys<sup>35</sup>-Lys<sup>47</sup>) shows the significantly decreased signal intensity as compared with that of spot no. 4 which contains only the epitope peptide Pro<sup>748</sup>-Ser<sup>760</sup> of EGFR. The other two spots (no. 2 and no. 3) which contain the peptide sequences with the same amino acid compositions but randomized in sequence orders derived from residues Lys<sup>35</sup>-Lys<sup>47</sup> of FKBP12 display the similar signal intensities as that of spot no. 4, and show the prominent difference to that of spot no. 1 ([Fig. 2-32](#)) as well.

The conclusions from the results in [Fig. 2-32](#) are that Janus-peptide chains with original primary sequences show interactions with each other whereas those with randomized

sequences do not. Therefore, it strongly indicates that the outputs of Janus-peptide array experiments could represent the naturally occurred interactions between the binding epitopes of the interacting complexes, and depend largely on the primary sequences in the original binding protein partners. Since the primary sequences of certain proteins are specified, it would lead to higher possibilities of the specificities achieved by Janus-peptide array experiments. The slight decrease in the signals of spot no. 2 and no. 3 as compared with that of spot no. 4 might due to the existing of some interference from the second peptide chain, however, such influences were not very significant.

### *2.3.2.5 Conclusions*

With all the information got from the experiments above, we can conclude that we can map the potential interaction sites between FKBP12 and EGFR cytoplasmic domain since several potential binding epitopes on both proteins had been found by combining standard SPOT method and Janus-peptide array. The observed inhibitory activities ( $IC_{50}$ ) of the soluble peptide epitopes derived from EGFR cytosolic domain found by the standard SPOT method on the PPIase activity of FKBP12 (Table 2-1, entry 1 to 3) show to be in the same range as the  $K_m$  of known peptide substrates for FKBP12 (Kofron, J.L., et al. 1991, Harrison, R.K. and Stein, R.L. 1992). These results indicate that also the soluble peptides derived from EGFR cytosolic domain are able to interact with the substrate binding site of FKBP12, and therefore suggesting the interaction between FKBP12 and EGFR cytosolic domain. Residues Met<sup>29</sup> to Ser<sup>67</sup> of FKBP12, corresponding to the found binding epitope on FKBP12 by using Janus-peptide array (Fig. 2-31) are located in the binding pocket of FKBP12 to FK506, and contain the key amino acids involved in the binding to FK506, as already discussed in section **2.3.1.3**. Again, it has been clearly shown that the active site of FKBP12 was involved in the interaction with EGFR cytosolic domain. However, the binding interface of FKBP12 to EGFR cytosolic domain is not necessarily exact the same as that binding to FK506.

## **2.4 General properties of Janus-peptide arrays**

The basic research of site-site interaction of two peptides immobilized on the solid support and the establishment of a novel approach in analyzing such matrix-bound peptide-

peptide interaction, called Janus-peptide array, using known protein-ligand interaction models were described in this dissertation. The further successful application in identifying the interaction sites of protein-protein complexes strongly indicates that Janus-peptide array approach based on the idea of matrix-bound peptide-peptide interaction to mimic protein-protein interactions is a very flexible and simple method in the study of protein recognition sites compared to conventional protein interaction analyses (Phizicky, E. and Fields, S. 1995).

Limitations are often met during the study of the interaction sites between two proteins, for instance, that one of the binding partners is not available or the chemical properties of the protein do not allow handling in biochemical analysis. The development of Janus-peptide array is to overcome such kind of limitations and to establish an approach for mapping binding sites of two proteins not necessarily depending on the availability of the proteins but on the primary sequences of the proteins. The knowledge of the existence of the direct interactions between two binding partners is required. The Janus method is based on the SPOT technology (Frank, R. 1992), so it keeps the advantages of SPOT method as well as potential drawbacks ([Table 1-2](#)). The benefits of using Janus-peptide array to depict the binding epitopes on protein to its peptide ligand are prominent, like in streptavidin/*Strep*-tag II interaction (section **2.2.1**) and 14-3-3/phosphopeptides interaction (section **2.2.2**). In case of mapping protein-protein interaction sites, the combination of conventional SPOT method and Janus-peptide array established here have shown to be efficient even when one of the interacting proteins is not available as native protein.

### **2.4.1 The properties of Janus-peptide arrays**

It is assumed that once two matrix-bound peptides representing the interacting linear epitopes derived from protein complex synthesized onto one carrier molecule, they will also interact. The analysis of matrix-bound peptide-peptide interactions, called Janus-peptide array, is based on the competition mechanism as depicted in [Scheme 2-1](#).

In a folded protein, normally amino-acid stretches form regular secondary structure elements such as the helices, sheets or turns. Secondary structures give ordered spatial arrangement of side chains, which is not found in the random coil like structures. Sequence stretches involved in the binding epitopes at protein-protein interfaces are frequently found to participate in the formation of secondary structure elements in the intact protein (Bogan, A.A. and Thorn, K.S. 1998). Protein-protein interactions via surface accessible interaction sites which involve amino acid residues and backbone contacts are often mediated by these

secondary structural elements, for instance, the interaction between c-Jun homodimer is mediated by helix-loop-helix leucine zipper domain (Junius, F.K., et al. 1996). Nevertheless, the chemical properties of the peptide stretches themselves regardless of structure formation are very important in contributing to the interaction, such as charged residues mediate low affinity protein-protein recognition at the cell surface (Davis, S.J., et al. 1998) and primary sequence of peptides usually plays important roles in antigen-antibody recognition events.

The conformation of the peptide on solid surface becomes to be a well-concerned question in Janus-peptide array, because the mapping of protein-protein interaction sites is based on exploring peptide-peptide interactions on solid surfaces. Although investigations have shown that peptides on beads (e.g. PEGA and POEPOP bead) could adopt certain local secondary structures (Furrer, J., et al. 2001, Jelinek, R., et al. 1997), it is yet unclear what happens on solid supports. However, it is known that sterically constrained oligopeptides will adopt induced conformations (section 1.1) or the structures of them will be stabilized, especially peptides being immobilized to the solid supports such as a resin and a cellulose membrane (section 1.1.2). The reduction of conformational entropy of peptides immobilized on solid supports could be the reason that induces the formation of the structures.

Recent results by SPOT synthesis may also help to support the conclusions that peptides on cellulose do form certain local structures. However, whether the structure on cellulose reflects exactly the conformation of the corresponding sequence range in the protein structure where these epitopes are derived from is still under question.

Bluthner and co-workers have shown that the PM/Scl-100 major epitope region might adopt a local alpha-helical secondary structure on cellulose through mutational analysis of the corresponding peptide LDVPPALADFIHQQR (Leu<sup>231</sup>-Arg<sup>245</sup> of PM/Scl-100) by glycine-walk followed by immunodetection (Bluthner, M., et al. 2002, Bluthner, M., et al. 2000). The successful work in the synthesis of functional *de novo* proteins on cellulose membrane based on a combination of the TASP concept (Mutter, M. and Tuchscherer, G. 1997) and the SPOT technique, gives another strong evidence that peptides once assembled onto solid phase coupled template will adopt secondary structures to form four-helix bundle protein motifs. The screening of *de novo* proteins by assembling peptides onto template in a combinatorial manner shows that synthetic proteins can adopt a correct and functional conformation on solid support (Rau, H.K., et al. 2000, Schnepf, R., et al. 2001).

The bases of the Janus-peptide array are: 1) the templates (Fig. 2-2) used in Janus-peptide array offer the advantage to position and to orient two anchored peptide chains; 2) the high peptide density (approx. 100 nmol/cm<sup>2</sup>); 3) the possible secondary structures adopted by

peptides due to the reduction of conformational entropy of covalently bound peptides on solid surface; 4) the existence of possible driving forces for two peptide chains association on the template. Thus, the interactions between two peptides representing the interacting epitopes are probably favored and enhanced once they are synthesized onto one template, because of the higher local peptide densities, in the close proximity they are and the structures they might adopt. Such kind of interactions can be detected in the Janus system, as an example demonstrated in [Fig. 2-8](#), some control Janus-peptide pairs (peptides derived from streptavidin and *Strep*-tag II pairs) either having interactions or not can be easily recognized. In comparison, it has been well accepted that the interactions between short peptides have very low affinities in solution and therefore are not measurable with conventional methods.

### **2.4.2 The potential drawbacks of Janus-peptide arrays**

Several protein-ligand and protein-protein interaction combinations have been selected to establish and evaluate Janus-peptide array. The results showed that most of the interaction sites in protein-protein/ligand complexes were screened out by exploring peptide-peptide interactions on solid supports using Janus method (see [Fig. 2-13](#), [Fig. 2-18](#), [Fig. 2-26](#)).

However, not all binding sites could be found by Janus method. For examples, in 14-3-3 and phosphopeptides complexes, it is known that residues apparently involved in binding to the phosphopeptides are Lys<sup>49</sup>, Arg<sup>56</sup>, Lys<sup>120</sup>, Arg<sup>127</sup>, Tyr<sup>128</sup>, Asn<sup>173</sup>, Leu<sup>216</sup>, Ile<sup>217</sup>, Leu<sup>220</sup>, Asn<sup>224</sup> and Trp<sup>228</sup> which are conserved in all 14-3-3 isotypes (Yaffe, M.B., et al. 1997). However, in 14-3-3 and RQRSTpSTPNV model (section **2.2.2.1**), only some of the major binding epitopes containing key amino acids Lys<sup>49</sup>, Arg<sup>56</sup> (in helix  $\alpha$ 3) as well as Trp<sup>228</sup> (in helix  $\alpha$ 9) have been observed by Janus-peptide array ([Fig. 2-15](#)). In contrast, other key amino acids like Lys<sup>120</sup>, Arg<sup>127</sup>, Tyr<sup>128</sup> (in helix  $\alpha$ 5) and Leu<sup>216</sup>, Ile<sup>217</sup>, Leu<sup>220</sup>, Asn<sup>224</sup> (in helix  $\alpha$ 9) contributing for the interaction (Petosa, C., et al. 1998) have not been detected. While in 14-3-3 and ARSHpSYPA model (section **2.2.2.2**) the key amino acids Leu<sup>216</sup>, Ile<sup>217</sup>, Leu<sup>220</sup>, Asn<sup>224</sup> (in helix  $\alpha$ 9) which are derived from the binding epitope on 14-3-3 were still not able to be detected by Janus-peptide array ([Fig. 2-16](#)), though most of the others were identified.

The incapability in discovering some of the binding epitopes is probably caused by limitations inherent in the Janus-peptide array using short peptides as interaction models. Since protein-protein interactions are usually mediated by relatively large contact interface (Jones, S. and Thornton, J.M. 1996), in most cases proteins have more than one binding sites

to interact with their binding partners. In such discontinuous binding sites the key residues contribution to the binding affinity are normally separated in the primary structure. Therefore, short peptides containing individual parts of these epitopes normally show low affinities to the respective binding partners. Even though Janus-peptide array has, several inherent advantages as already mentioned for increasing the binding affinities between two immobilized peptides on solid surface. Yet the Janus approach still has limitations due to: 1) the sensitivity of the Janus-peptide array is not high enough to promise to find out all the binding sites; 2) the binding epitopes of protein are rarely concentrated in a single element; 3) the immobilized peptide is influenced by the solid surface to have an environment different from that of the corresponding sequence in the intact protein and hence leading to false negative results.

The false positive results by Janus method also cannot be prevented. For example, spots D6-D8 in [Fig. 2-15](#) or spots A9-A16 and E18-F1 in [Fig. 2-16](#) have been found to give weak signals indicating possible interactions between respective anchored peptide pairs on the spots. However, the corresponding sequences were not involved in the binding sites of 14-3-3 to phosphopeptides according to X-ray crystallography (Petosa, C., et al. 1998, Rittinger, K., et al. 1999). The reasons for that could be: 1) regions of a protein which are not surface-exposed in the native structure will be displayed on the spot membrane and may therefore evoke false positive signals but they are not implicated in peptide-peptide interactions; 2) some peptide pairs with certain sequences and combinations have high propensity to induce unspecific electrostatic or hydrophobic interactions. Therefore, the results obtained by Janus-peptide array have to be interpreted with cautions.

The possible incorrectness of the synthetic peptide sequences (e.g. truncated peptide sequences) due to the incompleteness of synthesis caused by possible steric hinderance during synthesis or the unfavorable synthetic conditions SPOT synthesis suffers (e.g. the chemical reaction is processed not in an inert environment but exposure to air), could be another reason to cause false results.

### **2.4.3 The evaluation of the results from Janus-peptide arrays**

Janus-peptide array established herein only provides a semi-quantitative analytical system to determine the interactions between different immobilized peptide pairs individually. It is obvious that the efficiencies of synthesizing variable peptide sequences for the Janus method cannot be exactly same, therefore the amount of correct peptide sequences on each spots always fluctuates in a certain range. In this situation, the small difference can be

amplified during the Western blot analysis afterwards. Another related problem is that, the low signal variation in Janus-peptide arrays during the screening of peptide-peptide interactions should be noted. One example can be found in [Fig. 2-31](#) in the screening of interactions between peptide scan of FKBP12 and peptide Ac-PHVCRLLGICLTS. The differences of the visible signals are very difficult to be judged by eyes. In such situation, densitometry analysis is the best choice for quantifying the signal intensity of each spot objectively. An 'arbitrary unit' had been defined as criteria ([Fig. 2-15](#), legend) in judging the potential interactions between two peptides on each spot.

The preparation of array of peptide scan derived from the reverse sequence of protein can be used as a general way to evaluate the specificity of Janus-peptide array. The found binding epitopes based on the normal protein sequence by Janus method normally could not be detected when based on the reverse protein sequence, because of different primary sequences. However, when binding depends on side-chain interacting, or binding epitope contains symmetric sequence, both normal and reverse sequences could probably be found to be binding epitopes.

Nevertheless, Janus-peptide array provides a good and efficient high-throughput screen approach for preliminarily mapping unknown protein-protein/ligand interaction sites. The potential interaction sites found via Janus method in this report have good agreements with those already known in the literature or from crystal structure analysis. These results strongly indicated that there existed interactions between Janus-peptide pairs anchored on solid support and the site-site interactions of the immobilized peptide pairs could mimic protein-protein interactions. Therefore, Janus-peptide array will provide a good chance to study protein recognition events even in the absent of the native state proteins at hand, but only needs their primary sequences. After analysis by Janus-peptide array, it is possible to direct the further investigation to a binding site. The raw data obtained from Janus analysis can help to focus on the regions of interest and importance in a short time. Since it is the first description of Janus-peptide array, any data obtained by this new approach could be confirmed either through *in vitro* or *in vivo* mutation/deletion analysis or other biochemical assays (e.g. affinity blotting and coimmunoprecipitation). Ideally, structural analysis or theoretical prediction of protein-protein complexes or protein-peptide complexes would provide confirmation of a predicted interaction surface between two proteins.

## 2.5 Thermodynamic and kinetic parameters of the *cis/trans* isomerization of (4)-fluoroproline containing peptides and the influence of PPIases

### 2.5.1 *Cis/trans* isomerization of (4)-fluoroproline containing peptides

A chymotrypsin-coupled assay developed by Fischer (Fischer, G., et al. 1984) was used for delineating the kinetic and thermodynamic parameters of *cis/trans* isomerization of the tertiary amide bond preceding proline and (4)-fluoroproline in model peptides, namely, Suc-Ala-Ser-Pro-Phe-pNA (**1**), Suc-Ala-Ser-(4*R*)-F-Pro-Phe-pNA (**2**), Suc-Ala-Ser-(4*S*)-F-Pro-Phe-pNA (**3**), Suc-Ala-Ser-(4)-diF-Pro-Phe-pNA (**4**). This test exploits the *trans*-isomer specific hydrolysis of these model peptides by chymotrypsin. The fraction of tetrapeptide nitroaniline derivatives with the Xaa-Pro or Xaa-(4)F-Pro bond in *trans* conformation is eliminated from the equilibrium immediately because of the excess of chymotrypsin in the system liberating the chromophoric unit *para*-nitroaniline (*p*NA) in the fast hydrolysis reaction. The disturbed equilibrium and the immediate disappearing of the *trans* conformer allow the measurement of the *cis* → *trans* isomerization by following the UV absorption of liberated *p*NA at 390 nm time dependently.

The investigation of the kinetics of the isomerization and the determination of the *cis* and *trans* conformer ratios of the (4)-fluoroproline containing peptides (amplitudes) allowed the calculation of the rate constants of the *trans* → *cis* isomerization and the corresponding equilibrium constants summarized in [Table 2-2](#).

The *cis* contents of the model peptides studied in this work show an order of  $2 < 1 \leq 4 < 3$  ([Table 2-2](#)). Such tendencies in adopting a preferred conformation have also been found in the other model compounds with the comparative data obtained by NMR for the Ac-(4*R* or *S*)-F-Pro-OMe and the Ac-(4)-diF-Pro-OMe (Renner, C., et al. 2001). The observed preference of **3** for the *cis* conformation compared to the situation for **1** and particularly to that for **2** was confirmed by the different thermodynamic stabilities of the related barstar mutants that (4*S*)-FPro mutant showed a higher thermostability than (4*R*)-FPro mutant, where Pro<sup>48</sup> was replaced by proline surrogates (4-fluoroproline derivatives) (Renner, C., et al. 2001).

**Table 2-2** Parameters of the *cis/trans* isomerization of proline and (4)-fluoroproline containing compounds

Chemical compound	Content of the <i>cis</i> conformer (%)	<i>K</i>	$k_{cis \rightarrow trans}$ (s <sup>-1</sup> )	$k_{trans \rightarrow cis}$ (s <sup>-1</sup> )
Suc-Ala-Ser-Pro-Phe-pNA ( <b>1</b> )	15.4 <sup>b</sup>	5.5 <sup>c</sup>	0.0083 <sup>d</sup>	0.0015 <sup>e</sup>
Suc-Ala-Ser-(4 <i>R</i> )-F-Pro-Phe-pNA ( <b>2</b> )	11.0 <sup>b</sup>	8.1 <sup>c</sup>	0.0122 <sup>d</sup>	0.0015 <sup>e</sup>
Suc-Ala-Ser-(4 <i>S</i> )-F-Pro-Phe-pNA ( <b>3</b> )	22.0 <sup>b</sup>	3.6 <sup>c</sup>	0.0113 <sup>d</sup>	0.0032 <sup>e</sup>
Suc-Ala-Ser-(4)-diF-Pro-Phe-pNA ( <b>4</b> )	15.6 <sup>b</sup>	5.4 <sup>c</sup>	0.0310 <sup>d</sup>	0.0057 <sup>e</sup>
Ac-Pro-OMe <sup>a</sup>	17.3	4.8	0.0121	0.0025
Ac-(4 <i>R</i> )-F-Pro-OMe <sup>a</sup>	12.8	6.8	0.0260	0.0038
Ac-(4 <i>S</i> )-F-Pro-OMe <sup>a</sup>	28.5	2.5	0.0148	0.0059
Ac-(4)-diF-Pro-OMe <sup>a</sup>	23.0	3.4	0.0535	0.0160

<sup>a</sup> Parameters were calculated from thermodynamic data measured by NMR Renner, C., et al. 2001.

<sup>b</sup> Rate constants of the *cis* → *trans* isomerization were determined using the protease coupled assay. The peptide was dissolved in DMSO to a concentration of 10 mg/ml. The reaction was started by adding 3 μl of the stock peptide solution to 1.2 ml 35 mM HEPES buffer, pH 7.8 containing 0.83 mg/ml chymotrypsin giving a final peptide concentration of 25 μg/ml. The temperature was hold constant at 10 °C. The relative amplitude of the burst phase to the total one reflects the percentage of the *trans* conformer. The relative amplitude of the *cis* → *trans* isomerization phase to the total one reflects the percentage of the *cis* conformer.

<sup>c</sup> The equilibrium constant is defined as  $K = \frac{[trans]}{[cis]}$ , where  $[trans]$  and  $[cis]$  are the concentration of the *trans* and the *cis* conformer at equilibrium, respectively. These concentrations were determined by investigating the corresponding amplitudes of the kinetics as described above.

<sup>d</sup> The rate constant of the *cis* → *trans* isomerization  $k_{cis \rightarrow trans}$  was determined by fitting the progress curve measured in the protease-coupled assay to a single-exponential first-order reaction.

<sup>e</sup> The rate constant of the *trans* → *cis* isomerization  $k_{trans \rightarrow cis}$  was calculated based on the equilibrium constant  $K = \frac{[trans]}{[cis]} = \frac{k_{cis \rightarrow trans}}{k_{trans \rightarrow cis}}$  and the rate constant of the *cis* → *trans* isomerization  $k_{cis \rightarrow trans}$ .

The rate constants ( $k$ ) of the *cis*  $\rightarrow$  *trans* isomerization show an order of  $1 < 3 < 2 < 4$ , while the rate constants of the *trans*  $\rightarrow$  *cis* isomerization show another order of  $1 \leq 2 < 3 < 4$  (Table 2-2). The differences in the rate constant orders between *cis*  $\rightarrow$  *trans* and *trans*  $\rightarrow$  *cis* isomerization are due to the different *cis* contents of each model peptides. The increasing tendency of the *trans*  $\rightarrow$  *cis* isomerization in the order of  $1 \leq 2 < 3 < 4$  can be explained by the inductive effects of the fluorine substituents in strengthening of the carbonyl group C=O bond by weakening the double-bond character of the imidic bond preceding proline surrogates to facilitate *cis/trans* isomerization. Such an inductive effect was already shown by FT-IR spectroscopy study of Ac-Pro-OMe and Ac-4-FPro-OMe derivatives (Renner, C., et al. 2001). Furthermore, the  $pK_a$  values of the nitrogen atom of imidic group of the free amino acids decrease in the following order: Pro (10.8) > (4*R*)-FPro (9.23) > 4-diFPro (7.15) (Eberhardt, E.S., et al. 1996, Renner, C., et al. 2001).

The equilibrium constants  $K$  show an order of  $3 < 4 < 1 < 2$ . The  $K$  value for the difluoro derivative **4** is somewhat smaller than that of the native compound **1** (Table 2-2). The large difference in the  $K$  value of **2** and **3** relates to the different pucker of the proline ring, where the (4*R*)-derivative shows an intrinsic preference for  $\gamma$ -*exo* puckering and the (4*S*)-derivative for  $\gamma$ -*endo* puckering (Gerig, J.T. and McLeod, R.S. 1973, Renner, C., et al. 2001). Such phenomenon can be explained by the *gauche* effect (Panasik, N., Jr., et al. 1994). For the difluoro derivative, the *gauche* effects of both fluorine atoms counteract leading to behavior more similar to that of proline and preferring the *endo*-pucker, therefore the  $K$  values of both **1** and **4** are very similar.

The difference in free energy between the *cis* and *trans* isomer shows an order of  $3 < 4 < 1 < 2$  (Table 2-3). The (4*S*)-FPro derivative **3**, which adopts *endo*-pucker, shows the smallest free energy difference between the *cis* and *trans* isomer. Due to steric hinderance, the energy difference between the *cis* and *trans* isomer is significantly larger for the *exo*-pucker than for the *endo*-pucker according to molecular modeling. Such results would suggest a preference for the *endo*-pucker, which leads to a smaller energy difference between the *cis* and *trans* isomers, and therefore a larger population of the *cis* isomer at equilibrium, as indeed experimentally observed for (4*S*)-FPro in comparison to (4*R*)-FPro.

The activation free energy of *cis*  $\rightarrow$  *trans* of the model peptides shows an order of  $4 < 2 < 3 < 1$  (Table 2-3). This is in coincidence with the rate constants of the *cis*  $\rightarrow$  *trans* isomerization, which have an order of  $1 < 3 < 2 < 4$ . Since compound **4** has the lowest *cis*  $\rightarrow$  *trans* activation free energy, the rate constant of *cis*  $\rightarrow$  *trans* for **4** is the fastest.

**Table 2-3** Kinetic and Thermodynamic parameters of *cis* → *trans* isomerization of proline and (4)-fluoroproline containing peptides as determined by protease coupled assay in HEPES

Compound	<i>cis</i> (%)	$k_{cis \rightarrow trans}^a$ $\times 10^{-3} \text{ s}^{-1}$	$\Delta G_{cis \rightarrow trans}^0$ <sup>b</sup> kcal/mol	$\Delta G_{cis \rightarrow trans}^\ddagger$ <sup>c</sup> kcal/mol	$\Delta G_{trans \rightarrow cis}^\ddagger$ <sup>d</sup> kcal/mol
Suc-Ala-Ser-Pro-Phe-pNA ( <b>1</b> )	15.4	8.3	-0.958	19.22	20.18
Suc-Ala-Ser-(4 <i>R</i> )-F-Pro-Phe-pNA ( <b>2</b> )	11.0	12.2	-1.176	19.0	20.18
Suc-Ala-Ser-(4 <i>S</i> )-F-Pro-Phe-pNA ( <b>3</b> )	22.0	11.3	-0.720	19.05	19.76
Suc-Ala-Ser-(4)-diF-Pro-Phe-pNA ( <b>4</b> )	15.6	31.0	-0.948	18.48	19.43

<sup>a</sup> Measured at 283 K at substrate concentrations of 25 µg/ml.

<sup>b</sup> From  $\Delta G_{cis \rightarrow trans}^0 = -RT \ln K$  (at a temperature of 283 K), where  $K$  is equilibrium constant (*trans/cis* ratio).

<sup>c</sup> Calculated from equation  $k_{cis \rightarrow trans} = (k_B T/h) \exp(\Delta G_{cis \rightarrow trans}^\ddagger / RT)$ , Where  $k_B$  is the Boltzmann constant  $1.38066 \times 10^{-23}$  J/K,  $h$  is the Planck constant  $6.62618 \times 10^{-34}$  J·s,  $R$  is the general gas constant 8.315 J/K·mol and  $T$  is the absolute temperature (here is the experimental temperature 283 K).

<sup>d</sup> Calculated from equation  $k_{trans \rightarrow cis} = (k_B T/h) \exp(\Delta G_{trans \rightarrow cis}^\ddagger / RT)$

note: kJ = 0.2388459 kcal

### 2.5.2 Catalysis of the *cis/trans* isomerization of fluoroproline containing peptide substrates by PPIases

The catalytic efficiency of different PPIases on the *cis* → *trans* isomerization of the imidic prolyl peptide bond or the respective derivatives is summarized in [Table 2-4](#). Due to the very fast uncatalyzed *cis* → *trans* isomerization rate of the difluoro-proline derivative **4** with  $k_{cis \rightarrow trans}$  of  $0.031 \text{ s}^{-1}$ , the catalytic efficiency of different PPIases towards this peptide was not detectable with the standard PPIase assay.

The PPIases *hCyp18*, *hFKBP12*, and *E.coli* TF display the lowest catalytic efficiency towards the (4*R*)-fluoroproline containing peptide **2**. No catalytic action of *hPin1* and *hPar14* has been found towards the proline and the proline substitutions, since Ser-Pro bond was not well catalyzed by either *hPin1* (Schutkowski, M., et al. 1998) or *hPar14* (Uchida, T., et al. 1999). *E.coli* Par10 does not well tolerate the (4*S*)-fluoroproline substitution and shows only 1.8 % of the catalytic efficiency that *E.coli* Par10 displays towards peptide **1**. Generally

speaking, from [Table 2-4](#) we can assume that the fluorinated proline surrogates would prevent appropriate recognition or catalysis of certain isomerases towards these compounds resulting in a decreased catalysis of (4)-fluoroproline derivatives in comparison to the entire proline. Only *hFKBP12* shows some accelerated catalysis towards (4*S*)-fluoroproline derivative with 137 % of the catalytic efficiency that *hFKBP12* displays towards the proline-containing compound **1**. Different extents of the decreases in the activities of PPIases towards different substrates have been noticed, for example, *hCyp18* kept only 3.3 % of the activity towards **2** when its activity towards **1** was set at 100%. In comparison, *E.coli* Par10 showed 30.4 % of the catalytic efficiency towards **2** when its activity towards **1** was set at 100%.

Since PPIases have different specificities and catalytic efficiencies towards compound **1** due to different active binding pocket each enzyme contains, there exist large variations in the  $k_{cat}/K_m$  values of different PPIases towards **1**. The differences in the catalysis of a certain PPIase on the *cis* → *trans* isomerization of (4)-fluoroproline containing peptides in compare to proline containing peptide could also be due to the different electrostatic status, the steric conformation, and the orientation of the proline ring pucker adopted in the substrates.

**Table 2-4** Catalytic efficiency of peptidyl-prolyl *cis/trans* isomerases on the *cis* → *trans* isomerization of proline and (4)-fluoroproline containing peptides.<sup>a</sup>

compound	$\frac{k_{cat}}{K_m}$ (M <sup>-1</sup> ·s <sup>-1</sup> )					
	(Relative activity (%))					
	<i>hCyp18</i>	<i>hFKBP12</i>	<i>hPin1</i>	<i>E.coli</i> Par10	<i>E.coli</i> TF	<i>hPar14</i>
Suc-Ala-Ser-Pro-Phe-pNA <b>(1)</b>	3550000 (100)	19000 (100)	<10000	368000 (100)	78000 (100)	<10000
Suc-Ala-Ser-(4 <i>R</i> )-F-Pro-Phe-pNA <b>(2)</b>	118200 (3.3)	<10000	<10000	112000 (30.4)	<10000	<10000
Suc-Ala-Ser-(4 <i>S</i> )-F-Pro-Phe-pNA <b>(3)</b>	936300 (26.4)	26100 (137)	<10000	6800 (1.8)	11300 (14.5)	<10000

<sup>a</sup> Rate constants of the *cis* → *trans* isomerization were determined using the protease-coupled assay both in the absence and in the presence of the PPIase investigated. The peptide was dissolved in DMSO to a concentration of 10 mg/ml. The reaction was started by adding 3 μl of the stock peptide solution to 1.2 ml 35 mM HEPES buffer, pH 7.8 containing protease (0.83 mg/ml chymotrypsin) giving a final peptide concentration of 25 μg/ml. The temperature was kept constant at 10 °C. The progress curves were fitted to single exponential first-order kinetics.

The progress curves of the *cis*  $\rightarrow$  *trans* isomerization of either (4*R*)- or (4*S*)-fluoroproline containing substrates in the absence and in the presence of *hCyp18* are shown in [Fig. 2-33](#). The curves clearly demonstrate that the (4*S*)-fluoroproline derivative is a better substrate for the catalysis by *hCyp18* than the (4*R*)-fluoroproline derivative. The rate constant of the *cis*  $\rightarrow$  *trans* isomerization for (4*R*)-fluoroproline substrate in the presence of 11 nM *hCyp18* is  $0.0114\text{ s}^{-1}$  whereas that of the uncatalyzed reaction is  $0.0101\text{ s}^{-1}$  ([Fig. 2-33, B](#)). On the other hand, the rate constant of the *cis*  $\rightarrow$  *trans* isomerization for (4*S*)-fluoroproline substrate in the presence of 11 nM *hCyp18* is  $0.0238\text{ s}^{-1}$  whereas the rate constant of the uncatalyzed reaction is  $0.0135\text{ s}^{-1}$  ([Fig. 2-33, A](#)).

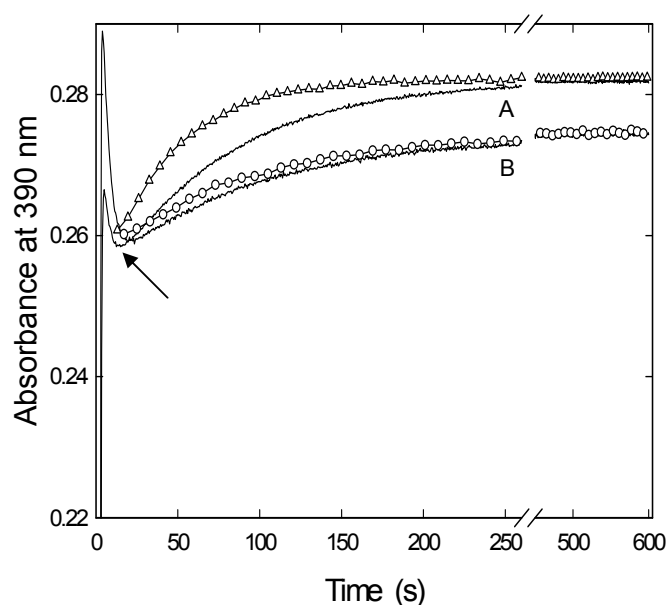


**Fig. 2-33** Progress curves for the  $\alpha$ -chymotrypsin mediated hydrolysis of Suc-Ala-Ser-4(*S*)-F-Pro-Phe-pNA (A) in the absence of (–) and in the presence of 11 nM Cyp18 (– $\Delta$ –), and hydrolysis of Suc-Ala-Ser-4(*R*)-F-Pro-Phe-pNA (B) in the absence (–) and in the presence of 11 nM Cyp18 (–O–). Data were collected using 35 mM HEPES buffer, pH 7.8 at 10 °C in the presence of 0.83 mg/ml chymotrypsin. A burst phase due to the *trans* isomers in equilibrium is observed (*arrow*). The spikes at the start of the curves are mixing artefacts. In panel A: (–) no Cyp18,  $k = 0.0135\text{ s}^{-1}$ ; (– $\Delta$ –) 11 nM Cyp 18,  $k = 0.0238\text{ s}^{-1}$ . In panel B: (–) no Cyp18,  $k = 0.0101\text{ s}^{-1}$ ; (–O–) 11 nM Cyp 18,  $k = 0.0114\text{ s}^{-1}$ .

The difference of the rate constants of *cis*  $\rightarrow$  *trans* isomerization between the (4*R*)- and (4*S*)- fluoroproline derivatives catalyzed by *hCyp18* might largely depend on the steric conformation and the orientation of the fluorine atom adopted when interacting with *hCyp18*. [Fig. 2-34](#) illustrates the stereochemical orientation and the interactions of (4*S*)-F-Pro and

(4*R*)-F-Pro when bound in the active site of *hCyp18*. The (4*S*)-fluorine substituent is surrounded by charged residues, such as the catalytically important Arg<sup>55</sup> and is directed to the carbonyl oxygen of the peptide bond preceding proline. The higher electronegativity of the fluorine atom might influence the electron density of the carbonyl oxygen and thus weaken the double bond character of the imidic prolyl bond facilitating the *cis/trans* isomerization by decreasing the activation energy barrier. In contrast, the (4*R*)-fluorine substituent is surrounded by aromatic and apolar residues (perturbation). It directs away from and displays a larger distance to the entire prolyl-peptide bond, which might be responsible for the much-impaired catalytic efficiency of *hCyp18* towards this variant.

The similar results have also been observed in the study of the catalysis of refolding of proteins containing (4)-fluoroproline surrogates by *hCyp18*. *hCyp18* catalyzes proline *trans* → *cis* isomerization of (4*S*)-FPro<sup>48</sup> surrogate of barstar C40A/C82A/P27A (b\*pwt) more than 2 times faster than that of the (4*R*)-FPro48 variant (Golbik, et al., unpublished data).

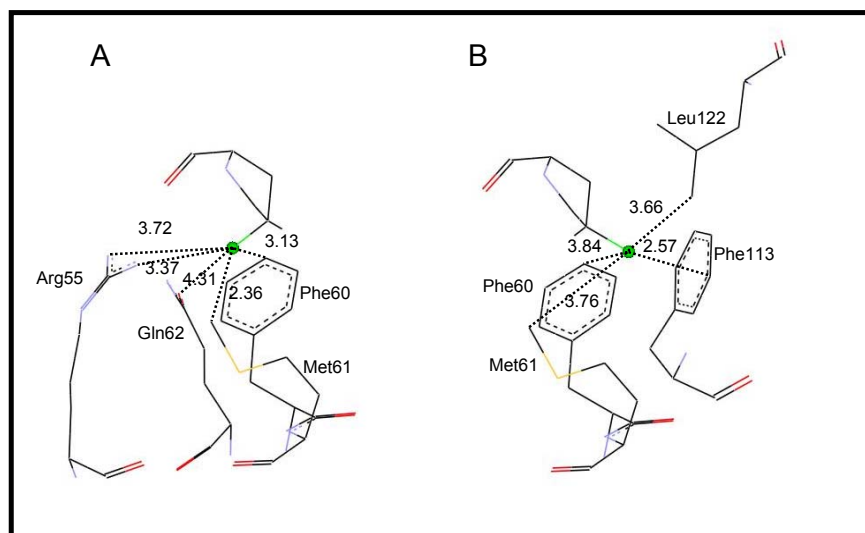


**Fig. 2-34** View of the key amino acids in the active site of *hCyp18*. (A) (4*S*)-fluoroproline and (B) (4*R*)-fluoroproline of an oligopeptide substrate coordinated in the active site of *hCyp18*. Fluorine is shown as green sphere. Figure was generated using WebLab ViewerPro based on the *hCyp18* structure in complex with Suc-Ala-Ala-Pro-Phe-pNA (PDB code 1RMH) (Zhao, Y. and Ke, H. 1996).

### 2.5.3 The influence of urea on the activity of different PPIases

The isomerization catalytic activity of different PPIases in the presence of denaturant urea towards peptide substrates has been studied. The study is important to provide relevant

data for the study of the protein folding relevancy and the *cis/trans* isomerization processes of b\*pwt variants containing proline-surrogates, (4)-fluoroproline, at position 48 to get the information about the folding as a result of the atomic mutation in a refolding system containing the denaturant urea.

Urea dependencies of the enzyme activities of different PPIases were determined by either the protease-coupled assay (*hCyp18*, *hFKBP12*, *hPar14*, *E.coli* TF) or the protease-free assay (*SlyD*, *E.coli* Par10) towards their specific peptide substrates at different denaturant concentrations. The using of protease-free assay for *SlyD* and *E.coli* Par10 is because of their instabilities in the presence of proteases. At increasing urea concentrations, the activities of different PPIases decrease (Fig. 2-35, A-E). The urea-dependent activity of *hCyp18* has already been reported (Golbik, R., et al. 1999).

The effects of the denaturant urea on the specific activities of different PPIases towards peptide substrates have been investigated by conducting the assays in the presence of appropriate concentrations of the denaturant, under the same conditions as for refolding of the different (4)-FPro48 substituted b\*pwt variants (Golbik, et al., unpublished data). The logarithm of the catalytic activities of different PPIases is found to be linearly dependent on the urea concentration in the range measured (Fig. 2-35, A-E) according to following equation

$$\ln\left(\frac{k_{cat}}{K_m}\right)^{[D]} = \ln\left(\frac{k_{cat}}{K_m}\right)^{[H_2O]} - m_c \cdot [D] \quad (2-1)$$

where  $\left(\frac{k_{cat}}{K_m}\right)^{[D]}$  is the catalytic efficiency at a given denaturant concentration,  $\left(\frac{k_{cat}}{K_m}\right)^{[H_2O]}$  is that in water,  $[D]$  is the concentration of the denaturant urea, and  $m_c$  is the slope of the logarithmic plot. The catalytic efficiency of the different enzymes was considered by extrapolation to 0 M denaturant concentration.

It is known that the equilibrium constant of the *cis/trans* equilibrium is independent of the denaturant concentration. Thus, the slopes of plots A-E in Fig. 2-35 which are derived from the isomerizations of the peptide substrates can be related to the isomerization values of the b\*pwt variants (Golbik, et al., unpublished data) under the assumption that the linear free relationship in Equation 2-1 is valid for both the *trans*  $\rightarrow$  *cis* and the *cis*  $\rightarrow$  *trans* isomerization activities of different PPIases.

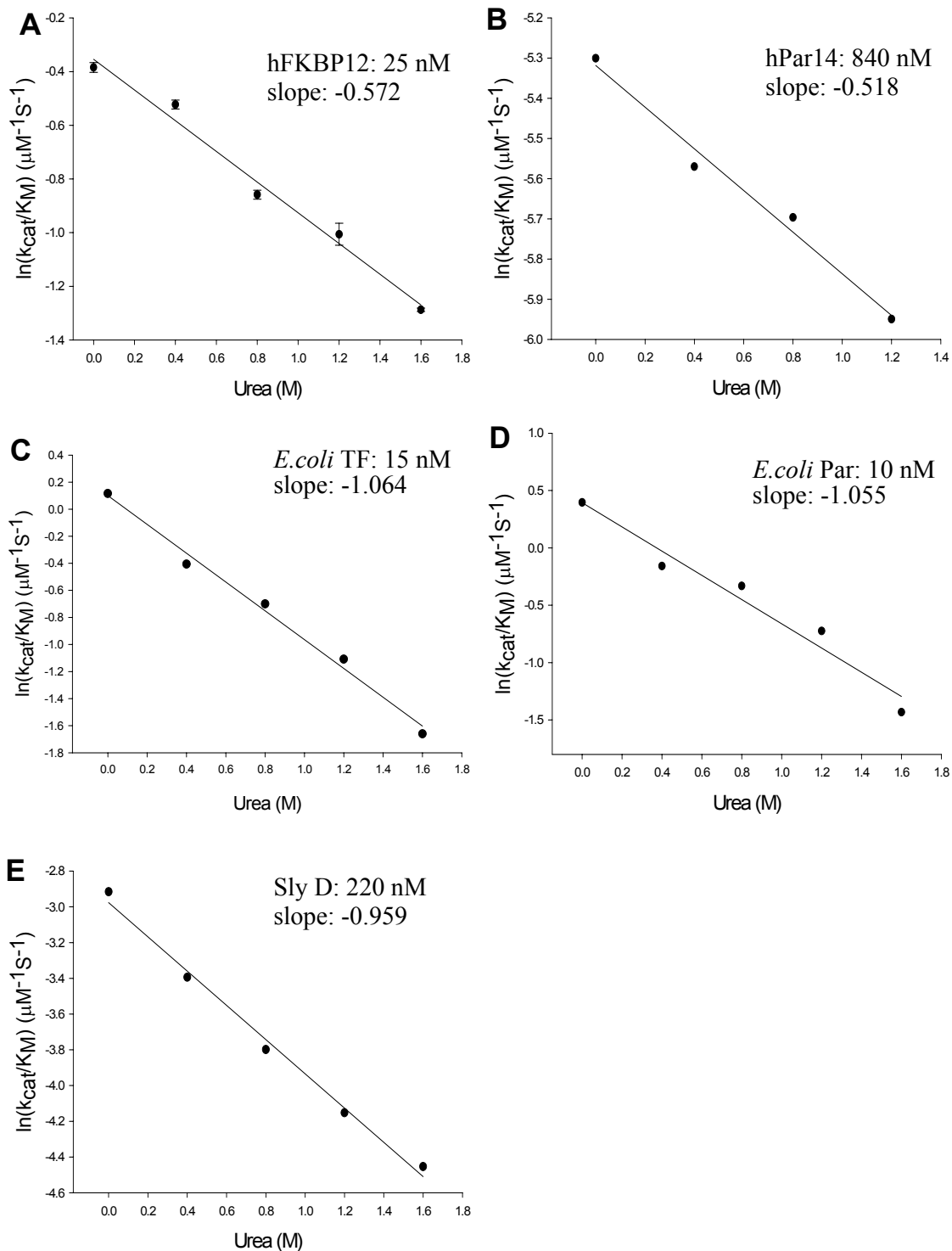


**Fig. 2-35** Urea dependence of the specific enzymatic activities of different PPIases towards their respective substrates. The enzymes were first incubated in 35 mM HEPES, pH 7.8 at 25 °C for 10 min. An aliquot of the incubation solution was added to the assay mixture containing the same concentration of urea in 35 mM HEPES, pH 7.8 and 0.83 mg/ml chymotrypsin [protease-coupled test]

according to (Fischer, G., et al. 1984, Harrison, R.K. and Stein, R.L. 1990), or 2  $\mu$ M BSA [protease-free test] according to (Janowski, B., et al. 1997). The assay mixture was incubated at 10 °C for 5 min. The reaction was started by adding 2-3  $\mu$ l of the respective peptide substrate. In the protease-coupled method, the substrate was dissolved in DMSO giving a stock concentration of 10 mg/ml. In the protease-free method, the substrate was dissolved in 0.5 M LiCl/TFE giving a stock concentration of 20 mg/ml. (A) Protease-coupled assay using Suc-Ala-Phe-Pro-Phe-pNA and 25 nM *hFKBP12*, (B) Protease-coupled assay using Suc-Ala-Arg-Pro-Phe-pNA and 840 nM *hPar14*, (C) Protease-coupled assay using Suc-Ala-Phe-Pro-Phe-pNA and 15 nM *E.coli* TF, (D) Protease-free assay using Suc-Ala-Phe-Pro-Phe-pNA and 10 nM *E.coli* Par10, (E) Protease-free assay using Suc-Ala-Phe-Pro-Phe-pNA and 220 nM SlyD. Data were fit according to Equation 2-1.

The catalytic activities of different PPIases on prolyl *trans*  $\rightarrow$  *cis* isomerization of b\*pwt and b\*pwt variants were measured in a refolding system containing 1.6 M urea. The knowledge of the influences of urea on different PPIases is very important to evaluate catalytic efficiencies of these PPIases towards the protein substrates. Therefore, the catalytic efficiencies of the PPIases to the barstar proteins can be simply corrected and normalized according to slopes  $m_c$  determined from the dependence of the individual enzymatic activity to the respective peptide substrates at different urea concentrations.

### 2.5.4 Conclusions

The observed kinetic and thermodynamic parameters of *cis*  $\rightarrow$  *trans* isomerization of proline and (4)-fluoroproline containing tetrapeptides studied in this work are comparable and in good agreement with those already studied like *N*-acetyl-proline methyl ester or *N*-acetyl-(4)-fluoroproline methyl esters (Renner, C., et al. 2001).

The specificity and catalytic efficiency of the peptidyl-prolyl *cis/trans* isomerases (PPIases) towards short peptide substrates containing (4)-fluoroproline as well as proline are varied. The observed differences were caused by different inherent properties of proline or (4)-fluoroproline, such as electrostatic status, the steric conformation, and the orientation of the proline ring pucker adopted in the substrates. The differences are also due to the differences in the substrate binding pockets of the different PPIases. The possible reasons that *hCyp18* showed different catalytic efficiencies towards (4*R*)- and (4*S*)-FPro derivatives can be discussed based on the core structure of *hCyp18* binding pocket as well as electrostatic withdrawing effects of fluorine from substrates.

The influences of urea on the activities of different PPIases have been studied using standard peptide substrates. Therefore the catalytic efficiencies of the PPIases to the *cis/trans* isomerization processes of b\*pwt variants containing (4)-fluoroproline surrogates measured in a refolding system containing denaturant urea can be simply corrected and normalized according to slopes  $m_c$  determined from the dependence of the individual enzymatic activity to the respective peptide substrates at different urea concentrations.

Fluorinated prolines have unique properties. They can be detected by  $^{19}\text{F}$  NMR spectroscopy and report conformational information. Dynamics of prolyl bond *cis/trans* isomerization gives rise to information on the conformational state, which can be altered by PPIases. The (4*S*)-FPro moiety appears to be most suitable for identification of *cis/trans* isomerization of a matrix-bound oligopeptides chain because of its unique properties in Cyp18 catalysis and the high content of *cis* isomer. However, the investigation on (4)-FPro containing matrix-bound peptides have not yet been performed in the course of this work.

## 3 Materials and Methods

### 3.1 Materials

#### Chemicals and materials

##### **Advanced ChemTech (Louisville, USA)**

Fmoc-Photolabile Linker (RT 1095)

##### **Amersham Pharmacia (Heidelberg, Germany)**

ECL™ Western blotting detection reagents

Hyperfilm™ ECL™

##### **AppliChem (Darmstadt, Germany)**

2-(*N*-Morpholin-o)ethanesulfonic acid (MES)

2-Amino-2-(hydroxymethyl)-1,3-propane-1,3-diol (Tris)

4-(2-Hydroxyethyl)-1-piperazine-1-ethanesulfonic acid (HEPES)

Agar

Ampicillin

Isopropyl β-D-thiogalactopyranoside (IPTG)

Kanamycin

##### **Bachem (Bubendorf, Switzerland)**

Suc-Ala-Leu-Pro-Phe-pNA

##### **BIOSOLVE (HA Valkenswaard, Netherlands)**

Acetonitrile (HPLC pure)

##### **Boehringer (Mannheim, Germany)**

Chloramphenicol

Tetracyclin

##### **Fluka (Buchs, Switzerland)**

Bromophenol blue (BPB)

Dichloromethane (DCM)

Diisopropylethylamine (DIPA)

Diisopropylcarbodiimide (DIC)

Dimethylformamide (DMF)

Hydrazine solution anhydrous

*N*-methylimidazole (NMI)

*N*-methylpyrrolidone (NMP)

Tetrahydrofurane (THF)

##### **GibcoBRL (Paisley, Scotland)**

Agarose

Peptone 140

**GLW, Ges.f.Laborbedarf mbH (Würzburg, Germany)**

Blotting paper

**ICN Biomedicals (Aurora, USA)**

Urea (ultra pure)

**Lidl UK (London, UK)**

Milk powder

**Merck (Darmstadt, Germany)**

$\alpha$ -Chymotrypsin (400 U/mg)

Dimethylsulfoxide (DMSO)

Fractogel EMD AF-Blue

Fractogel EMD DEAE-650(M)

Fractogel EMD SO<sub>3</sub><sup>-</sup>-650(M)

$\beta$ -Mercaptoethanol

Potassium chloride

Potassium hydroxide pellets

Sodium chloride

Sodium hydroxide pellets

Trypsin (40 U/mg)

**Merck-schuchardt (Hohenbrunn, Germany)**

Piperidine

Trifluoroacetic acid (TFA)

Triisopropylsilan

**MPG (Halle, Germany) (synthesized by chemistry group)**

Suc-Ala-Arg-Pro-Phe-pNA

Suc-Ala-Leu-Pro-Phe-pNA

Suc-Ala-Phe-Pro-Phe-pNA

Suc-Ala-Ser-(4)-diF-Pro-Phe-pNA

Suc-Ala-Ser-(4*R*)-F-Pro-Phe-pNA

Suc-Ala-Ser-(4*S*)-F-Pro-Phe-pNA

Suc-Ala-Ser-Pro-Phe-pNA

Other synthetic peptides used in this dissertation

**MPI (Martinsried, Germany) (kindly provided by Prof. L. Moroder)**

Fmoc-4,4-L-difluoroproline

Fmoc-4*R*-L-fluoroproline

Fmoc-4*S*-L-fluoroproline

**Novabiochem (Bad Soden, Germany)**

Boc-Lys(Fmoc)-OH

Fmoc-Lys(Dde)-OH

Fmoc-Rink linker

Fmoc-Ser(PO(OBzl)-OH)-OH

Fmoc-Xaa-Opfp

PyBOP

Rink Amide MBHA resin  
TBTU

**PALL Gelman (Dreieich, Germany)**  
Nitrocellulose

**Riedel-de Haën (Seelze, Germany)**  
Acetic anhydride

**Roth (Karlsruhe, Germany)**  
Dithiothreitol (DTT)  
EDTA  
Ethanol  
Rothiphorese Gel 30 (30% Acrylamide + 0.8% Bisacrylamide) ready for use  
TEMED

**SERVA (Heidelberg, Germany)**  
Ammonium Persulfate (APS)  
Coomassie brilliant blue (G-250)  
Dialysis tubing (MW cutoff 12 – 14 Kda)  
PEG 40000 (Polyethylenglycol, MW 40000 Da)  
SDS  
*N*-Tris(hydroxymethyl)-methylglycine (Tricine)  
Tween 20  
Yeast extract powder

**Sigma-Aldrich (Steinheim, Germany)**  
Albumin (Bovine)  
Biotin  
Sucrose  
PonceauS

All chemicals were purchased in their purest quality and used without further purification.

The amino acids (one-letter-code) for peptide synthesis on cellulose purchased from Novabiochem (Bad Soden, Germany) and Bachem (Bubendorf, Switzerland) were 9-fluorenylmethoxycarbonyl (Fmoc)-protected and pentafluorophenyl (Pfp)- or 3-hydroxy-2,3-dihydroxy-4-oxo-benzotriazolyl (Dhbt)-activated. The following side chain protecting groups were used: trityl for C, H, N and Q; *t*-butyl for D, E, S, T and Y; *t*-butoxycarbonyl for K; and pentamethyl dihydrobenzofurane sulfonyl for R.

**Proteins (recombinant proteins)**

**MPG (Halle, Germany)**

*E. coli* Par10

kindly provided by Dr. J. -U. Rahfeld

*E. coli* TF

hPar14

hPin1

SlyD

14-3-3  $\zeta/\delta$

kindly provided by Dr. H. Bang

hCyp18

self purification (see methods)

hFKBP12

**Sigma-Aldrich (Steinheim, Germany)**

Streptavidin

**Vectors**

**MPG (Halle, Germany)**

pQE60/hFKBP12

pQE70/hCyp18

**Invitrogen (Karlsruhe, Germany)**

pCRT7/GS<sup>©</sup>/14-3-3  $\zeta/\delta$

**Antibodies**

**MPG (Halle, Germany)**

anti FKBP12 serum

Pab productions, Herbertshausen

**Santa Cruz Biotechnology (Santa Cruz, USA)**

14-3-3 monoclonal antibody (14-3-3  $\beta$  (H8))

**Sigma-Aldrich (Steinheim, Germany)**

anti-mouse IgG peroxidase conjugate

anti-rabbit IgG peroxidase conjugate

anti-streptavidin antiserum from rabbit

**Bacterial cell strains**

BL21(DE3)pLysS

Stratagene (Heidelberg, Germany) *E. coli* B, pLysS

Plasmid coded for T7 Lysozyme

BL21RP c<sup>+</sup>

Stratagene (Heidelberg, Germany) *E. coli* B, contains

extra gene for *argU* und *proL* tRNA

DH5 $\alpha$

Invitrogen (Leek, Netherlands)

**Medium and buffers**

Blocking buffer	3 % milk powder in TBT buffer
Bradford buffer	0.1 g Coomassie Brilliant blue G-250 dissolved in: 100 ml 85 % phosphoric acid (w/v), 50 ml 95 % Ethanol (v/v), dilute to 1 L with H <sub>2</sub> O
Buffer A	10 mM Tricine, pH 8.0
Buffer B	10 mM HEPES, pH 7.8
Buffer C	10 mM MES, pH6.5
Coomassie blue buffer for SDS gel staining	2 g/l Coomassie brilliant blue R250, 0.5 g/l Coomassie brilliant blue G250, 10 % (v/v) acetic acid, 30 % methanol, 17.5 % Ethanol
Destaining buffer for SDS gel stained by coomassie blue	45 % (v/v) Methanol, 10 % (v/v) acetic acid
LB medium (Luria-Bertani)	10 g NaCl, 10 g Trypton, 5 g Yeast extract powder, dissolved in H <sub>2</sub> O to 1 L, pH 7.5 (adjusted by NaOH)
LB-medium for Agarplate	20 g/l Agar in LB medium
MP buffer	30 mM Tris pH 7.6 (HCl), 170 mM NaCl, 6.4 mM KCl 0.05 % (v/v) Tween 20, 5 % Saccharose (w/v)
PonceauS buffer	5 g/l PonceauS, 1 % acetic acid
Regeneration buffer A	480.5 g Urea, 10 g SDS, 1 ml 2-Mercaptoethanol, dissolved in H <sub>2</sub> O to 1 L
Regeneration buffer B	400 ml H <sub>2</sub> O, 500 ml EtOH, 100 ml Acetic acid
Sample buffer	156 mM Tris pH 6.8 (HCl), 80 mM SDS, 4 % (v/v) Glycerine, Bromophenol blue
Standard-buffer 7	10 mM HEPES, pH 7.8, 150 mM KCl, 1.5 mM MgCl <sub>2</sub> , 2 mM DTT
TBS buffer	30 mM Tris pH 7.6 (HCl), 170 mM NaCl, 6.4 mM KCl
TBT buffer	50 mM Tris pH 7.5 (HCl), 150 mM NaCl, 0.05 % (v/v) Tween 20
Transfer buffer	25 mM Tris, 150 mM Glycine, pH 8.3, 10 % (v/v) Methanol

**Standard used**

1 kb DNA ladder	New England Biolabs Inc (Oxford, UK)
Protein-10 kDa MW-Marker	GibcoBRL (Paisley, Scotland)
Protein-MW-Marker 4 / 5	Serva (Heidelberg, Germany)

**Final concentrations of antibiotics in LB medium or LB agarplate**

Ampicillin	100 µg/ml
Chloramphenicol	34 µg/ml
Kanamycin	50 µg/ml
Tetracyclin	10 µg/ml

## 3.2 **Methods**

### 3.2.1 **Expression and purification of *hCyp18***

1. Overnight cultures (3 x 100 ml) of *E. coli* cells grown in LB-medium bearing the Plasmid pQE70/*hCyp18* have been used to inoculate the main culture (6 x 1 liter of LB-medium). The cultures were incubated at 37 °C under severe shaking. At an OD<sub>600</sub> of 0.4 to 0.6 the protein expression was induced by adding IPTG to final concentration of 1 mM. After additional 4 hours at 37 °C, cells have been harvested by centrifugation (43000 × g, RC5B Plus, Kendro, 10 min, 4 °C).
2. Harvested cells were resuspended in buffer A and broken by passaging three times the French press cell (SLM Aminco, Büttelborn) at 4 °C under 1000 psi. By ultracentrifugation (240000 × g, Beckmann LE-80K ultracentrifuge, Beckmann, Palo Alto, California, USA, rotor SW 45Ti, 45 mins, 4 °C) cell particles and parts of the membrane could be separated from the supernatant.
3. Subsequently the supernatant has been applied to an anion exchanger column (Fractogel EMD DEAE-650 (M), Merck, Darmstadt, 1.6 × 14 cm) equilibrated in buffer A at a flow rate of 1 ml/min. The flow through fractions, containing *hCyp18*, were pooled and applied to an affinity column (Fractogel TSK AF-Blue, Merck, Darmstadt, 1 × 6 cm) which has also been equilibrated in buffer A and used at flow rate of 1 ml/min.
4. *hCyp18* was eluted with an increasing salt gradient from 0 to 3 M KCl in buffer A (100 / 100 ml). Afterwards the protein containing fractions were dialyzed against buffer B (3 × 2 l, 2 h, 4 °C). The dialyzed sample was loaded onto a cation exchange column (Fractogel EMD SO<sub>3</sub><sup>-</sup>-650 (M), Merck, Darmstadt, 1 × 14 cm), previously equilibrated with buffer B and run at 1 ml/min and eluted with an increasing salt gradient from 0 - 1 M NaCl in 50 ml of buffer B.
5. The *hCyp18* containing fractions were concentrated in a rotation cell device NOVA (3 bar overpressure, cut-off 3 kDa, PALL Filtron, NY, USA). By the use of a gel filtration column (Superdex Hiload 75, Pharmacia, Uppsala, Schweden, 1.6 × 60 cm) equilibrated in Standard 7 with a flow rate of 0.8 ml/min some impurity left could be successfully removed. Samples were again concentrated with a rotation cell device NOVA and finally stored at -80 °C.

### 3.2.2 Expression and purification of *hFKBP12*

1. Protein overexpression in *E. coli* with the plasmid pQE60/*hFKBP12* and the first purification step on an anion exchanger column (Fractogel EMD DEAE-650 (M), Merck, Darmstadt, 1.6 × 14 cm) have been conducted like described for the purification of *hCyp18*.
2. After pooling the flow through, the sample was dialyzed against buffer C.
3. The dialyzed sample was loaded onto an affinity column (Fractogel TSK AF-Blue, Merck, Darmstadt, 1 × 6 cm) equilibrated in buffer C (flow rate 1 ml/min). The protein has been eluted with a salt gradient from 0 to 3 M KCl in 75 ml of buffer C.
4. The pooled *hFKBP12* sample from the affinity column was applied to a cation exchanger column (Fractogel EMD SO<sub>3</sub><sup>-</sup>-650 (M), Merck, Darmstadt, 1 × 14 cm, equilibrated with *buffer C*). Elution of the bound protein took place by a linear increasing salt gradient (0 - 1 M KCl).
5. The purity of the sample has been analyzed after every purification step by SDS-PAGE and Coomassie staining.
6. Fractions containing *hFKBP12* were concentrated with a rotation cell device NOVA (3 bar overpressure, cut-off 3 kDa, PALL Filtron, USA) and afterwards loaded onto a gel filtration column (Superdex Hiload 75, Pharmacia, Sweden, 1.6 × 60 cm) equilibrated with Standard 7 at a flow rate of 0.8 ml/min. Eluted fractions containing *hFKBP12* were dialyzed 3 times against 10 mM HEPES-buffer pH 7.8 and stored at - 20°C.

### 3.2.3 MALDI-TOF analysis of cellulose bound peptide spots

#### Sample preparations

##### *Cellulose bound peptides – bound via Rink linker*

4 mm<sup>2</sup> pieces of the peptide spots were cut out and incubated in 10 µl HCCl<sub>3</sub>/TFA (98 %):1:1 for 60 min. 0.5 µl of the solution was spotted on a thinlayer matrix spot prepared on the MALDI steel target. The thinlayer preparation (Jensen, O.N., et al. 1996) was performed using a 1:1 solution of saturated α-cyano-4-hydroxycinnamic acid in acetone and 1 mg/ml nitrocellulose in acetone. The HCCl<sub>3</sub> containing sample dried immediately.

##### *Cellulose bound peptides – bound via photolabile linker*

4 mm<sup>2</sup> pieces of the peptide spots were irradiated with UV light until the color of the paper switch from white to light yellow (approximately 2 min). Subsequently, cellulose pieces

were fixed on the MALDI steel target using double-sided Tesa strip. 1  $\mu\text{l}$  of saturated matrix solution of  $\alpha$ -cyano-4-hydroxycinnamic acid in acetonitrile/water (0.1 % TFA) was spotted directly on the cellulose piece and sample were dried at room temperature.

### MALDI-TOF MS analysis

Dried samples were analysed by MALDI-TOF MS using a Bruker Reflex II mass spectrometer (Bruker Daltonik GmbH, Bremen, Germany) equipped with a pulsed ion extraction.

#### 3.2.4 Modification of cellulose membrane with $(\beta\text{-Ala})_2$ anchor functions

Cellulose membrane is the most commonly used continuous surface in SPOT synthesis, but the reactivity of hydroxyl group available from cellulose is not suitable for coupling amino acids. The common way is to transform the hydroxyl function into a more reactive amino function first, which is more nucleophilic than the hydroxyl group. The general procedures of this conversion step via esterification and the subsequent definition of the spots are depicted in [Fig. 3-1](#). Through the above steps, the cellulose membrane with the spotted amino functions on it contains many individual defined small reactors for the desired peptide synthesis. Using  $(\beta\text{-Ala})_2$  anchor has the advantage that it is not prone to self-catalyzed hydrolysis and the spacer arm is longer.

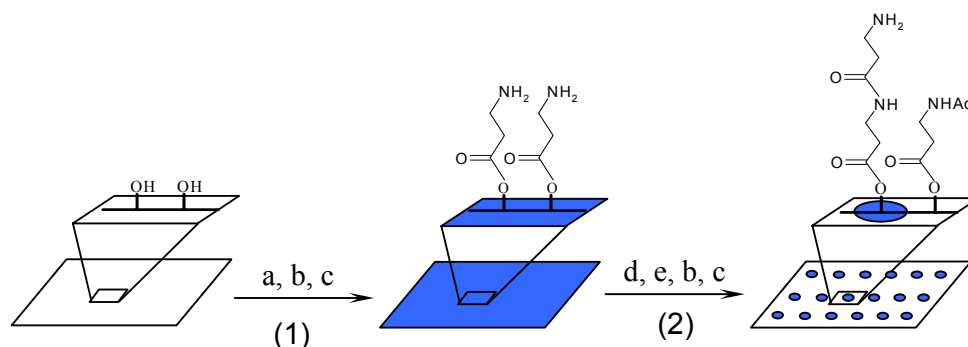


**Fig. 3-1** Functionalizing cellulose with amino group for SPOT synthesis (1) and defining the spots by addressable coupling of  $\beta$ -Ala (2). a) Fmoc- $\beta$ -Ala-OH/DIC/NMI, 12 h; b) 20% Piperidine/DMF; c) BPB/MeOH; d) Fmoc- $\beta$ -Ala-OPfp (spotwise); e) Ac<sub>2</sub>O/DIEA/DMF. Through acetylating (e) the free amino groups between spots are blocked and cannot be stained by Bromophenol blue (BPB).

As a solid support for peptide synthesis, a 9 X 13-cm Whatman paper (Maidstone, England) was used. The cellulose membrane was submerged in 0.2 M Fmoc- $\beta$ -Ala-OH solution (activated with 0.24 M DIC and 0.4 M NMI in DMF) without shaking for 3 h at room temperature to achieve an even distribution of amino functions by esterification of activated  $\beta$ -Ala to the hydroxyl groups of the cellulose. After washing 3 times for 5 min with DMF, the Fmoc protecting groups were cleaved by treatment with 20 % piperidine in DMF for 20 min. The membrane was washed with DMF five times and methanol twice and dried. The next step was to define the spots on cellulose with 0.2-0.3  $\mu$ l of 0.3 M Fmoc- $\beta$ -Ala-OPfp solution in DMF being spotted to predefined positions on the membrane by a pipetting robot (Abimed GmbH, Langenfeld, Germany). The coupling reactions normally lasted for 15-min, the remaining amino functions were acetylated by treatment of the membrane with 5 % acetic anhydride/2 % DIEA in DMF for 30 min. Then the membrane was washed four times with DMF, and the Fmoc groups were cleaved as described above. After washing four times with DMF, the free amino groups could be visualized with defined spots by staining with a 0.01 % BPB solution in DMF. The unbound BPB was removed by washing twice with methanol.

#### 3.2.5 The synthesis of templates used in Janus-peptide arrays

Two different templates (see Fig. 2-2) have been used in preparing Janus-peptide arrays.

1. Template 1 can be easily introduced through sequentially 2-time coupling of Fmoc-Lys(Dde)-OH and Boc-Lys(Fmoc)-OH to ( $\beta$ -Ala)<sub>2</sub> spacer on cellulose membrane. The amino acid derivatives (0.3 M) are activated by PyBOP (0.3 M) in DMF containing DIEA (10%, v/v) as a base. Two times coupling is necessary with 20 min for each. The N <sup>$\alpha$</sup> -Fmoc group of the immobilized peptide on membrane was cleaved by 20 % piperidine in DMF 2 times (5 min and 15 min respectively). After washing step with DMF (3 x 10 min), methanol (2 x 5 min), cellulose membrane was dried and ready for next round coupling of new amino acids. Thus, template 1 was introduced onto the cellulose membrane and ready for synthesis of Janus-peptide pairs.
2. Template 2 was prepared by first sequentially coupling Fmoc-Lys(Dde)-OH and Fmoc-Glu(OtBu)-OH to Rink Amide MBHA resin using Fmoc-based peptide synthesis strategy (Chan, W.C. and White, P.D. 2000, Fields, G.B. and Noble, R.L. 1990). The amino acid derivatives are activated by PyBOP. Then Fmoc-Glu-Lys(Dde)-CONH<sub>2</sub> was released from resin by 95 % TFA, 2 % Triisopropylsilan, 3 % water for 1 h at room temperature. The purified Fmoc-Glu-Lys(Dde)-CONH<sub>2</sub> (0.3 M) was activated on  $\gamma$ -carboxyl group of

Glu by PyBOP (0.3 M) in DMF with DIEA (10% v/v) and was then coupled to ( $\beta$ -Ala)<sub>2</sub> spacer on cellulose membrane three times (20 min each). The N<sup>α</sup>-Fmoc group of Fmoc-Glu( $\gamma$ -CO-NH-matrix)-Lys(Dde)-NH<sub>2</sub> on membrane was cleaved by 20 % piperidine in DMF 2 times (5 min and 15 min respectively). After washing step with DMF (3 x 10 min), methanol (2 x 5 min), cellulose membrane was dried and was then coupled with Boc-Lys(Fmoc)-OH (0.3 M) activated by PyBOP (0.3 M) in DMF containing DIEA (10% v/v) for two times (20 min each). Afterwards, template 2 was introduced onto the membrane and was ready for synthesis of peptide chains to prepare Janus-peptide arrays.

#### **3.2.6 The preparation of Janus-peptide membranes**

Janus-peptide arrays were prepared by automated SPOT synthesis (Frank, R. 1992, Kramer, A. and Schneider-Mergener, J. 1998, Kramer, A., et al. 1994). Peptides were C-terminally attached to the two amino functional groups of the templates anchored on cellulose individually. The amino functions are originally protected by two different orthogonal building blocks, namely Fmoc and Dde, which can be selectively and sequentially deprotected. The Fmoc protection group was deprotected by 20 % piperidine in DMF for 5 min and 15 min respectively, while Dde protection group was deprotected by 2 % hydrazine in DMF for 3 x 3 min (Bycroft, B.W., et al. 1993). After the deprotection of Fmoc protection groups on the templates, the first peptide chains were synthesized from C-terminal to N-terminal by SPOT synthesis. The free N-terminal amino groups of the first peptide chains were acetylated with 5 % acetic anhydride/2 % DIEA in DMF for 30 min after finishing the synthesis of the first chains. The second peptide chains were then synthesized to the amino functions using SPOT synthesis after removing of the Dde protection groups on the template. After the last synthesis step and Fmoc deprotection step of the second peptide chains, the free N-terminal amino groups of the second peptide chains were also blocked with 5 % acetic anhydride/2 % DIEA in DMF for 30 min. The final removal of the side protection groups is performed in 50 % TFA/DCM containing 2 % Triisopropylsilan and 3 % water for 3 h at room temperature with gentle shaking. After washing with DCM 2 x 5 min, DMF 3 x 15 min, MeOH 2 x 10 min, the peptide membrane was dried and kept in -20 °C ready for binding assays.

### 3.2.7 Western blot analysis

Before Western blot screening, the dry peptide-array membranes were rinsed in methanol for 10 min and for 3×20 min in TBS (30 mM Tris-HCl, pH 7.6, 170 mM NaCl, 6.4 mM KCl). The Probe proteins (e.g. streptavidin, 14-3-3 and hFKBP12) in a suitable concentration (50 nM ~ 200 nM) were allowed to react with peptide-array membranes in MP buffer (30 mM Tris-HCl, pH 7.6, 170 mM NaCl, 6.4 mM KCl, 0.05 % Tween 20, 5 % sucrose) overnight at 4°C with gentle shaking. Unbound probe protein was removed with TBS (4°C) and peptide-bound protein was electrotransferred onto nitrocellulose membranes (0.45 μM, PALL Gelman, Germany) using a semi-dry blotter (Biometra, Germany) (Kyhse-Andersen, J. 1984). The nitrocellulose membranes were sandwiched between blotting paper soaked with transfer buffer (25 mM Tris-HCl, pH 8.3, 150 mM Glycine, 10 % Methanol) kept at 4°C. Two nitrocellulose membranes were placed on both sides of the peptide membrane to be sure that all probe proteins have been captured during transferring. Electrotransfer was performed at a constant power of 0.8 mA/cm<sup>2</sup> peptide cellulose with suitable time courses (first electrotransfer step for 30-45 min, second electrotransfer step for 60-90 min).

Transferred probe protein was detected with protein-specific polyclonal rabbit antisera or monoclonal antibody. The immunoreactive complexes were further detected using peroxidase-conjugated anti-rabbit IgG or anti-mouse IgG. The final visualization was performed by using enhanced chemiluminescence ECL system with following steps:

1. Block the nitrocellulose with blocking buffer (3 % milk powder in TBT buffer) at room temperature for 2 h.
2. Incubate the nitrocellulose with first anti-probe protein polyclonal or monoclonal antibody with suitable dilution (1:1000 ~ 1:2000 in 0.5 % milk/TBT) at 4 °C overnight.
3. Wash the nitrocellulose membranes with TBT buffer 5 x 10 min, RT.
4. Probe nitrocellulose membrane with peroxidase conjugated antibody (anti-rabbit IgG or anti-mouse IgG) in a suitable dilution (1:1000 ~ 1:1500 in 0.5 % milk/TBT) for 3 h, RT.
5. Wash the nitrocellulose membranes with TBT buffer 5 x 10 min, RT.
6. Incubate nitrocellulose membrane with ECL Western blotting detection reagents for 1 min, and develop the film after exposure of the nitrocellulose membrane to Hyperfilm ECL for 30 seconds or other time courses to achieve the best signal to noise ratio.

**3.2.8 Membrane regeneration**

After probing, the cellulose peptide arrays can be regenerated using the following procedure. The membrane can be reprobed with the same or with a different ligand of interest.

1. Wash the peptide membrane with water, 3 x 10 min.
2. Wash the membrane with DMF, 3 x 10 min.
3. Wash the membrane with water, 2 x 10 min.
4. Incubate the membrane with regeneration buffer A, 3 x 10 min.
5. Incubate the membrane with regeneration buffer B, 3 x 10 min.
6. Wash the membrane twice with methanol for 10 min.
7. Dry the membrane and store it at -20 °C.

**3.2.9 SDS-Polyacrylamide Gel Electrophoreses (SDS-PAGE)**

SDS-PAGE is used to trace the expression and purification of recombinant proteins according to Laemmli (Laemmli, U.K. 1970). Protein-10 kDa-MW-Marker (GibcoBRL, Paisley, Scotland) is used as molecular mass standard. The samples were 1:1 (v/v) dissolved in 2-fold concentrated sample buffer and heated at 95 °C for 5 min. The samples were loaded onto the gel and 15 mA/gel was applied until the proteins are well concentrated into the stacking gel, then 30 mA/gel until the tracking dye reaches the bottom of the gel (gel size 9 x 8.5 cm). Coomassie blue buffer has been used to stain the gel for 30 min as described (Frey, M.D. and Radola, B.J. 1982).

**3.2.10 Determination of urea concentration**

The determination of the absolute urea concentration is based on the measuring of the difference in the refraction index between buffer and urea containing buffer. The concentration can be calculated according to equation 3-1 (Pace, C.N. 1986).

$$[\text{Urea}] = 117.66(\Delta N) + 29.753(\Delta N)^2 + 185.56(\Delta N)^3 \quad (3-1)$$

$\Delta N$             Difference of index of refraction between buffer with and without urea at RT

$[\text{Urea}]$         Concentration of urea in buffer (mol l<sup>-1</sup>)

**3.2.11 Determination of protein concentration with UV/VIS-spectroscopy**

Protein concentration can be determined by UV/VIS spectroscopy because molar extinction coefficients for proteins at 280 nm ( $\epsilon_{280}$ ) can be calculated according to amino acid sequence data (Gill, S.C. and von Hippel, P.H. 1989). Add protein solution in a quartz cuvette with 1 cm of pathlength and that use of a spectrophotometer (Hewlett Packard 8452A, USA) to scan UV/VIS spectrum of protein solution from 230 nm to 400 nm. The spectrum will give a hint how pure the protein is. The reference absorbance at 310 nm ( $A_{310}$ ) will give an information whether protein is aggregated (high  $A_{310}$  value) or not (low  $A_{310}$  value). The concentration of a measured protein is related to the amount of absorbed light by the sample by the Beer-Lambert Law:

$$A = \epsilon d c \quad (3-2)$$

In equation 3-2,  $A$  is absorbance,  $\epsilon$  is the molar extinction coefficient ( $M^{-1} \cdot cm^{-1}$ ),  $d$  is the pathlength of the sample cell (cm) and  $c$  is the concentration of the substance (M) that absorbs light. Once  $\epsilon$  and  $d$  are known,  $c$  can be calculated directly from  $A$ . Since protein  $\epsilon_{280}$  can be calculated (Gill, S.C. and von Hippel, P.H. 1989) and  $d$  is 1 cm, the protein concentration can be easily determined according to equation 3-3.

$$c = \frac{A_{280} - A_{310}}{\epsilon d} \quad (3-3)$$

**3.2.12 Determination of protein concentration with Bradford method**

The protein concentration can be determined by Bradford method (Bradford, M.M. 1976).

1. Prepare albumin standards by serial dilution in the same solvent as the protein of interest is. Prepare standards of 2 mg/ml down to 0.030 mg/ml of BSA solution.
2. For each protein standard and protein sample, add 200  $\mu$ l Bradford buffer into each microtiter plate wells and then add 50  $\mu$ l of each protein samples to the individual wells and mix. The reaction takes less than one minute at room temperature.
3. Read the absorbance of each sample at 590 nm wavelength ( $A_{590}$ ) by microtiter plate reader (Dynatech MR7000, Chantilly, USA). Bradford buffer alone is used as blank.
4. Plot the protein concentrations of the BSA standards versus the  $A_{590}$  on the SigmaPlot Graph program (SPSS Inc., USA). Plot the concentrations on the y-axis. To get a formula with which the unknown protein concentration can be determined by curve

fit. Determine what range of protein concentrations fall in a linear range. Omit the high and low numbers that fall outside the linear range, and re-plot. Use the revised graph to get a new formula for  $y$ . Insert the  $A_{590}$  value of the sample for  $x$ , find  $y$ , the sample concentration.

### 3.2.13 The catalytic efficiency of peptidyl-prolyl *cis/trans* isomerases

The catalytic efficiency of the PPIases used in this study was determined either by the protease-coupled assay (*hCyp18*, *hFKBP12*, *E.coli* TF) (Fischer, G., et al. 1984) or the protease-free assay (*SlyD*, *E.coli* Par10, *hPin1*) (Janowski, B., et al. 1997). The concentration of the protein substrates is less than the  $K_m$  for PPIases. The reaction proceeds according to first-order kinetics and can be described by equation 3-4 and 3-5.

$$v = -\frac{d[cis]}{dt} = k_{obs} \cdot [cis] \quad (3-4)$$

$$k_{obs} = k_0 + k_{enz} \quad (3-5)$$

Where  $[cis]$  is the time-dependent concentration of the *cis* conformer,  $k_{obs}$  is the observed,  $k_0$  is the uncatalyzed, and  $k_{enz}$  is the PPIase-catalyzed interconversion of the substrate. The catalytic efficiency  $\frac{k_{cat}}{K_m}$  of the enzyme was determined according to equation 3-6 assuming that the entire amount of the pure enzyme at a total concentration  $[E_0]$  represents catalytically active molecules.

$$\frac{k_{cat}}{K_m} = \frac{k_{obs} - k_0}{[E_0]} \quad (3-6)$$

The effect of the denaturant on the catalytic efficiency of the PPIases was determined by conducting the assays in the presence of appropriate concentrations of urea. The logarithm of the catalytic activity of the enzymes is found to be linearly dependent on the urea concentration according to equation 3-7.

$$\lg\left(\frac{k_{\text{cat}}}{K_m}\right)^{[\text{D}]} = \lg\left(\frac{k_{\text{cat}}}{K_m}\right)^{[\text{H}_2\text{O}]} - m_c \cdot [\text{D}] \quad (3-7)$$

Where,  $\left(\frac{k_{\text{cat}}}{K_m}\right)^{[\text{D}]}$  is the catalytic efficiency at a given denaturant concentration,  $\left(\frac{k_{\text{cat}}}{K_m}\right)^{[\text{H}_2\text{O}]}$  is that in water, and  $m_c$  is the slope of the logarithmic plot. The catalytic efficiency of the different enzymes was considered by extrapolation to 0 M denaturant concentration. The protein concentration of the PPIases was determined by measuring the absorbance at 280 nm and using the molar absorption coefficients determined according to the method of GILL and von HIPPEL (Gill, S.C. and von Hippel, P.H. 1989).

#### 3.2.14 Influence of PPIases on the *cis/trans* isomerization of (4)-fluoroproline containing peptides (protease-coupled assay)

The kinetics of the *cis* → *trans* isomerization of (4)-fluoroproline or proline containing peptide-4-nitroanilides was measured by using the protease-coupled test (Fischer, G., et al. 1984). The proteases chymotrypsin and trypsin will cleave off the chromogenic 4-nitroaniline only, if the peptide bond preceding proline is in *trans* conformation. The course of the reaction was followed by the absorbance change at 390 nm monitored by Dioden-Array UV/Vis-Spectrometer (Hewlett Packard 8452, USA). The protease concentration in the reaction mixture is in excess to ensure that the cleavage of the chromophore is not rate limiting. After a rapid burst phase, the amplitude that corresponds to the concentration of the *trans* conformer was cleaved immediately, the subsequent slow reaction phase corresponds to the *cis* → *trans* isomerization of the peptide bond preceding the proline derivative. The amplitude of the slow phase corresponds to the content of the *cis* conformer in solution. The reaction was carried out in 35 mM HEPES buffer, pH 7.8 at a temperature of 10 °C. The final protease concentration was either 0.83 mg/ml chymotrypsin (400 U/mg, Merck), or 50 µg/ml trypsin (40 U/mg, Merck). The substrate peptide was dissolved in DMSO to a concentration of 10 mg/ml. The reaction was started by adding 3 µl of the peptide to the protease mixture in a final volume of 1.2 ml giving a final peptide concentration of 25 µg/ml.

The influence of different PPIases on the *cis* → *trans* isomerization of the peptides was measured by performing the assay both in the absence and in the presence of the enzymes. The data was investigated as described above (Equations 3-4 to 3-6). The peptidyl-prolyl *cis/trans* isomerase SlyD is instable against the protease actions (supporting enzyme) and was

omitted in these studies. Furthermore, the (4)-fluoroproline containing peptides are not suitable for the protease-free assay (solvent-jump method) (Janowski, B., et al. 1997).

#### **3.2.15 Solvent-jump method (protease-free assay)**

If the catalytic efficiencies of some PPIases are not suitable to be determined by protease coupled assay (Fischer, G., et al. 1984) due to the instability of these PPIases against the protease action (supporting enzyme), one has to use the protease-free assay (solvent-jump method) (Garciaecheverria, C., et al. 1992, YliKauhaluoma, J.T., et al. 1996). The peptide substrates containing *p*-nitroaniline at C-terminal were dissolved in 0.5 M LiCl/TFE giving a stock concentration of 20 mg/ml. The largest changes in the absorption between the *cis* and *trans* conformer of substrates containing nitroaniline occurred at wavelength of 330 nm. Therefore, the course of *cis* → *trans* isomerization can be followed by the absorbance changes at 330 nm monitored by Diode-Array UV/Vis-Spectrometer (Hewlett Packard 8452, USA). The dissolving of substrates in LiCl/TFE buffer can increase the *cis* content of the substrate that has advantages in increasing the signal/noise ratio during spectroscopy analysis. The reaction was carried out in 35 mM HEPES buffer, pH 7.8, containing 2 μM BSA at a temperature of 10 °C. The reaction was started by adding 3 μl of the peptide to the mixture in a final volume of 1.2 ml giving a final peptide concentration of 50 μg/ml. The influence of different PPIases on the *cis* → *trans* isomerization of the peptides was measured by performing the assay both in the absence and in the presence of the enzymes. The data was investigated as described above (Equations 3-4 to 3-6).

#### **3.2.16 The inhibition of soluble peptides on the PPIase activity of hFKBP12**

The activity of hFKBP12 was measured towards substrate Suc-Ala-Phe-Pro-Phe-pNA by using protease-free method (Garciaecheverria, C., et al. 1992, Janowski, B., et al. 1997). The inhibition data for several soluble peptides derived from EGFR (section **2.3.2.2**) were analyzed according to the competitive model as already published for hCyp18 (Fischer, G. 1994). Protein hFKBP12 was first incubated with various concentrations of soluble peptides for 30 min at 10 °C and then the residual PPIase activity of hFKBP12 was measured. The residual enzymatic activity was plotted versus the inhibitor concentration and used for calculating the inhibitory constant (IC<sub>50</sub>) (Schutkowski, M., et al. 1995).

## Summary

The main aim of this work is to answer whether two oligopeptides, representing the linear binding epitopes of two interacting proteins, anchored side-by-side on solid supports on a single carrier molecule mutually orient chains and whether these matrix-bound oligopeptides mimic the conformation of interacting epitopes of native proteins.

We started with the investigation of protein-peptide complexes with known structures (e.g. streptavidin/*Strep*-tag II and 14-3-3/phosphopeptides), by parallel synthesizing arrays of two different peptide chains containing interacting sites from both binding partners on solid supports via a single carrier molecule, and analyzing the peptide-peptide interactions by newly established methodology, Janus-peptide array.

- We are able to synthesize two peptide chains onto cellulose membrane via a single template with high efficiency and give reproducible results in the following study.
- We have found that template 2 showed a higher signal to noise ratio in comparison to template 1, and therefore more suitable the Janus-peptide array study.
- We have found that cellulose membrane was more suitable to be used for Janus-peptide array, as compared with polypropylene membrane.
- In streptavidin/*Strep*-tag II interaction study, several main binding epitopes on streptavidin have been found by Janus-peptide array, which located in the same binding pocket of streptavidin to biotin.
- In 14-3-3/phosphopeptides interaction study, three main binding epitopes on 14-3-3 have been found by Janus-peptide array, which located directly in the binding groove of 14-3-3. Especially, one discovered binding epitope covering the sequence Ala<sup>47</sup>–Ser<sup>64</sup> (in helix  $\alpha$ 3) of 14-3-3 contains a cluster of basic residues (Lys<sup>49</sup>, Arg<sup>56</sup> and Arg<sup>60</sup>), which are important for the interaction with phosphoserine in phosphopeptides.

Further, protein-protein interacting complexes (e.g. FKBP12/FAP48 and FKBP12/EGF receptor cytosolic domain) were investigated by combining standard SPOT strategy and Janus-peptide arrays in deciphering the code of protein-protein interaction sites.

- In FKBP12/FAP48 interaction study, three out of total fifteen prolines in FAP48 have been observed to be involved in the binding epitopes to FKBP12 by standard SPOT strategy. Especially, two found binding epitopes corresponding to sequence Phe<sup>213</sup> – Glu<sup>231</sup> and sequence His<sup>299</sup> – Glu<sup>321</sup> of FAP48 contain Pro<sup>219</sup> and Pro<sup>309</sup>, respectively, which contribute significantly for the binding of FAP48 to FKBP12. In the following Janus-peptide assay study, one binding epitope region corresponding to sequence Met<sup>29</sup> – Glu<sup>61</sup> of FKBP12 has been found to have interaction with peptide epitopes derived from FAP48. This epitope on FKBP12 is exactly located in the known binding pocket of FKBP12 to FK506.
- In FKBP12/EGFR cytosolic domain interaction study, five potential binding epitopes on EGFR cytosolic domain have been found by using standard SPOT strategy. Three soluble peptides derived from these observed epitopes showed that their inhibitory activities (IC<sub>50</sub>) on the PPIase activity of FKBP12 were in the same range (hundreds of μM) of the *K<sub>m</sub>* of known peptide substrates for FKBP12. By using Janus-peptide array, one binding region corresponding to sequence Met<sup>29</sup> – Ser<sup>67</sup> of FKBP12 has been found to have interaction with one peptide epitope derived from EGFR cytosolic domain. This found binding epitope is located in the known binding pocket of FKBP12 to FK506.

The results obtained indicated that two peptides, potentially interacting, do interact with each other when immobilized on a solid support, and such interaction is detectable by Janus-peptide array. The capability in analyzing the main contact sites of protein-protein/peptide complexes by Janus-peptide array strongly indicated that matrix-bound peptide-peptide interactions could mimic protein-protein interactions.

Fluorinated prolines have unique properties. They can be detected by <sup>19</sup>F NMR spectroscopy and provide conformational information. Dynamics of *cis/trans* isomerization of prolyl bond preceding (4)-fluoroproline gives rise to information on the conformational state, which can be altered by PPIases. The (4*S*)-fluoroproline moiety appears to be most suitable for investigation of *cis/trans* isomerization of a matrix-bound oligopeptides chain because of its unique properties in Cyp18 catalysis and the high content of *cis* isomer.

## References

- Aitken, A.**, 14-3-3 and its possible role in co-ordinating multiple signalling pathways, *Trends Cell Biol.* **1996**, *6*, 341-347.
- Akerfeldt, K.S., Kim, R.M., Camac, D., Groves, J.T., Lear, J.D. and Degrado, W.F.**, Tetraphilin - a 4-Helix Proton Channel Built on a Tetraphenylporphyrin Framework, *J. Am. Chem. Soc.* **1992**, *114*, 9656-9657.
- Altmann, K.H. and Mutter, M.**, A General Strategy for the Denovo Design of Proteins Template Assembled Synthetic Proteins, *Int. J. Biochem.* **1990**, *22*, 947-956.
- An, S.S.A., Lester, C.C., Peng, J.L., Li, Y.J., Rothwarf, D.M., Welker, E., Thannhauser, T.W., Zhang, L.S., Tam, J.P. and Scheraga, H.A.**, Retention of the cis proline conformation in tripeptide fragments of bovine pancreatic ribonuclease A containing a non-natural proline analogue, 5,5-dimethylproline, *J. Am. Chem. Soc.* **1999**, *121*, 11558-11566.
- Arnold, F.H. and Zhang, J.H.**, Metal-mediated protein stabilization, *Trends Biotechnol.* **1994**, *12*, 189-192.
- Ast, T., Heine, N., Germeroth, L., Schneider-Mergener, J. and Wenschuh, H.**, Efficient assembly of peptomers on continuous surfaces, *Tetrahedron Lett.* **1999**, *40*, 4317-4318.
- Beausoleil, E. and Lubell, W.D.**, Steric effects on the amide isomer equilibrium of prolyl peptides. Synthesis and conformational analysis of N-acetyl-5- tert-butylproline N'-methylamides, *J. Am. Chem. Soc.* **1996**, *118*, 12902-12908.
- Beausoleil, E. and Lubell, W.D.**, An examination of the steric effects of 5-tert-butylproline on the conformation of polyproline and the cooperative nature of type II to type I helical interconversion, *Biopolymers* **2000**, *53*, 249-256.
- Beausoleil, E., Sharma, R., Michnick, S.W. and Lubell, W.D.**, Alkyl 3-position substituents retard the isomerization of prolyl and hydroxyprolyl amides in water, *J. Org. Chem.* **1998**, *63*, 6572-6578.
- Bierer, B.E.**, Cyclosporin A, FK506, and rapamycin: binding to immunophilins and biological action, *Chem. Immunol.* **1994**, *59*, 128-155.
- Bluthner, M., Koch, J. and Mahler, M.**, Mutational Analysis and Structure Predictions in *Peptide Arrays on Membrane Supports - Synthesis and Applications* (Eds.: J. Koch and M. Mahler), Springer Verlag, Berlin, Heidelberg, **2002**, pp. 123.
- Bluthner, M., Mahler, M., Muller, D.B., Dunzl, H. and Bautz, F.A.**, Identification of an alpha-helical epitope region on the PM/Scl-100 autoantigen with structural homology to a region on the heterochromatin p25beta autoantigen using immobilized overlapping synthetic peptides, *J. Mol. Med.* **2000**, *78*, 47-54.
- Bogan, A.A. and Thorn, K.S.**, Anatomy of hot spots in protein interfaces, *J. Mol. Biol.* **1998**, *280*, 1-9.
- Bradford, M.M.**, Rapid and Sensitive Method for Quantitation of Microgram Quantities of Protein Utilizing Principle of Protein-Dye Binding, *Anal. Biochem.* **1976**, *72*, 248-254.

- Brandts, J.F., Halvorson, H.R. and Brennan, M.**, Consideration of the Possibility that the slow step in protein denaturation reactions is due to cis-trans isomerism of proline residues, *Biochemistry (Mosc)*. **1975**, *14*, 4953-4963.
- Bray, A.M., Maeji, N.J., Jhingran, A.G. and Valerio, R.M.**, Gas-Phase Cleavage of Peptides from a Solid Support with Ammonia Vapor - Application in Simultaneous Multiple Peptide-Synthesis, *Tetrahedron Lett*. **1991**, *32*, 6163-6166.
- Bretscher, L.E., Jenkins, C.L., Taylor, K.M., DeRider, M.L. and Raines, R.T.**, Conformational stability of collagen relies on a stereoelectronic effect, *J. Am. Chem. Soc.* **2001**, *123*, 777-778.
- Brown, E.J., Albers, M.W., Shin, T.B., Ichikawa, K., Keith, C.T., Lane, W.S. and Schreiber, S.L.**, A mammalian protein targeted by G1-arresting rapamycin-receptor complex, *Nature* **1994**, *369*, 756-758.
- Bycroft, B.W., Chan, W.C., Chhabra, S.R. and Hone, N.D.**, A Novel Lysine-Protecting Procedure for Continuous-Flow Solid- Phase Synthesis of Branched Peptides, *J. Chem. Soc.-Chem. Commun.* **1993**, 778-779.
- Cameron, A.M., Steiner, J.P., Roskams, A.J., Ali, S.M., Ronnett, G.V. and Snyder, S.H.**, Calcineurin associated with the inositol 1,4,5-trisphosphate receptor-FKBP12 complex modulates Ca<sup>2+</sup> flux, *Cell* **1995a**, *83*, 463-472.
- Cameron, A.M., Steiner, J.P., Sabatini, D.M., Kaplin, A.I., Walensky, L.D. and Snyder, S.H.**, Immunophilin FK506 binding protein associated with inositol 1,4,5-trisphosphate receptor modulates calcium flux, *Proc. Natl. Acad. Sci. U. S. A.* **1995b**, *92*, 1784-1788.
- Cardenas, M.E., Hemenway, C., Muir, R.S., Ye, R., Fiorentino, D. and Heitman, J.**, Immunophilins interact with calcineurin in the absence of exogenous immunosuppressive ligands, *EMBO J.* **1994**, *13*, 5944-5957.
- Cavelier, F., Vivet, B., Martinez, J., Aubry, A., Didierjean, C., Vicherat, A. and Marraud, M.**, Influence of silaproline on peptide conformation and bioactivity, *J. Am. Chem. Soc.* **2002**, *124*, 2917-2923.
- Chalmers, D.K. and Marshall, G.R.**, Pro-D-Nme-Amino Acid and D-Pro-Nme-Amino Acid - Simple, Efficient Reverse-Turn Constraints, *J. Am. Chem. Soc.* **1995**, *117*, 5927-5937.
- Chambraud, B., Radanyi, C., Camonis, J.H., Shazand, K., Rajkowski, K. and Baulieu, E.E.**, FAP48, a new protein that forms specific complexes with both immunophilins FKBP59 and FKBP12. Prevention by the immunosuppressant drugs FK506 and rapamycin, *J. Biol. Chem.* **1996**, *271*, 32923-32929.
- Chan, W.C. and White, P.D.**, Fmoc solid phase peptide synthesis : a practical approach, vol edn. Edited by. Oxford University Press, New York, **2000**.
- Chandrasekhar, K., Profy, A.T. and Dyson, H.J.**, Solution Conformational Preferences of Immunogenic Peptides Derived from the Principal Neutralizing Determinant of the Hiv- 1 Envelope Glycoprotein Gp120, *Biochemistry (Mosc)*. **1991**, *30*, 9187-9194.
- Chen, Y.G., Liu, F. and Massague, J.**, Mechanism of TGFbeta receptor inhibition by FKBP12, *EMBO J.* **1997**, *16*, 3866-3876.
- Cheng, H.N. and Bovey, F.A.**, Cis-Trans Equilibrium and Kinetic Studies of Acetyl-L-Proline and Glycyl-L-Proline, *Biopolymers* **1977**, *16*, 1465-1472.

- Chilkoti, A., Tan, P.H. and Stayton, P.S.**, Site-directed mutagenesis studies of the high-affinity streptavidin-biotin complex: contributions of tryptophan residues 79, 108, and 120, *Proc. Natl. Acad. Sci. U. S. A.* **1995**, *92*, 1754-1758.
- Davis, S.J., Davies, E.A., Tucknott, M.G., Jones, E.Y. and van der Merwe, P.A.**, The role of charged residues mediating low affinity protein-protein recognition at the cell surface by CD2, *Proc. Natl. Acad. Sci. U. S. A.* **1998**, *95*, 5490-5494.
- DeRider, M.L., Wilkens, S.J., Waddell, M.J., Bretscher, L.E., Weinhold, F., Raines, R.T. and Markley, J.L.**, Collagen stability: insights from NMR spectroscopic and hybrid density functional computational investigations of the effect of electronegative substituents on prolyl ring conformations, *J. Am. Chem. Soc.* **2002**, *124*, 2497-2505.
- Diaz, H., Espina, J.R. and Kelly, J.W.**, A Dibenzofuran-Based Amino-Acid Designed to Nucleate Antiparallel Beta-Sheet Structure - Evidence for Intramolecular Hydrogen-Bond Formation, *J. Am. Chem. Soc.* **1992**, *114*, 8316-8318.
- Dill, K.A.**, Dominant Forces in Protein Folding, *Biochemistry (Mosc)*. **1990**, *29*, 7133-7155.
- Dumy, P., Keller, M., Ryan, D.E., Rohwedder, B., Wöhr, T. and Mutter, M.**, Pseudo-prolines as a molecular hinge: Reversible induction of cis amide bonds into peptide backbones, *J. Am. Chem. Soc.* **1997**, *119*, 918-925.
- Dyson, H.J. and Wright, P.E.**, Defining solution conformations of small linear peptides, *Annu. Rev. Biophys. Biophys. Chem.* **1991**, *20*, 519-538.
- Eberhardt, E.S., Panasik, N. and Raines, R.T.**, Inductive effects on the energetics of prolyl peptide bond isomerization: Implications for collagen folding and stability, *J. Am. Chem. Soc.* **1996**, *118*, 12261-12266.
- Fields, G.B. and Noble, R.L.**, Solid phase peptide synthesis utilizing 9-fluorenylmethoxycarbonyl amino acids, *Int. J. Pept. Protein Res.* **1990**, *35*, 161-214.
- Fields, G.B., Tian, Z. and Barany, G.**, Solid-Phase Peptide-Synthesis Utilizing 9-Fluorenylmethoxycarbonyl Amino-Acids in *Synthetic Peptides: A Users Guide* (Eds.: G.A. Grant), W.H. Freeman and Co., New York, **1992**, pp. 77-183.
- Fischer, G.**, Peptidyl-Prolyl Cis/Trans Isomerases and Their Effectors, *Angew. Chem. Int. Ed. Engl.* **1994**, *33*, 1415-1436.
- Fischer, G.**, Chemical aspects of peptide bond isomerisation, *Chemical Society Reviews* **2000**, *29*, 119-127.
- Fischer, G., Bang, H., Berger, E. and Schellenberger, A.**, Conformational specificity of chymotrypsin toward proline-containing substrates., *Biochim. Biophys. Acta* **1984**, *791*, 87-97.
- Fischer, G., Bang, H. and Mech, C.**, [Determination of enzymatic catalysis for the cis-trans-isomerization of peptide binding in proline-containing peptides], *Biomed. Biochim. Acta* **1984**, *43*, 1101-1111.
- Fischer, G. and Schmid, F.X.**, The mechanism of protein folding. Implications of in vitro refolding models for de novo protein folding and translocation in the cell, *Biochemistry (Mosc)*. **1990**, *29*, 2205-2212.
- Fischer, S., Dunbrack, R.L. and Karplus, M.**, Cis-Trans Imide Isomerization of the Proline Dipeptide, *J. Am. Chem. Soc.* **1994**, *116*, 11931-11937.

- Frank, R.**, Spot-Synthesis - an Easy Technique for the Positionally Addressable, Parallel Chemical Synthesis on a Membrane Support, *Tetrahedron* **1992**, *48*, 9217-9232.
- Frank, R.**, The SPOT-synthesis technique. Synthetic peptide arrays on membrane supports--principles and applications, *J. Immunol. Methods* **2002**, *267*, 13-26.
- Frank, R. and Doring, R.**, Simultaneous Multiple Peptide-Synthesis under Continuous-Flow Conditions on Cellulose Paper Disks as Segmental Solid Supports, *Tetrahedron* **1988**, *44*, 6031-6040.
- Frank, R., Güler, S., Krause, S. and Lindenmaier, W.**, Facile and rapid 'spot synthesis' of large numbers of peptides on membrane sheet in *Peptides 1990, Proceedings of 21<sup>st</sup> European Peptide Symposium* (Eds.: E. Giralt and D. Andreu), ESCOM, Leiden, **1991**, pp 151.
- Frank, R. and Overwin, H.**, SPOT synthesis - Epitope analysis with arrays of synthetic peptides prepared on cellulose membranes, *Methods Mol. Biol.* **1996**, *66*, 149-169.
- Frank, R. and Schneider-Mergener, J.**, SPOT Synthesis - Scope of Application in *Peptide Arrays on Membrane Supports - Synthesis and Applications* (Eds.: J. Koch and M. Mahler), Springer Verlag, Berlin, Heidelberg, **2002**, pp. 1.
- Freidinger, R.M., Veber, D.F., Perlow, D.S., Brooks, J.R. and Saperstein, R.**, Bioactive conformation of luteinizing hormone-releasing hormone: evidence from a conformationally constrained analog, *Science* **1980**, *210*, 656-658.
- Frey, M.D. and Radola, B.J.**, Rapid Staining of Proteins in Ultrathin-Layer Isoelectric- Focusing in Polyacrylamide Gels, *Electrophoresis* **1982**, *3*, 27-32.
- Furrer, J., Piotto, M., Bourdonneau, M., Limal, D., Guichard, G., Elbayed, K., Raya, J., Briand, J.P. and Bianco, A.**, Evidence of secondary structure by high-resolution magic angle spinning NMR spectroscopy of a bioactive peptide bound to different solid supports, *J. Am. Chem. Soc.* **2001**, *123*, 4130-4138.
- Futaki, S., Aoki, M., Ishikawa, T., Kondo, F., Asahara, T., Niwa, M., Nakaya, Y., Yagami, T. and Kitagawa, K.**, Chemical ligation to obtain proteins comprising helices with individual amino acid sequences, *Bioorg. Med. Chem.* **1999**, *7*, 187-192.
- Galat, A. and Metcalfe, S.M.**, Peptidylproline Cis/Trans Isomerases, *Prog. Biophys. Mol. Biol.* **1995**, *63*, 67-118.
- Garciaecheverria, C., Kofron, J.L., Kuzmic, P., Kishore, V. and Rich, D.H.**, Continuous Fluorometric Direct (Uncoupled) Assay for Peptidyl Prolyl Cis-Trans-Isomerases, *J. Am. Chem. Soc.* **1992**, *114*, 2758-2759.
- Gerig, J.T.**, Fluorine Nmr of Proteins, *Progress in Nuclear Magnetic Resonance Spectroscopy* **1994**, *26*, 293-370.
- Gerig, J.T. and McLeod, R.S.**, Conformations of Cis-4-Fluoro-L-Proline and Trans-4-Fluoro-L-Proline in Aqueous-Solution, *J. Am. Chem. Soc.* **1973**, *95*, 5725-5729.
- Geysen, H.M., Meloen, R.H. and Barteling, S.J.**, Use of peptide synthesis to probe viral antigens for epitopes to a resolution of a single amino acid, *Proc. Natl. Acad. Sci. U. S. A.* **1984**, *81*, 3998-4002.
- Ghadiri, M.R. and Choi, C.**, Secondary Structure Nucleation in Peptides - Transition-Metal Ion Stabilized Alpha-Helices, *J. Am. Chem. Soc.* **1990**, *112*, 1630-1632.

- Ghadiri, M.R., Soares, C. and Choi, C.**, A Convergent Approach to Protein Design - Metal Ion-Assisted Spontaneous Self-Assembly of a Polypeptide into a Triple-Helix Bundle Protein, *J. Am. Chem. Soc.* **1992**, *114*, 825-831.
- Ghadiri, M.R., Soares, C. and Choi, C.**, Design of an Artificial 4-Helix Bundle Metalloprotein Via a Novel Ruthenium(II)-Assisted Self-Assembly Process, *J. Am. Chem. Soc.* **1992**, *114*, 4000-4002.
- Gill, S.C. and von Hippel, P.H.**, Calculation of protein extinction coefficients from amino acid sequence data, *Anal. Biochem.* **1989**, *182*, 319-326.
- Golbik, R., Fischer, G. and Fersht, A.R.**, Folding of barstar C40A/C82A/P27A and catalysis of the peptidyl-prolyl cis/trans isomerization by human cytosolic cyclophilin (Cyp18), *Protein Sci.* **1999**, *8*, 1505-1514.
- Gothel, S.F. and Marahiel, M.A.**, Peptidyl-prolyl cis-trans isomerases, a superfamily of ubiquitous folding catalysts, *Cell. Mol. Life Sci.* **1999**, *55*, 423-436.
- Goudsmit, J., Debouck, C., Meloen, R.H., Smit, L., Bakker, M., Asher, D.M., Wolff, A.V., Gibbs, C.J., Jr. and Gajdusek, D.C.**, Human immunodeficiency virus type 1 neutralization epitope with conserved architecture elicits early type-specific antibodies in experimentally infected chimpanzees, *Proc. Natl. Acad. Sci. U. S. A.* **1988**, *85*, 4478-4482.
- Grathwohl, C. and Wuthrich, K.**, Nmr-Studies of the Rates of Proline Cis-Trans Isomerization in Oligopeptides, *Biopolymers* **1981**, *20*, 2623-2633.
- Guillier, F., Orain, D. and Bradley, M.**, Linkers and cleavage strategies in solid-phase organic synthesis and combinatorial chemistry, *Chem. Rev.* **2000**, *100*, 2091-2157.
- Haack, T. and Mutter, M.**, Serine Derived Oxazolidines as Secondary Structure Disrupting, Solubilizing Building-Blocks in Peptide-Synthesis, *Tetrahedron Lett.* **1992**, *33*, 1589-1592.
- Haar, W., Femandjian, S., Robert, F., Lefebvresoubeyran, O. and Savrda, S.**, Conformational Studies of Cyclo-Gly-Pro(S) by X-Ray-Diffraction and Proton Magnetic-Resonance, *Tetrahedron* **1976**, *32*, 2811-2815.
- Harrison, R.K. and Stein, R.L.**, Mechanistic studies of peptidyl prolyl cis - trans isomerase: evidence for catalysis by distortion, *Biochemistry (Mosc)*. **1990**, *29*, 1684-1689.
- Heine, N., Germeroth, L., Schneider-Mergener, J. and Wenschuh, H.**, A modular approach to the SPOT synthesis of 1,3,5-trisubstituted hydantoins on cellulose membranes, *Tetrahedron Lett.* **2001**, *42*, 227-230.
- Hendrickson, W.A., Pahler, A., Smith, J.L., Satow, Y., Merritt, E.A. and Phizackerley, R.P.**, Crystal structure of core streptavidin determined from multiwavelength anomalous diffraction of synchrotron radiation, *Proc. Natl. Acad. Sci. U. S. A.* **1989**, *86*, 2190-2194.
- Holmes, D.L., Smith, E.M. and Nowick, J.S.**, Solid-phase synthesis of artificial beta-sheets, *J. Am. Chem. Soc.* **1997**, *119*, 7665-7669.
- Huse, M., Chen, Y.G., Massague, J. and Kuriyan, J.**, Crystal structure of the cytoplasmic domain of the type I TGF beta receptor in complex with FKBP12, *Cell* **1999**, *96*, 425-436.

- Improta, R., Benzi, C. and Barone, V.**, Understanding the role of stereoelectronic effects in determining collagen stability. 1. A quantum mechanical study of proline, hydroxyproline, and fluoroproline dipeptide analogues in aqueous solution, *J. Am. Chem. Soc.* **2001**, *123*, 12568-12577.
- Inouye, K., Sakakibara, S. and Prockop, D.J.**, Effects of Stereo-Configuration of Hydroxyl Group in 4- Hydroxyproline on Triple-Helical Structures Formed by Homogeneous Peptides Resembling Collagen, *Biochim. Biophys. Acta* **1976**, *420*, 133-141.
- Janowski, B., Wollner, S., Schutkowski, M. and Fischer, G.**, A protease-free assay for peptidyl prolyl cis/trans isomerases using standard peptide substrates, *Anal. Biochem.* **1997**, *252*, 299-307.
- Jelinek, R., Terry, T.D., Gesell, J.J., Malik, P., Perham, R.N. and Opella, S.J.**, NMR structure of the principal neutralizing determinant of HIV-1 displayed in filamentous bacteriophage coat protein, *J. Mol. Biol.* **1997**, *266*, 649-655.
- Jelinek, R., Valente, A.P., Valentine, K.G. and Opella, S.J.**, Two-dimensional NMR spectroscopy of peptides on beads, *J. Magn. Reson.* **1997**, *125*, 185-187.
- Jensen, O.N., Podtelejnikov, A. and Mann, M.**, Delayed extraction improves specificity in database searches by matrix-assisted laser desorption/ionization peptide maps, *Rapid Commun. Mass Spectrom.* **1996**, *10*, 1371-1378.
- Jones, S. and Thornton, J.M.**, Principles of protein-protein interactions, *Proc. Natl. Acad. Sci. U. S. A.* **1996**, *93*, 13-20.
- Junius, F.K., O'Donoghue, S.I., Nilges, M., Weiss, A.S. and King, G.F.**, High resolution NMR solution structure of the leucine zipper domain of the c-Jun homodimer, *J. Biol. Chem.* **1996**, *271*, 13663-13667.
- Kang, Y.K.**, Cis-trans isomerization and puckering of pseudoproline dipeptides, *Journal of Physical Chemistry B* **2002**, *106*, 2074-2082.
- Kang, Y.K.**, cis-trans isomerization of N-acetyl-N'-methylamides of 5- methylproline and 5,5-dimethylproline, *Journal of Molecular Structure-Theochem* **2002**, *585*, 209-221.
- Kang, Y.K., Jhon, J.S. and Han, S.J.**, Conformational study of Ac-Xaa-Pro-NHMe dipeptides: proline puckering and trans/cis imide bond., *J. Pept. Res.* **1999**, *53*, 30-40.
- Karas, M., Bachmann, D., Bahr, U. and Hillenkamp, F.**, Matrix-Assisted Ultraviolet-Laser Desorption of Nonvolatile Compounds, *International Journal of Mass Spectrometry and Ion Processes* **1987**, *78*, 53-68.
- Keller, M., Sager, C., Dumy, P., Schutkowski, M., Fischer, G.S. and Mutter, M.**, Enhancing the proline effect: Pseudo-prolines for tailoring cis/trans isomerization, *J. Am. Chem. Soc.* **1998**, *120*, 2714-2720.
- Kemp, D.S. and Bowen, B.R.**, Conformational-Analysis of Peptide-Functionalized Diacylaminoepindolidiones H-1-Nmr Evidence for Beta-Sheet Formation, *Tetrahedron Lett.* **1988**, *29*, 5081-5082.
- Kemp, D.S. and Bowen, B.R.**, Synthesis of Peptide-Functionalized Diacylaminoepindolidiones as Templates for Beta-Sheet Formation, *Tetrahedron Lett.* **1988**, *29*, 5077-5080.

- Kemp, D.S., Boyd, J.G. and Muendel, C.C.**, The helical  $\alpha$  constant for alanine in water derived from template-nucleated helices, *Nature* **1991**, 352, 451-454.
- Kern, D., Schutkowski, M. and Drakenberg, T.**, Rotational barriers of cis/trans isomerization of proline analogues and their catalysis by cyclophilin, *J. Am. Chem. Soc.* **1997**, 119, 8403-8408.
- Kiefhaber, T. and Schmid, F.X.**, Kinetic coupling between protein folding and prolyl isomerization. II. Folding of ribonuclease A and ribonuclease T1, *J. Mol. Biol.* **1992**, 224, 231-240.
- Koepf, E.K., Petrassi, H.M., Sudol, M. and Kelly, J.W.**, WW: An isolated three-stranded antiparallel beta-sheet domain that unfolds and refolds reversibly; evidence for a structured hydrophobic cluster in urea and GdnHCl and a disordered thermal unfolded state, *Protein Sci.* **1999**, 8, 841-853.
- Kofron, J.L., Kuzmic, P., Kishore, V., Colon-Bonilla, E. and Rich, D.H.**, Determination of kinetic constants for peptidyl prolyl cis-trans isomerases by an improved spectrophotometric assay, *Biochemistry (Mosc)*. **1991**, 30, 6127-6134.
- Kortemme, T., Ramirez-Alvarado, M. and Serrano, L.**, Design of a 20-amino acid, three-stranded beta-sheet protein, *Science* **1998**, 281, 253-256.
- Kramer, A., Reineke, U., Dong, L., Hoffmann, B., Hoffmuller, U., Winkler, D., Volkmer-Engert, R. and Schneider-Mergener, J.**, Spot synthesis: observations and optimizations, *J. Pept. Res.* **1999**, 54, 319-327.
- Kramer, A. and Schneider-Mergener, J.**, Synthesis and screening of peptide libraries on continuous cellulose membrane supports, *Methods Mol. Biol.* **1998**, 87, 25-39.
- Kramer, A., Schuster, A., Reineke, U., Malin, R., Volkmer-Engert, R., Landgraf, C. and Schneider-Mergener, J.**, Combinatorial Cellulose-Bound Peptide Libraries: Screening Tools for the Identification of Peptides That Bind Ligands with Predefined Specificity, *Methods (Comp. Meth. Enzymol.)* **1994**, 6, 388-395.
- Krummrei, U., Baulieu, E.E. and Chambraud, B.**, The FKBP-associated protein FAP48 is an antiproliferative molecule and a player in T cell activation that increases IL2 synthesis, *Proc. Natl. Acad. Sci. U. S. A.* **2003**,
- Kukhar, V.P.**, Fluorine-Containing Amino-Acids, *Journal of Fluorine Chemistry* **1994**, 69, 199-205.
- Kyhse-Andersen, J.**, Electroblotting of multiple gels: a simple apparatus without buffer tank for rapid transfer of proteins from polyacrylamide to nitrocellulose, *J. Biochem. Biophys. Methods* **1984**, 10, 203-209.
- Lacombe, J.M., Andriamanampisoa, F. and Pavia, A.A.**, Solid-phase synthesis of peptides containing phosphoserine using phosphate tert.-butyl protecting group, *Int. J. Pept. Protein Res.* **1990**, 36, 275-280.
- Laemmli, U.K.**, Cleavage of structural proteins during the assembly of the head of bacteriophage T4, *Nature* **1970**, 227, 680-685.
- Lam, K.S., Salmon, S.E., Hersh, E.M., Hruby, V.J., Kazmierski, W.M. and Knapp, R.J.**, A new type of synthetic peptide library for identifying ligand-binding activity, *Nature* **1991**, 354, 82-84.

- Lebl, M., Solid-phase synthesis on planar supports, *Biopolymers* **1998**, *47*, 397-404.
- Licha, K., Bhargava, S., Rheinlander, C., Becker, A., Schneider-Mergener, J. and Volkmer-Engert, R., Highly parallel nano-synthesis of cleavable peptide-dye conjugates on cellulose membranes, *Tetrahedron Lett.* **2000**, *41*, 1711-1715.
- Lieberman, M. and Sasaki, T., Iron(II) Organizes a Synthetic Peptide into 3-Helix Bundles, *J. Am. Chem. Soc.* **1991**, *113*, 1470-1471.
- Liu, Y.C., Liu, Y., Elly, C., Yoshida, H., Lipkowitz, S. and Altman, A., Serine phosphorylation of Cbl induced by phorbol ester enhances its association with 14-3-3 proteins in T cells via a novel serine-rich 14-3-3-binding motif, *J. Biol. Chem.* **1997**, *272*, 9979-9985.
- Lopez-Illasaca, M., Schiene, C., Kullertz, G., Tradler, T., Fischer, G. and Wetzker, R., Effects of FK506-binding protein 12 and FK506 on autophosphorylation of epidermal growth factor receptor, *J. Biol. Chem.* **1998**, *273*, 9430-9434.
- MacArthur, M.W. and Thornton, J.M., Influence of proline residues on protein conformation, *J. Mol. Biol.* **1991**, *218*, 397-412.
- Macias, M.J., Hyvonen, M., Baraldi, E., Schultz, J., Sudol, M., Saraste, M. and Oschkinat, H., Structure of the WW domain of a kinase-associated protein complexed with a proline-rich peptide, *Nature* **1996**, *382*, 646-649.
- Makhatadze, G.I. and Privalov, P.L., Energetics of protein structure, *Adv. Protein Chem.* **1995**, *47*, 307-425.
- Mathias, L.J., Esterification and Alkylation Reactions Employing Isoureas, *Synthesis-Stuttgart* **1979**, 561-576.
- McCafferty, D.G., Slate, C.A., Nakhle, B.M., Graham, H.D., Austell, T.L., Vachet, R.W., Mullis, B.H. and Erickson, B.W., Engineering of a 129-Residue Tripod Protein by Chemoselective Ligation of Proline-Ii Helices, *Tetrahedron* **1995**, *51*, 9859-9872.
- Meldal, M., Pega - a Flow Stable Polyethylene-Glycol Dimethyl Acrylamide Copolymer for Solid-Phase Synthesis, *Tetrahedron Lett.* **1992**, *33*, 3077-3080.
- Merrifield, R.B., Solid-Phase Peptide Synthesis. 1. The synthesis of a tetrapeptide, *J. Am. Chem. Soc.* **1963**, *85*, 2149-2154.
- Merrifield, R.B., Solid-phase peptide synthesis in *Peptides : synthesis, structures, and applications* (Eds.: B. Gutte), Academic Press, San Diego, **1995**, pp 93-169.
- Mihara, H., Nishino, N., Hasegawa, R. and Fujimoto, T., A Hybrid of Amphiphilic Alpha-Helical Peptides and Meso- Tetra(Alpha,Alpha,Alpha,Alpha-Ortho-Carboxyphenyl)-Porphyrin - Membrane-Penetrating Porphyrin-4-Alpha-Helix Artificial Protein, *Chem. Lett.* **1992**, 1805-1808.
- Muslin, A.J., Tanner, J.W., Allen, P.M. and Shaw, A.S., Interaction of 14-3-3 with signaling proteins is mediated by the recognition of phosphoserine, *Cell* **1996**, *84*, 889-897.
- Mutter, M., The Construction of New Proteins and Enzymes - a Prospect for the Future, *Angew. Chem. Int. Ed. Engl.* **1985**, *24*, 639-653.
- Mutter, M., Nature's Rules and Chemists Tools - a Way for Creating Novel Proteins, *Trends Biochem.Sci.* **1988**, *13*, 260-265.

- Mutter, M., Altmann, E., Altmann, K.H., Hersperger, R., Koziej, P., Nebel, K., Tuchscherer, G., Vuilleumier, S., Gremlich, H.U. and Muller, K.**, The Construction of New Proteins .3. Artificial Folding Units by Assembly of Amphiphilic Secondary Structures on a Template, *Helv. Chim. Acta* **1988**, *71*, 835-847.
- Mutter, M. and Altmann, K.H.**, The Construction of New Proteins, *Angew. Makromol. Chem.* **1986**, *145*, 211-229.
- Mutter, M., Altmann, K.H., Tuchscherer, G. and Vuilleumier, S.**, Strategies for the Denovo Design of Proteins, *Tetrahedron* **1988**, *44*, 771-785.
- Mutter, M., Hersperger, R., Gubernator, K. and Muller, K.**, The Construction of New Proteins .5. A Template-Assembled Synthetic Protein (Tasp) Containing Both a 4-Helix Bundle and Beta-Barrel-Like Structure, *Proteins: Struct Funct Genet* **1989**, *5*, 13-21.
- Mutter, M., Nefzi, A., Sato, T., Sun, X., Wahl, F. and Woehr, T.**, Pseudo-Prolines (Psi-Pro) for Accessing Inaccessible Peptides, *Pept. Res.* **1995**, *8*, 145-153.
- Mutter, M. and Tuchscherer, G.**, Non-native architectures in protein design and mimicry, *Cell. Mol. Life Sci.* **1997**, *53*, 851-863.
- Mutter, M. and Vuilleumier, S.**, A Chemical Approach to Protein Design - Template-Assembled Synthetic Proteins (Tasp), *Angew. Chem. Int. Ed. Engl.* **1989**, *28*, 535-554.
- Mutter, M., Woehr, T., Gioria, S. and Keller, M.**, Pseudo-prolines: induction of cis/trans-conformational interconversion by decreased transition state barriers., *Biopolymers* **1999**, *51*, 121-128.
- Neye, H.**, Mutation of FKBP associated protein 48 (FAP48) at proline 219 disrupts the interaction with FKBP12 and FKBP52, *Regul. Pept.* **2001**, *97*, 147-152.
- Pace, C.N.**, Determination and analysis of urea and guanidine hydrochloride denaturation curves, *Methods Enzymol.* **1986**, *131*, 266-280.
- Panasik, N., Jr., Eberhardt, E.S., Edison, A.S., Powell, D.R. and Raines, R.T.**, Inductive effects on the structure of proline residues, *Int. J. Pept. Protein Res.* **1994**, *44*, 262-269.
- Peng, Z.H.**, Solid phase synthesis and NMR conformational studies on cyclic decapeptide template molecule, *Biopolymers* **1999**, *49*, 565-574.
- Perich, J.W., Ede, N.J., Eagle, S. and Bray, A.M.**, Synthesis of phosphopeptides by the Multipin method: Evaluation of coupling methods for the incorporation of Fmoc-Tyr(PO(3)Bzl,H)-OH, Fmoc-Ser(PO(3)Bzl,H)-OH and Fmoc-Thr(PO(3)Bzl,H)-OH, *Letters in Peptide Science* **1999**, *6*, 91-97.
- Petosa, C., Masters, S.C., Bankston, L.A., Pohl, J., Wang, B., Fu, H. and Liddington, R.C.**, 14-3-3zeta binds a phosphorylated Raf peptide and an unphosphorylated peptide via its conserved amphipathic groove, *J. Biol. Chem.* **1998**, *273*, 16305-16310.
- Phizicky, E. and Fields, S.**, Protein-protein interactions: methods for detection and analysis, *Microbiol. Rev.* **1995**, *59*, 94-123.
- Pliyev, B.K. and Gurvits, B.Y.**, Peptidyl-prolyl cis-trans isomerases: structure and functions, *Biochemistry (Mosc).* **1999**, *64*, 738-751.
- Ramachandran, G.N. and Sasisekharan, V.**, Conformation of polypeptides and proteins, *Adv. Protein Chem.* **1968**, *23*, 283-438.

- Rau, H.K., DeJonge, N. and Haehnel, W.**, Modular synthesis of de novo-designed metalloproteins for light-induced electron transfer, *Proc. Natl. Acad. Sci. U. S. A.* **1998**, *95*, 11526-11531.
- Rau, H.K., DeJonge, N. and Haehnel, W.**, Combinatorial Synthesis of Four-Helix Bundle Hemoproteins for Tuning of Cofactor Properties, *Angew. Chem. Int. Ed. Engl.* **2000**, *39*, 250-253.
- Rau, H.K. and Haehnel, W.**, Design, synthesis, and properties of a novel cytochrome b model, *J. Am. Chem. Soc.* **1998**, *120*, 468-476.
- Reimer, U., Scherer, G., Drewello, M., Kruber, S., Schutkowski, M. and Fischer, G.**, Side-chain effects on peptidyl-prolyl cis/trans isomerisation, *J. Mol. Biol.* **1998**, *279*, 449-460.
- Reineke, U., Kramer, A. and Schneider-Mergener, J.**, Antigen sequence- and library-based mapping of linear and discontinuous protein-protein-interaction sites by spot synthesis, *Curr. Top. Microbiol. Immunol.* **1999**, *243*, 23-36.
- Reineke, U., Sabat, R., Kramer, A., Stigler, R.D., Seifert, M., Michel, T., Volk, H.D. and SchneiderMergener, J.**, Mapping protein-protein contact sites using cellulose-bound peptide scans, *Mol. Divers.* **1996**, *1*, 141-148.
- Renil, M. and Meldal, M.**, POEPOP and POEPS: Inert polyethylene glycol crosslinked polymeric supports for solid synthesis, *Tetrahedron Lett.* **1996**, *37*, 6185-6188.
- Renner, C., Alefelder, S., Bae, J.H., Budisa, N., Huber, R. and Moroder, L.**, Fluoroprolines as tools for protein design and engineering, *Angew. Chem. Int. Ed. Engl.* **2001**, *40*, 923-925.
- Reznik, G.O., Vajda, S., Smith, C.L., Cantor, C.R. and Sano, T.**, Streptavidins with intersubunit crosslinks have enhanced stability, *Nat. Biotechnol.* **1996**, *14*, 1007-1011.
- Rittinger, K., Budman, J., Xu, J., Volinia, S., Cantley, L.C., Smerdon, S.J., Gamblin, S.J. and Yaffe, M.B.**, Structural analysis of 14-3-3 phosphopeptide complexes identifies a dual role for the nuclear export signal of 14-3-3 in ligand binding, *Mol. Cell* **1999**, *4*, 153-166.
- Ruan, F.Q., Chen, Y.Q. and Hopkins, P.B.**, Metal-Ion Enhanced Helicity in Synthetic Peptides Containing Unnatural, Metal-Ligating Residues, *J. Am. Chem. Soc.* **1990**, *112*, 9403-9404.
- Rudiger, S., Germeroth, L., Schneider-Mergener, J. and Bukau, B.**, Substrate specificity of the DnaK chaperone determined by screening cellulose-bound peptide libraries, *EMBO J.* **1997**, *16*, 1501-1507.
- Rusche, J.R., Javaherian, K., McDanal, C., Petro, J., Lynn, D.L., Grimaila, R., Langlois, A., Gallo, R.C., Arthur, L.O., Fischinger, P.J. and et al.**, Antibodies that inhibit fusion of human immunodeficiency virus-infected cells bind a 24-amino acid sequence of the viral envelope, gp120, *Proc. Natl. Acad. Sci. U. S. A.* **1988**, *85*, 3198-3202.
- Sabatini, D.M., Erdjument-Bromage, H., Lui, M., Tempst, P. and Snyder, S.H.**, RAFT1: a mammalian protein that binds to FKBP12 in a rapamycin-dependent fashion and is homologous to yeast TORs, *Cell* **1994**, *78*, 35-43.
- Sano, T., Vajda, S., Smith, C.L. and Cantor, C.R.**, Engineering subunit association of multisubunit proteins: a dimeric streptavidin, *Proc. Natl. Acad. Sci. U. S. A.* **1997**, *94*, 6153-6158.

- Sasaki, T. and Kaiser, E.T.**, Synthesis and Structural Stability of Helichrome as an Artificial Hemeproteins, *Biopolymers* **1990**, *29*, 79-88.
- Schaefer, G., Akita, R.W. and Sliwkowski, M.X.**, A discrete three-amino acid segment (LVI) at the C-terminal end of kinase-impaired ErbB3 is required for transactivation of ErbB2, *J. Biol. Chem.* **1999**, *274*, 859-866.
- Scharn, D., Germeroth, L., Schneider-Mergener, J. and Wenschuh, H.**, Sequential nucleophilic substitution on halogenated triazines, pyrimidines, and purines: A novel approach to cyclic peptidomimetics, *J. Org. Chem.* **2001**, *66*, 507-513.
- Scharn, D., Wenschuh, H., Reineke, U., Schneider-Mergener, J. and Germeroth, L.**, Spatially addressed synthesis of amino- and amino-oxy-substituted 1, 3,5-triazine arrays on polymeric membranes, *J. Comb. Chem.* **2000**, *2*, 361-369.
- Schiene, C. and Fischer, G.**, Enzymes that catalyse the restructuring of proteins, *Curr. Opin. Struct. Biol.* **2000**, *10*, 40-45.
- Schiene-Fischer, C. and Yu, C.**, Receptor accessory folding helper enzymes: the functional role of peptidyl prolyl cis/trans isomerases, *FEBS Lett.* **2001**, *495*, 1-6.
- Schmid, F.X.**, Prolyl isomerase: enzymatic catalysis of slow protein-folding reactions, *Annu. Rev. Biophys. Biomol. Struct.* **1993**, *22*, 123-142.
- Schmid, F.X.**, Prolyl isomerases, *Adv. Protein Chem.* **2002**, *59*, 243-282.
- Schmid, F.X., Mayr, L.M., Mucke, M. and Schonbrunner, E.R.**, Prolyl isomerases: role in protein folding, *Adv. Protein Chem.* **1993**, *44*, 25-66.
- Schmidt, T.G., Koepke, J., Frank, R. and Skerra, A.**, Molecular interaction between the Strep-tag affinity peptide and its cognate target, streptavidin, *J. Mol. Biol.* **1996**, *255*, 753-766.
- Schmidt, T.G. and Skerra, A.**, The random peptide library-assisted engineering of a C-terminal affinity peptide, useful for the detection and purification of a functional Ig Fv fragment, *Protein Eng.* **1993**, *6*, 109-122.
- Schneider, J.P. and Kelly, J.W.**, Templates That Induce Alpha-Helical, Beta-Sheet, and Loop Conformations, *Chemical Reviews* **1995a**, *95*, 2169-2187.
- Schneider, J.P. and Kelly, J.W.**, Synthesis and Efficacy of Square-Planar Copper-Complexes Designed to Nucleate Beta-Sheet Structure, *J. Am. Chem. Soc.* **1995b**, *117*, 2533-2546.
- Schnepf, R., Hörth, P., Bill, E., Wiegardt, K., Hildebrandt, P. and Haehnel, W.**, De novo Design and Characterization of Copper Centers in Synthetic Four-Helix-Bundle Proteins, *J. Am. Chem. Soc.* **2001**, *123*, 2186-2195.
- Schoetz, G., Trapp, O. and Schurig, V.**, Determination of the cis-trans isomerization barrier of several L-peptidyl-L-proline dipeptides by dynamic capillary electrophoresis and computer simulation, *Electrophoresis* **2001**, *22*, 2409-2415.
- Schreiber, S.L.**, Chemistry and biology of the immunophilins and their immunosuppressive ligands, *Science* **1991**, *251*, 283-287.
- Schutkowski, M., Bernhardt, A., Zhou, X.Z., Shen, M., Reimer, U., Rahfeld, J.U., Lu, K.P. and Fischer, G.**, Role of phosphorylation in determining the backbone dynamics of the serine/threonine-proline motif and Pin1 substrate recognition, *Biochemistry (Mosc.)* **1998**, *37*, 5566-5575.

- Schutkowski, M., Wollner, S. and Fischer, G.**, Inhibition of peptidyl-prolyl cis/trans isomerase activity by substrate analog structures: thioxo tetrapeptide-4-nitroanilides, *Biochemistry (Mosc)*. **1995**, *34*, 13016-13026.
- Shaw, B.R. and Schurr, J.M.**, Association Reaction of Collagen Model Polypeptides (Pro-Pro-Gly)N, *Biopolymers* **1975**, *14*, 1951-1985.
- Shi, Z., Olson, C.A., Rose, G.D., Baldwin, R.L. and Kallenbach, N.R.**, Polyproline II structure in a sequence of seven alanine residues, *Proc. Natl. Acad. Sci. U. S. A.* **2002**, *99*, 9190-9195.
- Skerra, A. and Schmidt, T.G.**, Use of the Strep-Tag and streptavidin for detection and purification of recombinant proteins, *Methods Enzymol.* **2000**, *326*, 271-304.
- Smythe, M.L., Huston, S.E. and Marshall, G.R.**, The Molten Helix - Effects of Solvation on the Alpha-Helical to 3(10)-Helical Transition, *J. Am. Chem. Soc.* **1995**, *117*, 5445-5452.
- Stamos, J., Sliwowski, M.X. and Eigenbrot, C.**, Structure of the epidermal growth factor receptor kinase domain alone and in complex with a 4-anilinoquinazoline inhibitor, *J. Biol. Chem.* **2002**, *277*, 46265-46272.
- Standaert, R.F., Galat, A., Verdine, G.L. and Schreiber, S.L.**, Molecular cloning and overexpression of the human FK506-binding protein FKBP, *Nature* **1990**, *346*, 671-674.
- Stapley, B.J. and Creamer, T.P.**, A survey of left-handed polyproline II helices, *Protein Sci.* **1999**, *8*, 587-595.
- Stein, R.L.**, Mechanism of enzymatic and nonenzymatic prolyl cis-trans isomerization, *Adv. Protein Chem.* **1993**, *44*, 1-24.
- Stewart, D.E., Sarkar, A. and Wampler, J.E.**, Occurrence and role of cis peptide bonds in protein structures, *J. Mol. Biol.* **1990**, *214*, 253-260.
- Toepert, F.**, Synthesis of an Array Comprising 837 Variants of the hYAP WW Protein Domain, *Angew. Chem. Int. Ed. Engl.* **2001**, *40*, 897-900.
- Tradler, T., Stoller, G., Rucknagel, K.P., Schierhorn, A., Rahfeld, J.U. and Fischer, G.**, Comparative mutational analysis of peptidyl prolyl cis/trans isomerases: active sites of Escherichia coli trigger factor and human FKBP12, *FEBS Lett.* **1997**, *407*, 184-190.
- Tsang, K.Y., Diaz, H., Graciani, N. and Kelly, J.W.**, Hydrophobic Cluster Formation Is Necessary for Dibenzofuran- Based Amino-Acids to Function as Beta-Sheet Nucleators, *J. Am. Chem. Soc.* **1994**, *116*, 3988-4005.
- Tuchscherer, G., Domer, B., Sila, U., Kamber, B. and Mutter, M.**, The Tasp Concept - Mimetics of Peptide Ligands, Protein Surfaces and Folding Units, *Tetrahedron* **1993**, *49*, 3559-3575.
- Tuchscherer, G. and Mutter, M.**, Templates in protein de novo design, *J. Biotechnol.* **1995**, *41*, 197-210.
- Tuchscherer, G., Servis, C., Corradin, G., Blum, U., Rivier, J. and Mutter, M.**, Total Chemical Synthesis, Characterization, and Immunological Properties of an Mhc Class-I Model Using the Tasp Concept for Protein De Novo Design, *Protein Sci.* **1992**, *1*, 1377-1386.
- Tuchscherer, G., Steiner, V., Altmann, K.H. and Mutter, M.**, De novo design of proteins. Template-assembled synthetic proteins (TASP), *Methods Mol. Biol.* **1994**, *36*, 261-285.

- Tugarinov, V., Zvi, A., Levy, R. and Anglister, J.**, A cis proline turn linking two beta-hairpin strands in the solution structure of an antibody-bound HIV-1IIIB V3 peptide, *Nat. Struct. Biol.* **1999**, *6*, 331-335.
- Uchida, T., Fujimori, F., Tradler, T., Fischer, G. and Rahfeld, J.U.**, Identification and characterization of a 14 kDa human protein as a novel parvulin-like peptidyl prolyl cis/trans isomerase, *FEBS Lett.* **1999**, *446*, 278-282.
- Van Duyne, G.D., Standaert, R.F., Karplus, P.A., Schreiber, S.L. and Clardy, J.**, Atomic structure of FKBP-FK506, an immunophilin-immunosuppressant complex, *Science* **1991**, *252*, 839-842.
- Van Duyne, G.D., Standaert, R.F., Karplus, P.A., Schreiber, S.L. and Clardy, J.**, Atomic structures of the human immunophilin FKBP-12 complexes with FK506 and rapamycin, *J. Mol. Biol.* **1993**, *229*, 105-124.
- van Hemert, M.J., Steensma, H.Y. and van Heusden, G.P.**, 14-3-3 proteins: key regulators of cell division, signalling and apoptosis, *Bioessays* **2001**, *23*, 936-946.
- Vandenbroeck, K., Alloza, I., Brehmer, D., Billiau, A., Proost, P., McFerran, N., Rudiger, S. and Walker, B.**, The conserved Helix C region in the superfamily of interferon-gamma /Interleukin-10-related cytokines corresponds to a high-affinity binding site for the HSP70 chaperone DnaK, *J. Biol. Chem.* **2002**,
- Veber, D.F., Strachan, R.G., Bergstrand, S.J., Holly, F.W., Homnick, C.F., Hirschmann, R., Torchiana, M.L. and Saperstein, R.**, Non-Reducible Cyclic Analogs of Somatostatin, *J. Am. Chem. Soc.* **1976**, *98*, 2367-2369.
- Venkatraman, J., Shankaramma, S.C. and Balaram, P.**, Design of folded peptides, *Chem. Rev.* **2001**, *101*, 3131-3152.
- Veronese, F.D.M., Willis, A.E., Boyerthompson, C., Appella, E. and Perham, R.N.**, Structural Mimicry and Enhanced Immunogenicity of Peptide Epitopes Displayed on Filamentous Bacteriophage - the V3 Loop of Hiv-1 Gp120, *J. Mol. Biol.* **1994**, *243*, 167-172.
- Vincenz, C. and Dixit, V.M.**, 14-3-3 proteins associate with A20 in an isoform-specific manner and function both as chaperone and adapter molecules, *J. Biol. Chem.* **1996**, *271*, 20029-20034.
- Vitagliano, L., Berisio, R., Mastrangelo, A., Mazzarella, L. and Zagari, A.**, Preferred proline puckerings in cis and trans peptide groups: Implications for collagen stability, *Protein Sci.* **2001**, *10*, 2627-2632.
- Volkmer-Engert, R., Hoffmann, B. and SchneiderMergener, J.**, Stable attachment of the HMB-linker to continuous cellulose membranes for parallel solid phase spot synthesis, *Tetrahedron Lett.* **1997**, *38*, 1029-1032.
- Wakamiya, T., Saruta, K., Yasuoka, J. and Kusumoto, S.**, An Efficient Procedure for Solid-Phase Synthesis of Phosphopeptides by the Fmoc Strategy, *Chemistry Letters* **1994**, 1099-1102.
- Warrass, R., Wieruszkeski, J.M., Boutillon, C. and Lippens, G.**, High-resolution magic angle spinning NMR study of resin-bound polyalanine peptides, *J. Am. Chem. Soc.* **2000**, *122*, 1789-1795.
- Weber, P.C., Ohlendorf, D.H., Wendoloski, J.J. and Salemme, F.R.**, Structural origins of high-affinity biotin binding to streptavidin, *Science* **1989**, *243*, 85-88.

- Wenschuh, H., Volkmer-Engert, R., Schmidt, M., Schulz, M., Schneider-Mergener, J. and Reineke, U.**, Coherent membrane supports for parallel microsynthesis and screening of bioactive peptides, *Biopolymers* **2000**, *55*, 188-206.
- Wilchek, M. and Bayer, E.A.**, Avidin-biotin technology ten years on: has it lived up to its expectations?, *Trends Biochem. Sci.* **1989**, *14*, 408-412.
- Wilson, K.P., Yamashita, M.M., Sintchak, M.D., Rotstein, S.H., Murcko, M.A., Boger, J., Thomson, J.A., Fitzgibbon, M.J., Black, J.R. and Navia, M.A.**, Comparative X-Ray Structures of the Major Binding-Protein for the Immunosuppressant Fk506 (Tacrolimus) in Unliganded Form and in Complex with Fk506 and Rapamycin, *Acta Crystallogr. Sect. D-Biol. Crystallogr.* **1995**, *51*, 511-521.
- Wohr, T., Wahl, F., Nefzi, A., Rohwedder, B., Sato, T., Sun, X.C. and Mutter, M.**, Pseudo-prolines as a solubilizing, structure-disrupting protection technique in peptide synthesis, *J. Am. Chem. Soc.* **1996**, *118*, 9218-9227.
- Wong, A.K., Jacobsen, M.P., Winzor, D.J. and Fairlie, D.P.**, Template Assembled Synthetic Proteins (TASPs). Are template size, shape, and directionality important in formation of four-helix bundles?, *J. Am. Chem. Soc.* **1998**, *120*, 3836-3841.
- Yaffe, M.B., Rittinger, K., Volinia, S., Caron, P.R., Aitken, A., Leffers, H., Gamblin, S.J., Smerdon, S.J. and Cantley, L.C.**, The structural basis for 14-3-3:phosphopeptide binding specificity, *Cell* **1997**, *91*, 961-971.
- YliKauhaluoma, J.T., Ashley, J.A., Lo, C.H.L., Coakley, J., Wirsching, P. and Janda, K.D.**, Catalytic antibodies with peptidyl-prolyl cis-trans isomerase activity, *J. Am. Chem. Soc.* **1996**, *118*, 5496-5497.
- Zhao, Y. and Ke, H.**, Crystal structure implies that cyclophilin predominantly catalyzes the trans to cis isomerization, *Biochemistry (Mosc)*. **1996**, *35*, 7356-7361.
- Zou, J. and Sugimoto, N.**, Complexation of peptide with Cu<sup>2+</sup> responsible to inducing and enhancing the formation of alpha-helix conformation, *Biomaterials* **2000**, *13*, 349-359.
- Zvi, A., Hiller, R. and Anglister, J.**, Solution Conformation of a Peptide Corresponding to the Principal Neutralizing Determinant of Hiv-1(Iiib) - a 2- Dimensional Nmr-Study, *Biochemistry (Mosc)*. **1992**, *31*, 6972-6979.

# Acknowledgements

First I would like to thank my supervisor, Professor Dr. Gunter Fischer; for giving me the chance to pursue my Ph.D. work in your group, for your guides, suggestions and instructions throughout my study period. Mere words can not express the role you have played in my life. Your boundless energy and enthusiasm for science pushed me to new limits.

Many thanks to Dr. Cordelia Schiene-Fischer, my advisor during my Ph.D. time, for your good advices and discussions on my research work. I thank you for being first reader of this dissertation in the midst of your busy schedule, your careful reading and giving me so many good suggestions for the manuscript.

Thanks to Dr. Frank Bordusa, for providing me support and facilities for the chemical synthesis work and for lots of interesting scientific discussions.

Thanks to Dr. Ralph Golbik for the nice cooperation in fluoroproline project and thank you for your reading of this part of my dissertation.

Thanks to PD. Dr. Jahreis Günther and Mario Drewello, for synthesizing peptides for my research project.

Thanks to Dr. Marc Kipping for measuring mass spectra of peptides immobilized on solid surface, for the discussion and suggestion on the project of matrix-bound peptide array.

Thanks to our former group members, Dr. Mike Schutkowski and Dr. Ulf Reimer, for your suggestions, ideas and information in the Janus peptide array project.

I am grateful to my Chinese colleagues, Dr. Yixin Zhang and Dr. Sen Li, for many of your suggestions, discussions and helps in my research work.

Special appreciation to my colleague, Markus Liebscher, who not only discussed with me about different scientific topics, provided me a lot of help and information in computer skills and knowledge, but also gave a lot of help in my daily life.

I appreciate all other colleagues in Max Planck Research Unit for Enzymology of Protein Folding, for your cooperation, helps and friendship, which are very important for a foreign student and make me feel very happy to work with you.

Lastly, I would like to give special thankfulness to my family: Mom, Dad and Carol for all of your faith, patience, and love.

Chao Yu

# Appendix A

## CURRICULUM VITAE

### PERSONAL DATA:

Name: YU, Chao  
Place of Birth: Shanghai, P. R. China  
Date of Birth: 25 June 1971  
Nationality: P. R. China

### EDUCATION:

- 2000,3-2003, 6: Ph.D. candidate in Biochemistry, at  
Max-Planck Research Unit Enzymology of Protein Folding, Halle, Germany  
Supervisor: Prof. Dr. Gunter Fischer  
Dissertation: "Matrix-bound peptides modeling protein-protein interactions"
- 1996,9-1999,9: M.S. in Biochemistry and Molecular Biology, at  
Shanghai Institute of Biochemistry, Chinese Academy of Sciences, Shanghai, China  
Supervisor: Prof. Dafu Cui  
Thesis: "Structures and functions of bone metabolism related peptides--synthesis, expression and biological activities study."
- 1989,9-1993,7: B.S. in Biochemistry, at  
East China University of Science and Technology, Shanghai, China  
Thesis: "Studies of the structures and functions of insulin like growth factor 1"
- 1983,9-1986,7: Secondary and high school study, Shanghai Wei-Yu High School, Shanghai, China

### PROFESSIONAL EXPERIENCE:

- 2000-2003      **Ph.D. student and research fellow**  
Max-Planck Research Unit Enzymology of Protein Folding, Halle, Germany
- 1996-1999      **Graduate student and research associate**  
Shanghai Institute of Biochemistry, Chinese Academy of Sciences, Shanghai, China
- 1993-1996      **Biochemistry research assistant**  
Shanghai Institute of Biochemistry, Chinese Academy of Sciences, Shanghai, China

Chao Yu

## **Appendix B**

### **Eidesstattliche Erklärung:**

Hiermit versichere ich, daß ich die vorliegende Arbeit “ Matrix-bound peptides modeling protein-protein interactions“ selbständig und nur unter Verwendung der genannten Hilfsmittel und angeführten Literaturzitate angefertigt habe. Die Arbeit wurde an keiner anderen Universität zur Promotion eingereicht.

Chao Yu